UNIVERSITÀ DEGLI STUDI DI TRENTO

Facoltà di Scienze Matematiche, Fisiche e Naturali

Dipartimento di Fisica

Tesi di Dottorato di Ricerca in Fisica
Ph.D. Thesis in Physics

Non-Symmetrized Hyperspherical Harmonics Method Applied to Light Hypernuclei

Candidate:
Fabrizio
Ferrari Ruffino

Supervisor:
Prof. Giuseppina
Orlandini

Dottorato di Ricerca in Fisica, XXIX ciclo

April 18, 2017

Contents

2

List of Abbreviations

HH	Hyperspherical Harmonics
NSHH	Non-Symmetrized Hyperspherical Harmonics
EIHH	Effective Interaction Hyperspherical Harmonics
FY	Faddeev Yakubovsky
MC	Monte Carlo
AFDMC	Auxiliary Field Diffusion Monte Carlo
GFMC	Green Function Monte Carlo
NCSM	No-Core Shell Model
GEM	Gaussian Expansion Method
CRCGV	Coupled-Rearrangement-Channel Gaussian basis
SVM	Stochastic Variational Method
EFT	Effective Field Theory
LMM	Lagrange Mesh Method
RR	Raynal-Revai
CM	Center of Mass
HO	Harmonic Oscillator
L-S	Lee-Suzuki
OPE	One Pion Exchange
TPE	Two Pion Exchange
NN	Nucleon-Nucleon
YN	hYperon-Nucleon
YY	hYperon-hYperon

Introduction

The present work is conducted in the field of few-body methods and it concerns the extension of the Non-Symmetrized Hyperspherical Harmonics method in order to treat quantum systems with different species of particles and additional degrees of freedom, like particle mixing. The aim is to introduce it as a new tool in the ab-initio study of light hypernuclei, namely nuclei with at least one hyperon, and, more in general, of few-body quantum systems composed by a variety of different objects.

In the last decades the physics of hypernuclei has seen increasing interest, testified by the intense experimental activity on strange systems. However, due to the instability of hyperons in the vacuum and to the consequent difficulty to produce stable beams, a very limited hyperon-nucleon (YN) database is available. The standard one comprises only 35 selected Λp low-energy scattering data [1] and some ΛN and ΣN data at higher energies for a total of 52 YN scattering data. Almost no information is available in the YY sector. In comparison, the Nijmegen NN scattering database includes over 4300 NN data in the range $0 \div 350$ MeV [2].
Quite a variety of potential models involving hyperons exist. They include purely phenomenological models (e.g. [3, 4]), meson-theoretical models [5], and descriptions in chiral effective field theory (χEFT) [6, 7]. However, the evidently limited information available for strange nuclear systems highlights the necessity of instruments to test the quality of the interaction models, and ab-initio methods are the natural ones. In fact, the accuracy of the results can be systematically controlled and this makes the comparison theory-experiment conclusive with respect to the input dynamics. Moreover, ab-initio methods allow to partially compensate the lack of scattering data by exploiting the experimental information on hypernuclear bound states in order to provide new constraints on the YN potential. Therefore, in the strange sector, ab-initio calculations for bound states play an even more important role compared to the nuclear case.
However, at present, a limited number of ab-initio calculations is available for hypernuclei, mainly focused on 3- and 4-body systems (see, for example, refs. [8–14]). An improvement in the maximal number of particles treatable

would allow to better exploit the experimental information available on hypernuclei with $A > 4$ in order to test and upgrade the available interaction models. In chapter 1 a brief review on hypernuclear bound states calculations is provided.

The main purpose of the present work is to generalize the Non-Symmetrized Hyperspherical Harmonics Method (NSHH) [15, 16] to make it a new ab-initio method for bound state calculations in the hypernuclear sector.
The NSHH approach is a recent development of the more classical Hyperspherical Harmonics (HH) expansion method. One of the main difficulties of the latter approach is the organization of the HH basis into irreducible representations of the symmetry group. The NSHH has been designed to simplify this task from a numerical point of view. The general method was developed by Gattobigio et al. [15] and later extended by Barnea et al. [16] to handle the modern realistic NN interactions like the Argonne Vn' potentials. It has been employed in order to perform bound state benchmark calculations of light nuclei up to $A = 6$. The method is based on the use of the HH basis without previous symmetrization. The identification of the eigenstates with good symmetries of the Hamiltonian of a system of A identical particles is done by means of the Casimir operator of the group of permutations of A objects. Such an approach is easily adaptable to a variety of physical systems with arbitrary permutational symmetry.

The original part of the present work is the extension of the NSHH method in order to treat systems of non-identical particles and on the incorporation of specific kinds of interaction models that require additional degrees of freedom, like the mixing of different species of particles (for example most of the modern hyperon-nucleon potentials take explicitly into account the conversion of a Λ hyperon into a Σ hyperon and vice versa). To do this we show a way to treat systems where the mass of one or more particles is "state-dependent" and we include the mixing degrees of freedom in the NSHH framework. We have also implemented the three body ΛNN forces by exploiting the pre-existing implementation of the NNN potential.
Although such extensions are general, we apply them on hypernuclei by providing benchmark results for binding energies and Λ-separation energies (the difference between the binding energy of the system without and with the Λ particle) for systems with $A = 3 \div 5$. We have also set up $\Lambda\Lambda$-hypernuclei calculations.
In order to treat systems with $A \geq 5$ the implementation of an efficient parallelization procedure is needed and part of the work has also been devoted to this, even if with partial results which demand for additional study.

The thesis is organized as follows:

In **Chapter 1** we provide a brief review on the experimental investigation on hypernuclei and on the available interaction models. We also show the general features of the few-body hypernuclear problem and motivate the extensions applied to the NSHH method and described in the following chapters.

In **Chapter 2** we show the adopted system of coordinates and their properties and we introduce the A-body Hyperspherical Harmonics basis that we adopt to approach the few-body bound state problem.

In **Chapter 3** the NSHH method is presented in its generalized form in order to treat systems with different species of particles and interactions.

In **Chapter 4** we show the further extensions done to the NSHH method in order to treat the interaction models with particle mixing or 3-body terms. In addition we show the adopted parallelization scheme avoiding technical details.

In **Chapter 5** we provide a number of selected benchmark results for binding and separation energies of light hypernuclei up to $A = 5$.

Conclusions and future perspectives are drawn at the end.

Chapter 1

Hypernuclear Systems

Although the present work is mainly devoted to the few-body method more than to the physics of hypernuclei, in this chapter we provide some historical hints on the hypernuclear investigation and we briefly introduce the general features of an hypernuclear few-body problem. The aim is to account for the NSHH extensions described in the next chapters and to show where the method is mainly intended to be employed in future investigations.

As mentioned in the introduction, hypernuclei are nuclei with at least one hyperon, namely a baryon with non-zero strangeness. In table 1.1 the hyperons and their main properties are listed. They are weakly decaying particles with a lifetime of the order of 10^{-10} s and their mass is heavier than the nucleon one by about $80 \div 680$ MeV. The standard notation adopted for

TABLE 1.1: Table of hyperons and their properties. In order: quark components, total isospin, total spin and parity, rest mass, mean lifetime and main decay modes [17, 18].

Hyperon	qqq	T	S^{π}	m (MeV)	τ (10^{-10}s)	Decay
Λ	uds	0	$1/2^+$	1115.683(6)	2.63(2)	$p\pi^-$,$n\pi^0$
Σ^+	uus	1	$1/2^+$	1189.37(7)	0.802(3)	$p\pi^0$,$n\pi^+$
Σ^0	uds	1	$1/2^+$	1192.64(2)	7.4(7)·10^{-10}	$\Lambda\gamma$
Σ^-	dds	1	$1/2^+$	1197.45(3)	1.48(1)	$n\pi^-$
Ξ^0	uss	1/2	$1/2^+$	1314.9(2)	2.90(9)	$\Lambda\pi^0$
Ξ^-	dss	1/2	$1/2^+$	1321.71(7)	1.64(2)	$\Lambda\pi^-$
Ω^-	sss	0	$3/2^+$	1672.5(3)	0.82(1)	$\Lambda K^-,\Xi^0\pi^-,\Xi^-\pi^0$

hypernuclei is:

$$^A_Y X \rightarrow A-1 \text{ nucleons (N)} , \quad 1 \text{ hyperon (Y);}$$
$$^A_{YY} X \rightarrow A-2 \text{ nucleons} , \quad\quad 2 \text{ hyperons,}$$

where X is the nuclear element and ^{A-1}X is the *core* nucleus. The separation energy of the hyperon in an hypernucleus is defined as:

$$B_Y(^A_Y X) = E(^{A-1}X) - E(^A_Y X) \, . \tag{1.1}$$

For an hypernucleus with two hyperons the double separation energy is defined:

$$B_{YY}(^A_{YY} X) = E(^{A-2}X) - E(^A_{YY} X) \, , \tag{1.2}$$

and the incremental YY energy is given by:

$$\Delta B_{YY}(^A_{YY} X) = B_{YY}(^A_{YY} X) - 2B_Y(^{A-1}_Y X) \, . \tag{1.3}$$

The evaluation of the hyperon separation energies is thus based on the calculation of the binding energies of the hypernuclei and of the corresponding core nuclei.

1.1   Brief Review on Experimental Discoveries of Hypernuclei

Among the known hypernuclei, the Λ-hypernuclei constitute by far the largest set. At present fourty-one of them have been discovered, four $\Lambda\Lambda$-hypernuclei and only one bound Σ-hypernucleus. Almost no information is available on hypernuclei with other hyperons [17].
The discovery of hypernuclei goes back to 1953 when Danysz and Pniewski observed the first decay of the hypertritium [19]:

$$^3_\Lambda \text{H} \rightarrow {}^3\text{He} + \pi^- \, ,$$
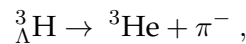
in an emulsion stack, as product of a fragmentation induced by cosmic rays. Emulsion experiments became then the main line of experimental investigation on light and medium-light Λ-hypernuclei (from $A = 5$ to $A = 15$) until the 70's, when kaon beams were first produced at CERN, providing hypernuclear spectroscopic data ranging from the light to the medium region ($A = 18 \div 40$) through the reaction (K^-, π^-). By means of the same reaction the heaviest hypernucleus was also found, the $^{209}_\Lambda$Bi. It followed an intense experimental investigation through the 80's in particular by means of the reaction (π^+, K^+) at the Alternating Gradient Syncrotron of Brookhaven National Laboratory and then at the proton syncrotron of the High Energy Accelerator Organization in Japan [17], with a number of new discoveries in the heavy region, from $^{51}_\Lambda$V to $^{208}_\Lambda$Pb (see fig. 1.1). A jump of quality in the resolution of the hypernuclear γ-ray spectroscopy took place thanks to

a new germanium detector (the Hyperball) and the high quality and intensity electron beams produced at the Thomas Jefferson National Accelerator Facility (JLab), allowing the reaction $(e, e'K^+)$ [17, 20].

Thanks to new facilities like J-PARC new reaction channels became available for the production of neutron rich Λ-hypernuclei, like (K^-, π^0), (π^-, K^0) and double charge exchange reactions (π^-, K^+) and (K^-, π^+) [21]. In fig. 1.1 the association between the different reaction channels and the hypernuclei produced is shown.

At present, several research facilities are actively involved in hypernuclear production and spectroscopy investigations. Some of the main ones are J-PARC, ALICE (at LHC), JLab, MAMI (Mainz) and DAΦNE (Frascati, Italy). Part of the reports and future prospects can be found in refs. [22–25].

Very recent examples of high precision γ-ray spectroscopy measurements, especially in the light sector, can be found in refs. [26–28].

The lightest hypernucleus known at present is the hypertritium $^3_\Lambda$H. No Λp nor $^3_\Lambda$He were found. In 2014 some hints on a possible Λnn bound state were found [29], although, at present, theoretical investigations do not conciliate such observation with the available informations on the nuclear and hypernuclear interactions [14, 30, 31].

In general, by looking at the separation energies of Λ hypernuclei, there is an increase of B_Λ with A by about 1 MeV/nucleon, and stable hypernuclei with unstable core nuclei appear, like $^6_\Lambda$He, $^8_\Lambda$He, $^7_\Lambda$Be, $^9_\Lambda$Be. This is the confirmation that the Λ hyperon has a "glue" like effect, by increasing the binding energy and stability of the whole system [17]. In tab. 1.2 the separation energies B_Λ of a selected number of hypernuclei in the light sector ($A = 3 \div 15$) are shown.

Only four $\Lambda\Lambda$-hypernuclei were found up to now: $^{\ 6}_{\Lambda\Lambda}$He, $^{10}_{\Lambda\Lambda}$Be, $^{12}_{\Lambda\Lambda}$Be and $^{13}_{\Lambda\Lambda}$B [35, 36]. Although almost no $\Lambda\Lambda$ scattering data are available, some hints on a weakly attractive character of the $\Lambda\Lambda$ interaction have been found.

1.2 Review on Hypernuclear Interactions

As anticipated in the introduction, the YN scattering database is limited and bound state energies are employed to fill only partially the lack of information on the hypernuclear interaction. By consequence, the quality of hypernuclear potentials is not comparable to the nuclear counterpart.

The Nijmegen YN meson-theoretical interaction model has probably been the most used in theoretical calculations over the last twenty years. Soft-core Nijmegen potentials for the YY sector have also been developed [38],

TABLE 1.2: Quantum numbers and experimental separation energies B_Λ of a partial set of Λ-hypernuclei in the light sector $A = 3 \div 15$ [32–34].

$^A_\Lambda$X	T	T_z	J^π	B_Λ (MeV)	$^A_\Lambda$X	T	T_z	J^π	B_Λ (MeV)
$^3_\Lambda$H	0	0	$1/2^+$	0.13(5)	$^9_\Lambda$Li	1	1	-	8.53(15)
$^4_\Lambda$H	1/2	1/2	0^+	2.04(4)	$^9_\Lambda$Be	0	0	1/2	6.71(4)
$^4_\Lambda$He	1/2	-1/2	0^+	2.39(3)	$^9_\Lambda$B	-	-	-	8.29(18)
$^5_\Lambda$He	0	0	$1/2^+$	3.12(2)	$^{10}_\Lambda$Be	1/2	1/2	-	9.11(22)
$^6_\Lambda$He	0	0	(1)	4.18(10)	$^{10}_\Lambda$B	1/2	-1/2	-	8.89(12)
$^7_\Lambda$He	1	1	-	5.68(3)	$^{11}_\Lambda$B	0	0	$5/2^+$	10.24(5)
$^7_\Lambda$Li	0	0	(1/2)	5.58(3)	$^{12}_\Lambda$B	1/2	1/2	1^-	11.37(6)
$^7_\Lambda$Be	1	-1	1/2	5.16(8)	$^{12}_\Lambda$C	-	-	1	10.76(19)
$^8_\Lambda$He	-	-	-	7.16(70)	$^{13}_\Lambda$C	0	0	1/2	11.69(12)
$^8_\Lambda$Li	1/2	1/2	1^-	6.80(3)	$^{14}_\Lambda$C	1/2	1/2	-	12.17(33)
$^8_\Lambda$Be	1/2	-1/2	-	6.84(5)	$^{15}_\Lambda$N	-	-	-	13.59(15)

leading to the extended soft-core 08 (ESC08) interaction model which represented the only interaction model unifying the NN, NY and YY sector [39], until the very recent development of the χEFT YY model [40, 41]. Hypernuclear calculations have been performed with this kind of potentials, in particular G-matrix based density functional calculations for medium-heavy hypernuclei (from $^{13}_\Lambda$C to $^{208}_\Lambda$Pb) and hypermatter [39, 42, 43]. However discrepancies with experiments are still evident. For example, six different parametrizations of the Nijmegen YN potential fit equally well the scattering data but produce different scattering lenghts [17, 44]. Moreover the Nijmegen models do not predict precisely all the hypernuclear binding energies in the light region, for example the correct separation energies of the mirror hypernuclei $^4_\Lambda$H and $^4_\Lambda$He.

A χEFT approach has been developed starting in 2006 when a Leading Order (LO) expansion for the YN interaction was provided [6] and then in 2013, when the Next to Leading Order (NLO) has been developed [7]. In addition a NLO potential has been developed also for the S=-2 sector [40, 41]. Calculations empolying such interactions are mainly limited to $A = 3 \div 4$ systems, and are based on the Faddeev Yakubovski (FY) [7] equations and on the No-Core Shell Model (NCSM) [9, 10], showing results of quality comparable to ESC08 ones.

Phenomenological models fitted on the Nijmegen set of data have been widely used by the Riken groups in order to investigate the structure of light hypernuclei up to $A = 5$ and heavier systems by means of cluster models and the Gaussian Expansion Method (GEM) [45]. For example the $^6_{\Lambda\Lambda}$He has been studied in terms of $\alpha + \Lambda + \Lambda$ and the $^{10}_{\Lambda\Lambda}$Be as $\alpha + \alpha + \Lambda + \Lambda$ by employing phenomenological $\alpha\Lambda$ interaction models.

All the mentioned YN interaction models are based on the explicit $\Lambda - \Sigma$
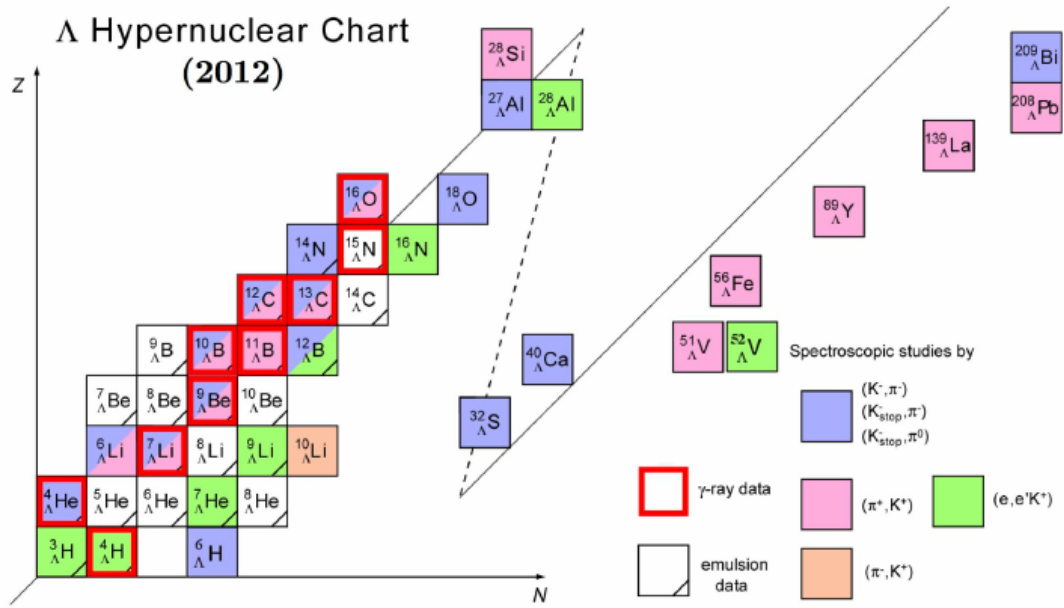
FIGURE 1.1: Hypernuclear chart of Λ hypernuclei. Figure
taken from ref. [37]

coupling. In fact the $\Lambda\pi\Lambda$ coupling is prohibited due to the isospin conservation. This means that the long range part of the ΛN interaction is caused by the $\Lambda - \Sigma$ conversion potential, where one pion exchange is possible.

A class of purely phenomenological Argonne-like interactions have been developed by Bodmer, Usmani and Carlson [3, 46] in the same way as the Argonne nuclear potential. They have been built by taking into account different diagrammatic contributions mainly related to pion exchange. Instead of the explicit $\Lambda - \Sigma$ coupling, they contain two body ΛN and three-body ΛNN terms, which are at the same two-pion exchange level. This last interaction model has been used only for Monte Carlo calculations, both for finite systems and nuclear matter, with consistent results [3, 12, 47].

1.3 The Hypernuclear Hamiltonian

Hypernuclei are systems composed by at least two different species of particles, namely nucleons and hyperons, which are both fermions. The permutational symmetry of such systems is obviously limited to the nucleons and hyperons subsets composing the A-body system. In the most common case of hypernuclei with a single hyperon, the permutational symmetry is limited to the core nuclei. The total hypernuclear Hamiltonian:

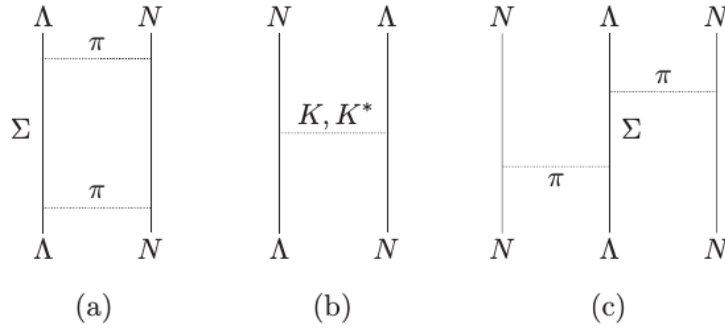$$H = H_N + H_Y + V_{YN} . \tag{1.4}$$

FIGURE 1.2: Examples of meson exchange processes between nucleons and hyperons at the 2- and 3-body level. In (*a*) and (*c*) two pion exchange processes are shown, while in (*c*) a K,K^* exchange process is represented. Figure extracted from ref. [12].

where H_N is the Hamiltonian of the core nucleus, H_Y of the hyperonic part and V_{YN} is the potential between the particles belonging to the two different species.

We denote the internal set of coordinates of the system as $\boldsymbol{\eta}$. The wave function of the hypernucleus satisfies the fermionic permutational symmetry both for nucleons and hyperons:

$$\begin{aligned} \hat{P}_{N_i N_j} \, \Psi(\boldsymbol{\eta}) &= - \, \Psi(\boldsymbol{\eta}) \; ; \\ \hat{P}_{Y_i Y_j} \, \Psi(\boldsymbol{\eta}) &= - \, \Psi(\boldsymbol{\eta}) \; , \end{aligned} \qquad (1.5)$$

where the $\hat{P}$ operators represent two-particle permutations. Therefore a proper symmetrization procedure must be applied separately on the core nucleus and on the hyperonic set.

Since the Λ hyperon has isospin $t = 0$, the strong $\Lambda\pi\Lambda$ vertex is forbidden due to isospin conservation. Thus the Λ particle can exchange one pion only via the $\Lambda\pi\Sigma$ vertex. This means that a YN force at the one pion exchange (OPE) level must explicitly take into account the $\Lambda - \Sigma$ coupling.

One-meson exchange processes involving a nucleon N and a Λ without Σ conversion can only occour through the exchange of a K,K^* pair, which contributes in exchanging strangeness between the Λ and the N baryons. However the K,K^* exchange potential is short range and it is expected to be quite weak due to the opposite sign of the K and K^* tensor contributions [12].

In fig. 1.2 the main meson exchange processes involving a Λ hyperon among nucleons are shown. In particular we see that a Λ-hypernuclear interaction model defined at the two-pion exchange (TPE) level must involve 2- and 3-body forces, namely ΛN and ΛNN terms.

Such coupling scheme is adopted by the phenomenological Bodmer-Usmani interaction model [3], which avoids the explicit inclusion of the Σ hyperon degree of freedom by introducing 3-body terms related to the two pion exchange diagrams of fig. 1.2 (and other TPE diagrams):

$$H_{\Lambda\text{-hyp}}^{BU} = T + V_{NN} + V_{\Lambda N} + V_{\Lambda NN} \,. \tag{1.6}$$

However, except for the Bodmer-Usmani model, all the available hypernuclear interactions are based on the explicit $\Lambda - \Sigma$ coupling. This means that additional degrees of freedom due to the mixing between the Λ and the Σ particle have to be included.

For a Λ-hypernucleus the Hamiltonian has the following block structure:

$$H = \begin{pmatrix} T_{m_\Lambda} & \\ & T_{m_\Sigma} \end{pmatrix} + \begin{pmatrix} 0 & \\ & \Delta M \end{pmatrix} \\ + \begin{pmatrix} V_{NN-NN} & \\ & V_{NN-NN} \end{pmatrix} + \begin{pmatrix} V_{N\Lambda-N\Lambda} & V_{N\Sigma-N\Lambda} \\ V_{N\Lambda-N\Sigma} & V_{N\Sigma-N\Sigma} \end{pmatrix} , \tag{1.7}$$

where the upper diagonal blocks are related to the system with the Λ hyperon and the lower diagonal ones to the same system with the Σ hyperon. We see that the YN potential operator couples the Λ part of the basis with the Σ one through the mixing terms $V_{N\Lambda-N\Sigma}$ and $V_{N\Sigma-N\Lambda}$. The ΔM matrix is related to the mass difference in energy units between the Λ and the Σ particles and the T_{m_Λ} and T_{m_Σ} matrices are the kinetic energy operators related to the system with the Λ and the Σ hyperon respectively.

If more hyperons are present, the block structure of the Hamiltonian becomes more complex. Moreover in the double strangeness $S = -2$ sector new coupling channels open up, involving Ξ hyperons too.

The aim of the present work is to extend the Hyperspherical Harmonics method in order to approach such systems. In particular we generalize the method in order to treat systems with different species of particles and we implement some extensions that allow the incorporation of particle-mixing interaction models as the YN ones. We also implement the ΛNN 3-body force.

Chapter 2

The A-Body Hyperspherical Harmonics Basis

In this chapter we present the basis we adopt for the bound state calculations this work is based on.

In configuration space, our system is described by the spatial coordinates besides the spin and the isospin quantum numbers. By consequence our basis is composed by a spatial part and a spin/isospin part. The coordinate system is the hyperspherical one and it is built over the mass-weighted Jacobi coordinates: it includes a single radial coordinate, i.e. the hyperradius ρ, a set of $N-1$ hyperangles $\{\phi_i ; \ i = 2, \ldots, N\}$ and a set of $2N$ angles $\{(\theta_i, \varphi_i) ; \ i = 1, \ldots, N\}$.

The spatial part of each of our basis functions is a product of an hyperradial polynomial (we use a set of Laguerre polynomials) and a hyperangular and angular function belonging to the Hyperspherical Harmonics (HH) set. However, when we generically refer to "HH basis", we often intend the complete basis, including the hyperradial part.

The aim is to extend the NSHH formalism to the general case of systems composed by different species of particles, so we do not assume any specific feature on our A-body system.

In section 2.1 we introduce the hyperspherical system of coordinates by starting from the Jacobi basis for $\mathbb{R}^{3A}$. We define first the properties of the mass-weighted Jacobi set and we generalize some of them by introducing the transformations which change the mass parameters. They will turn useful in the extensions of the HH method presented in chapter 3 that are necessary to treat most of the modern hypernuclear interactions. Then we illustrate the transformation to the hyperspherical coordinates and the consequent derivation of the so called *grand angular momentum operator*, the angular part of the kinetic energy operator in hyperspherical coordinates: the hyperspherical harmonics are its eigenfunctions.

In section 2.3 we show the complete NSHH basis in details including the

construction of the spin and isospin part. The main properties of the adopted basis and their applications will be shown in the next chapters. Finally, some remarks on the symmetrized HH basis are provided.

2.1   The Jacobi System of Coordinates

Two different systems of coordinates are combined in the definition of our HH basis: the mass-weighted Jacobi set and the hyperspherical set. The former allows to separate the center of mass (CM) term from the internal ones in the kinetic operator and it is particularly convenient when only the internal degrees of freedom of the physical system are of interest. The latter is composed by a single radial coordinate and $3A-4$ angles (if we exclude the CM) and it provides the natural set where the A-body HH basis is defined. In fact the angular dependence of the kinetic operator in hyperspherical coordinates is contained only in the *grand angular momentum operator* and the HH functions are its eigenfunctions. The adopted coordinate system is then the Jacobi internal set parametrized in hyperspherical coordinates.

The Jacobi set is order-dependent so different choices in the particles ordering and coupling correspond to different sets. We show the transformations which allow to pass from one set to another and we extend them in order to introduce the possiblity to change the mass parameters from one set to another. On this basis in chapter 3 we will define spatial permutations operators and we will introduce a way to treat systems with particle resonance degrees of freedom.

2.1.1   The Standard Set of Mass-Weighted Coordinates

In a system of A particles, where $\mathbf{r}_i$ and m_i are the cartesian position and the mass of the i-th particle respectively, we introduce the mass-weighted Jacobi coordinates by adopting the reversed order convention [48]:

$$\boldsymbol{\eta}_{A-i} = \sqrt{\frac{m_{i+1}M_i}{mM_{i+1}}}\left(\mathbf{r}_{i+1} - \frac{1}{M_i}\sum_{j=1}^{i} m_j\mathbf{r}_j\right) \ ; \quad i = 1, ..., N \ , \qquad (2.1)$$

where $N = A - 1$, the constant m is a reference mass (for convenience the nucleon mass in our case) and:

$$M_i = \sum_{j=1}^{i} m_j \ . \qquad (2.2)$$

Each $\boldsymbol{\eta}_{A-i}$ vector represents the $(i+1)$-th particle position with respect to the center of mass of the first i particles. In case of identical masses, with

$m_i = m$ for $i = 1, \ldots, A$, eq. (2.1) becomes:

$$\boldsymbol{\eta}_{A-i}^{\mathrm{id}} = \sqrt{\frac{i}{i+1}}\left(\mathbf{r}_{i+1} - \frac{1}{i}\sum_{j=1}^{i}\mathbf{r}_j\right) \; ; \quad i = 1, \ldots, N \; . \tag{2.3}$$

Of course the complete set of mass-weighted Jacobi coordinates includes the rescaled CM coordinate:

$$\boldsymbol{\eta}_0 = \sqrt{\frac{M_A}{m}}\mathbf{R}_{\mathrm{cm}} = \frac{1}{\sqrt{mM_A}}\sum_i m_i\mathbf{r}_i \; . \tag{2.4}$$

The basis $\{\boldsymbol{\eta}_i\}$ is orthonormal in case of equal masses. The matrix S defines the passage from cartesian to Jacobi basis:

$$S = \begin{pmatrix} -\sqrt{\frac{m_2}{m_1 M_2}} & \sqrt{\frac{m_1}{m_2 M_2}} & 0 & \cdots & 0 \\ -\sqrt{\frac{m_3}{M_2 M_3}} & -\sqrt{\frac{m_3}{M_2 M_3}} & \sqrt{\frac{M_2}{m_3 M_3}} & \cdots & 0 \\ -\sqrt{\frac{m_4}{M_3 M_4}} & -\sqrt{\frac{m_4}{M_3 M_4}} & -\sqrt{\frac{m_4}{M_3 M_4}} & \cdots & 0 \\ \vdots & \vdots & \vdots & \ddots & \vdots \\ \frac{1}{\sqrt{M_A}} & \frac{1}{\sqrt{M_A}} & \frac{1}{\sqrt{M_A}} & \cdots & \frac{1}{\sqrt{M_A}} \end{pmatrix} \cdot \mathcal{M} \; , \tag{2.5}$$

where:

$$\mathcal{M}_{ij} = \sqrt{m_i}\,\delta_{ij} \; . \tag{2.6}$$

It can be verified that the orthogonality conditions are always satisfied for any set of masses $\{m_1, \ldots, m_A\}$:

$$S^T \cdot S = \mathbb{I} \quad ; \quad \det(S) = 1 \; . \tag{2.7}$$

If $\mathbf{v}_r$ and $\mathbf{v}_\eta$ are the same vector defined, respectively, on the cartesian and on the Jacobi basis, the change of coordinates is defined by:

$$\mathbf{v}_r = \frac{1}{\sqrt{m}}\mathcal{M} \cdot S^T \cdot \mathbf{v}_\eta \; , \tag{2.8}$$

and the volume elements are related by:

$$dV_\eta = \prod_{i=0}^{N} d\boldsymbol{\eta}_i = \prod_{i=1}^{A}\sqrt{\frac{m_i}{m}}d\mathbf{r}_i = \left(\prod_{i=1}^{A}\sqrt{\frac{m_i}{m}}\right)dV_r \; . \tag{2.9}$$

Eq. (2.8) allows to convert the kinetic energy operator from cartesian to Jacobi coordinates. The following relations hold:

$$
\begin{aligned}
T = -\sum_{i=1}^{A} \frac{\hbar^2}{2m_i} \Delta_{r_i} &= -\frac{\hbar^2}{2} \nabla_r^T \cdot (\mathcal{M}^{-1})^2 \cdot \nabla_r \\
&= -\frac{\hbar^2}{2m} \nabla_\eta^T \cdot S \cdot \mathcal{M} \cdot (\mathcal{M}^{-1})^2 \cdot \mathcal{M} \cdot S^T \cdot \nabla_\eta \qquad (2.10) \\
&= -\frac{\hbar^2}{2m} \sum_{i=0}^{N} \Delta_{\eta_i} ,
\end{aligned}
$$

where $\nabla_r^T = (\nabla_{r_1}^T, \nabla_{r_2}^T, \ldots)$ and an analogue definition for ∇_η^T. We note that the above operator is proportional to the $3A$-dimensional laplacian only in case of identical masses. In case of different masses, the Gram matrix g associated to the Jacobi set is not the identity matrix anymore, due to the non-orthogonality of the basis:

$$
\sum_{i=0}^{N} \Delta_{\eta_i} \underset{g \neq \mathbb{I}}{\neq} \nabla_\eta^T \cdot g \cdot \nabla_\eta = \Delta . \qquad (2.11)
$$

2.1.2   The Kinematic Rotations

Several different schemes of mass-weighted Jacobi coordinates are possible besides the standard one shown in eq. (2.1). In general, they differ by the sequence of coupling among each of the A particles composing the system and by the orientation of each $\boldsymbol{\eta}_i$ vector.

All the applications which allow to pass from one scheme to another belong to the group $O(N)$, since they do not involve the CM coordinate nor the relative orientation of the x, y and z components of each $\boldsymbol{\eta}_i$ vector. They are compositions of three basic types of transformations, called *kinematic rotations* [49]: exchange between adjacent particles, change in sign of a vector and recoupling of two particles. In fig. 2.1 two examples of, respectively, exchange and recoupling of two particles are shown.

The standard set of eq. (2.1) is based on a sequence of couplings which goes neatly from particle 1 to particle A. However, all the $A!$ possible dispositions are allowed and the transformations from one sequence to another are compositions of exchanges between adjacent particles which, in the generic case of particles i and $i + 1$, involve the $\boldsymbol{\eta}_{A-i}$ and $\boldsymbol{\eta}_{A-i+1}$ coordinates only:

$$
\begin{pmatrix} \vdots \\ \boldsymbol{\eta}'_{A-i} \\ \boldsymbol{\eta}'_{A-i+1} \\ \vdots \end{pmatrix} = p_{(i,i+1)} \cdot \begin{pmatrix} \vdots \\ \boldsymbol{\eta}_{A-i} \\ \boldsymbol{\eta}_{A-i+1} \\ \vdots \end{pmatrix} \qquad (2.12)
$$

FIGURE 2.1: Two alternatives to the standard scheme a) of a 5-body Jacobi set of coordinates. In b) a recoupling of particles 4 and 5 is shown: the vector describing their relative positions is connected to the CM of the remaining three particles. In c) the order of coupling of particle 4 and 5 is exchanged with respect to a).

where:

$$
p_{(i,i+1)} = \begin{pmatrix} \mathbb{I}_{N-i} & & & \\ & -\cos\beta_i & \sin\beta_i & \\ & \sin\beta_i & \cos\beta_i & \\ & & & \mathbb{I}_{i-2} \end{pmatrix}, \tag{2.13}
$$

with β_i called the *kinematic angle* and defined as:

$$
\cos^2\beta_i = \frac{m_i m_{i+1}}{M_i(M_{i-1} + m_{i+1})} . \tag{2.14}
$$

In case of identical particles: $\cos^2\beta_i = i^{-1}$. In fig. 2.1 c) the $p_{(4,5)}$ transformation in a 5-body set is graphically shown.

Although the standard set of Jacobi coordinates is based on a sequential coupling, other coupling schemes are possible. The simplest is the one where the i-th and $(i+1)$-th particles are coupled to each other and their CM is coupled to the CM of the previous $(i-1)$ particles:

$$
\boldsymbol{\eta}''_{A-i} = \sqrt{\frac{m_i m_{i+1}}{m(m_i + m_{i+1})}} (\mathbf{r}_{i+1} - \mathbf{r}_i)
$$

$$
\boldsymbol{\eta}''_{A-i+1} = \sqrt{\frac{(m_{i-1} + m_i)M_{i-2}}{mM_i}} \left(\frac{1}{M_{i-1}} \sum_{j=1}^{i-2} m_j \mathbf{r}_j - \frac{m_i \mathbf{r}_i + m_{i+1}\mathbf{r}_{i+1}}{m_i + m_{i+1}} \right) .
$$

$$
\tag{2.15}
$$

The matrix of change of basis has a structure similar to the one in eq. (2.12):

$$
c_{(i,i+1)} = \begin{pmatrix} \mathbb{I}_{N-i} & & & \\ & \cos\gamma_i & \sin\gamma_i & \\ & \sin\gamma_i & -\cos\gamma_i & \\ & & & \mathbb{I}_{i-2} \end{pmatrix}, \tag{2.16}
$$

and the kinematic angle γ_i is given by [49]:

$$
\cos^2\gamma_i = \frac{M_{i-1}m_i}{M_i(m_i + m_{i+1})} . \tag{2.17}
$$

In fig. 2.1 b) the $c_{(4,5)}$ transformation is shown.

For both p and c kinematic rotations the moduli of the transformed basis vectors satisfy the relation:

$$
\eta_{A-i}^2 + \eta_{A-i+1}^2 = \eta_{A-i}'^2 + \eta_{A-i+1}'^2 = \eta_{A-i}''^2 + \eta_{A-i+1}''^2 \tag{2.18}
$$

2.1.3   Coupling Permutations and Spatial Permutations

We note that, in case of identical particles, the transformation $p_{(i,i+1)}$ is a true spatial transposition between particles i and $i+1$ and any composition of p transformations corresponds to a spatial permutation. However, this is not a general statement, in fact the kinematic rotations always maintain the association between $\mathbf{r}_i$ and m_i and this prevents the identification with spatial permutations in case of different masses. If we call $\boldsymbol{\eta}[(m_1, \mathbf{r}_1), (m_2, \mathbf{r}_2), \ldots]$ the complete set of Jacobi vectors as function of the mass-position pairs $(m_i, \mathbf{r}_i)$, a spatial transposition $P_{(i,i+1)}$ between particles i and $i+1$ exchanges, by definition, the $\mathbf{r}_i$ and $\mathbf{r}_{i+1}$ vectors only:

$$
\begin{aligned}
P_{(i,i+1)} \cdot \boldsymbol{\eta}[(m_1, \mathbf{r}_1), \ldots, &(m_i, \mathbf{r}_i), (m_{i+1}, \mathbf{r}_{i+1}), \ldots] = \\
& \boldsymbol{\eta}[(m_1, \mathbf{r}_1), \ldots, (m_i, \mathbf{r}_{i+1}), (m_{i+1}, \mathbf{r}_i), \ldots] .
\end{aligned} \tag{2.19}
$$

The effect is a change in all the $\boldsymbol{\eta}_j$ definitions from $j = 0$ to $j = A - i$. In the next subsection we extend the set of transformations by including the possibility to change the m_i parameters and we show how the $P_{i,j}$ permutations are defined.

On the contrary, it can be easily checked that the action of a $p_{(i,i+1)}$ kinematic rotation on the $\boldsymbol{\eta}$ set keeps the $(m_i, \mathbf{r}_i)$ and $(m_{i+1}, \mathbf{r}_{i+1})$ pairs unchanged:

$$
\begin{aligned}
p_{(i,i+1)} \cdot \boldsymbol{\eta}[(m_1, \mathbf{r}_1), \ldots, &(m_i, \mathbf{r}_i), (m_{i+1}, \mathbf{r}_{i+1}), \ldots] = \\
& \boldsymbol{\eta}[(m_1, \mathbf{r}_1), \ldots, (m_{i+1}, \mathbf{r}_{i+1}), (m_i, \mathbf{r}_i), \ldots] ,
\end{aligned} \tag{2.20}
$$

in fact only the $\boldsymbol{\eta}_{A-i}$ and $\boldsymbol{\eta}_{A-i+1}$ basis vectors change, as shown in eq. (2.12). In most of the cases this distinction is meaningless, since permutations are

usually employed in symmetrization procedures which are limited to identical particles. However, as we will see in chapter 4, there are interaction models that include potential terms proportional to space exchange operators, like, for example, the Bodmer-Usmani hyperon-nucleon (YN) potential [46]:

$$V_{\Lambda N} = [(V_c(r_{\Lambda N}) - \overline{V})(1 - \epsilon + \epsilon \hat{P}_{\Lambda N}) + \frac{1}{4} V_\sigma \boldsymbol{\sigma}_\Lambda \cdot \boldsymbol{\sigma}_N] \, T_\pi^2(r_{\Lambda N}) \,, \quad (2.21)$$

where the operator $\hat{P}_{\Lambda N}$ is a spatial permutation between the Λ hyperon and the nucleon N (which have different masses), and it should not be confused with $p_{\Lambda N}$. For this reason, from now on, we refer to the p_{ij} transformations as coupling permutations and to the P_{ij} as spatial permutations (or transpositions).

2.1.4 Transformations between Different Sets of Mass Parameters

Regardless of the arrangement or of the chosen mass parameters, the Jacobi set of coordinates constitutes a basis for $\mathbb{R}^{3A}$. In the previous section we saw that the transformations from one scheme to another are compositions of elementary transformations called kinematic rotations which belong to the group $O(N)$.

Here we introduce a new type of transformations that allow to pass from one Jacobi basis defined on a given set of masses, ζ, to another basis defined on a different set ζ', with:

$$\zeta = \{m_i > 0 \,; \;\; i = 1, \dots, A\} \,. \quad (2.22)$$

It is easy to prove that the subspace defined by the last $\boldsymbol{\eta}_{N-i}, \dots, \boldsymbol{\eta}_N$ coordinates is invariant under any change in the set of mass parameters:

$$\boldsymbol{\eta}_{N-i}^{\zeta'} = c_N \boldsymbol{\eta}_N^{\zeta} + c_{N-1} \boldsymbol{\eta}_{N-1}^{\zeta} + \dots + c_{N-i} \boldsymbol{\eta}_{N-i}^{\zeta} \,, \quad (2.23)$$

where the c's are real positive coefficients. A useful consequence is the invariance of the subspace given by the internal coordinates $\langle \boldsymbol{\eta}_1, \dots, \boldsymbol{\eta}_N \rangle$, which allows to describe the internal motion of a system by employing a set of mass parameters different from the physical one and by keeping the separation of the CM coordinate $\boldsymbol{\eta}_0$.

The matrix of the transformation from the ζ set to ζ' is given by:

$$W_{\zeta'\zeta} = S_{\zeta'} \, \mathcal{M}_{\zeta'}^{-1} \, \mathcal{M}_\zeta \, S_\zeta^T \,. \quad (2.24)$$

We look for a more useful form of the matrix elements of W.

Such transformations are compositions of kinematic rotations and scaling transformations. This can be seen by noting that the first vector of a given

Jacobi set, $\boldsymbol{\eta}_1$, is proportional to the first vector of another set, $\boldsymbol{\eta}'_1$, where all the mass parameters are equal but the last one, denoted as m'_A. Moreover the first Jacobi vector is the only one that depends on the mass-position pair $(m_A, \mathbf{r}_A)$, except the CM $\boldsymbol{\eta}_0$ which can be neglected as explained above. We have:

$$\boldsymbol{\eta}_i^\zeta = \begin{cases} a_A\, \boldsymbol{\eta}_1^{\zeta'} & i = 1 \\ \boldsymbol{\eta}_i^{\zeta'} & i = 2, \ldots, N \end{cases} \tag{2.25}$$

with:

$$a_A = \sqrt{\frac{m_A}{m'_A}\frac{M'_A}{M_A}} \qquad ; \qquad M'_A = M_A - m_A + m'_A\,. \tag{2.26}$$

We see that in this case the transformation $W_{\zeta'\zeta} \equiv W_{(A)}$ is a pure scaling transformation:

$$W_{(A)} = \begin{pmatrix} a_A & \\ & \mathbb{I}_{N-1} \end{pmatrix}\,. \tag{2.27}$$

However, if the mass to change is located in the generic i-th position, one can always apply a sequence of kinematic rotations in order to move the $(m_i, \mathbf{r}_i)$ couple in the last coupling position, and then come back after the application of the scaling transformation $W_{(A)}$:

$$W_{(i)} = \left[\prod_{\alpha=N}^{i} p_{\alpha,\alpha+1}^{\zeta'} \right] W_{(A)} \left[\prod_{\alpha=i}^{N} p_{\alpha,\alpha+1}^{\zeta} \right]\,, \tag{2.28}$$

where we made a distinction between p^ζ and $p^{\zeta'}$ since, after the scaling transformation $W_{(i)}$, the mass parameter m_i changes into m'_i, so the kinematic angle changes too.

Of course any transformation $W_{\zeta'\zeta}$ which changes a part of the mass parameters or all of them is a composition of the above transformations:

$$W_{\zeta'\zeta} = \prod_{i=1}^{A} W_{(i)}\,. \tag{2.29}$$

By means of the W matrices and the kinematic rotations we can now define the permutation matrices P_{ij}. We have:

$$\begin{aligned} P_{ij}\, \boldsymbol{\eta} &= W_{ij} \cdot p_{i,j} \cdot \boldsymbol{\eta}\left[(m_1, \mathbf{r}_1), \ldots, (m_i, \mathbf{r}_i), \ldots, (m_j, \mathbf{r}_j), \ldots\right] \\ &= W_{ij} \cdot \boldsymbol{\eta}\left[(m_1, \mathbf{r}_1), \ldots, (m_j, \mathbf{r}_j), \ldots, (m_i, \mathbf{r}_i), \ldots\right] \\ &= \boldsymbol{\eta}\left[(m_1, \mathbf{r}_1), \ldots, (m_i, \mathbf{r}_j), \ldots, (m_j, \mathbf{r}_i), \ldots\right]\,. \end{aligned} \tag{2.30}$$

2.2 The Hyperspherical System of Coordinates

The aim is now to show the structure of a generic hyperspherical set of coordinates and express the kinetic energy operator in terms of the hyperradius and of the hyperangles.

Different choices of hyperangular coordinate schemes are possible and the transformations to pass from one scheme to another are compositions of elementary transformations that involve only two adjacent hyperangles. Accordingly, the kinetic energy operator can be parametrized in different ways, however the angular and hyperangular dependence is always contained in a single operator called the grand angular momentum operator.

2.2.1 The Hyperangular Scheme

We start from the N vectors of the Jacobi set defined in eq. (2.1) leaving out the CM coordinate and express them in terms of N spherical sets of coordinates:

$$\boldsymbol{\eta}_i(\eta_i^x, \eta_i^y, \eta_i^z) \Rightarrow \boldsymbol{\eta}_i(\eta_i, \theta_i, \varphi_i), \quad i = 1, \ldots, N . \tag{2.31}$$

The N radial parameters η_i are then expressed in terms of an hyperspherical set composed by a radial coordinate ρ, the so called *hyperradius*, and $N-1$ hyperangles. The former is given by:

$$\rho^2 = \sum_{i=1}^{N} \eta_i^2 = \frac{1}{2mM_A} \sum_{i,j=1}^{A} m_i m_j r_{ij}^2 , \tag{2.32}$$

while the hyperangular set is defined as:

$$\sin\phi_i = \frac{\eta_i}{\sqrt{\eta_1^2 + \ldots + \eta_i^2}} \; ; \quad i = 2, \ldots, N . \tag{2.33}$$

The resulting parametrization of the N-dimensional radial set $\{\eta_1, \eta_2, \ldots, \eta_N\}$ is:

$$\eta_N = \rho \sin\phi_N ,$$
$$\eta_{N-1} = \rho \cos\phi_N \sin\phi_{N-1} ,$$
$$\vdots$$
$$\eta_i = \rho \cos\phi_N \ldots \cos\phi_{i+1} \sin\phi_i , \tag{2.34}$$
$$\vdots$$
$$\eta_2 = \rho \cos\phi_N \ldots \cos\phi_3 \sin\phi_2 ,$$
$$\eta_1 = \rho \cos\phi_N \ldots \cos\phi_3 \cos\phi_2 .$$

The angular plus hyperangular set is usually denoted in a compact form as:

$$\Omega_N = (\theta_1, \varphi_1, \ldots, \theta_N, \varphi_N; \phi_2, \ldots, \phi_N) . \tag{2.35}$$

The chosen hyperspherical parametrization of the N Jacobi vectors has then the following domain:

$$\boldsymbol{\eta}(\rho, \Omega_N) : \ \mathbb{R}_+ \times S_+^{N-1} \times (S^2)^N \longrightarrow \mathbb{R}^{3N} , \tag{2.36}$$

where S_+^{N-1} corresponds to the hyperangular part of the domain and it is the positive sector of the S^{N-1} hypersphere in $\mathbb{R}^N$ (each η_i is positive-definite). $(S^2)^N = S_{\eta_1}^2 \times S_{\eta_2}^2 \times \ldots \times S_{\eta_N}^2$ is the angular part, given by the cartesian product of the unit spheres defining the orientation of each $\boldsymbol{\eta}_i$ in $\mathbb{R}^3$. Of course $\mathbb{R}_+$ is the hyperradial domain. The range of each ϕ_i angle is:

$$0 \le \phi_i \le \frac{\pi}{2} \quad ; \ i = 2, \ldots, N , \tag{2.37}$$

while the spherical angles span the ordinary S^2 range:

$$\begin{aligned} & 0 \le \theta_i \le \pi ; \\ & 0 \le \varphi_i \le 2\pi \quad ; \ i = 2, \ldots, N . \end{aligned} \tag{2.38}$$

The total hyperspherical (and hyperradial) volume element is [15]:

$$\begin{aligned} dV_{\text{hh}} &= dV_\rho \, dV_{\Omega_N} \\ &= \rho^{3N-1} d\rho \, \sin\theta_1 d\theta_1 d\varphi_1 \prod_{i=2}^{N} \sin\theta_i d\theta_i d\varphi_i (\sin\phi_i)^2 (\cos\phi_i)^{3i-4} d\phi_i . \end{aligned} \tag{2.39}$$

As in the case of Jacobi coordinates, different sets of hyperspherical coordinates exist and they are usually represented by the so called *tree diagrams*, first introduced by N. Ya. Vilenkin et al. in ref. [50]. In fig. 2.2 the standard set of eq. (2.34) is schematized.

Each hyperangle ϕ_i is related to the i-th node: if the segment joining this node with the upper one extends to the right, a factor equal to $\sin\phi_i$ is associated, otherwise $\cos\phi_i$. Each η_i is obtained by the product of ρ with each sine or cosine factor associated to each node starting from the lowest vertex and following the track to the η_i termination.

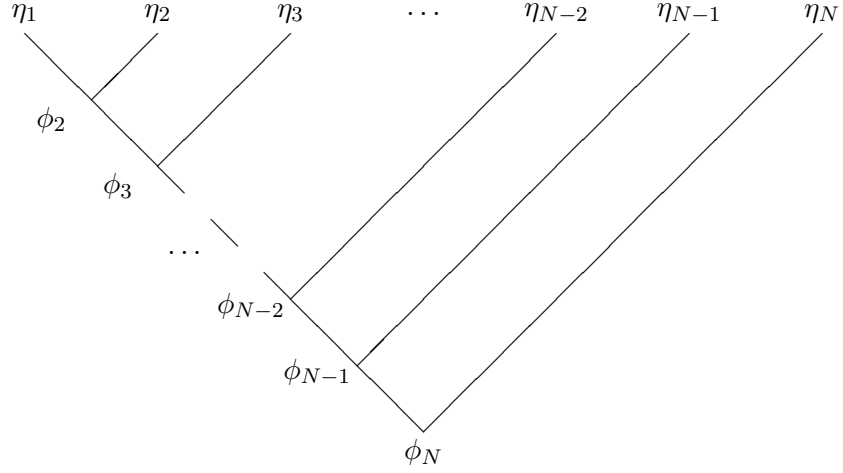In fig. 2.3 an alternative scheme of hyperspherical coordinates is shown.

FIGURE 2.2: Tree diagram representing the standard scheme of hyperangular coordinates. The explicit relations are shown in eq. (2.34).

The corresponding alternative parametrization:

$$\eta_N = \rho \sin \tilde{\phi}_N \sin \phi_{N,N-1} \, ,$$
$$\eta_{N-1} = \rho \sin \tilde{\phi}_N \cos \phi_{N,N-1} \, ,$$
$$\vdots \tag{2.40}$$
$$\eta_2 = \rho \cos \tilde{\phi}_N \cos \phi_{N-2}... \cos \phi_3 \sin \phi_2 \, ,$$
$$\eta_1 = \rho \cos \tilde{\phi}_N \cos \phi_{N-2}... \cos \phi_3 \cos \phi_2 \, .$$

2.2.2 The Kinetic Energy and the Grand Angular Momentum Operator

By excluding the CM term, the kinetic energy operator of eq. (2.10) expressed in terms of the N-spherical set of coordinates of eq. (2.31) is:

$$T_{\text{int}} = -\frac{\hbar^2}{2m} \sum_{i=1}^{N} \left(\frac{\partial^2}{\partial \eta_i^2} + \frac{2}{\eta_i} \frac{\partial}{\partial \eta_i} - \frac{\hat{l}_i^2}{\eta_i^2} \right) \tag{2.41}$$

where $\hat{l}_i$ is the angular momentum operator associated to the $\boldsymbol{\eta}_i$ coordinate. By parametrizing the η_i coordinates into the hyperspherical set of eq. (2.34) we obtain:

$$T_{\text{int}} = -\frac{\hbar^2}{2m} \left(\frac{\partial^2}{\partial \rho^2} + \frac{3N-1}{\rho} \frac{\partial}{\partial \rho} + \frac{\hat{K}_N^2(\Omega_N)}{\rho^2} \right) \, . \tag{2.42}$$

The operator $\hat{K}_N$ is the total *grand angular momentum*. For a generic n, with $2 \leq n \leq N$, the operator $\hat{K}_n^2$ is iteratively defined as [16]:

$$\hat{K}_n^2 = -\frac{\partial^2}{\partial\phi_n^2} + \frac{3n - 6 - (3n - 2)\cos(2\phi_n)}{\sin(2\phi_n)}\frac{\partial}{\partial\phi_n} + \frac{1}{\cos^2(\phi_n)}\hat{K}_{n-1}^2$$
$$+ \frac{1}{\sin^2(\phi_n)}\hat{l}_n^2 , \tag{2.43}$$

For $n = 1$ we have: $\hat{K}_1^2 = \hat{l}_1^2$.

In analogy to the two particles case, where the relative square angular momentum $\hat{l}^2$ is the projection of the laplacian on the angular domain S^2, the square grand angular momentum $\hat{K}_N^2$ can be interpreted as the kinetic operator (up to constants) defined on the N-body hyperangular and angular domain $S_+^{N-1} \times (S^2)^N$. By lowering the n index starting from N, the same analogy holds for $\hat{K}_n^2$, defined on the restricted $S_+^{n-1} \times (S^2)^n$ domain. Moreover the dependence of $\hat{K}_n^2$ on the $(S^2)^n$ domain is restricted to the $\hat{l}_n^2$ operators, in fact in the $n = 1$ case we recover the two particle domain, and we have the coincidence between $\hat{K}_1^2$ and $\hat{l}_1^2$.

We note that, with the chosen parametrization, there is no difference in the form of the kinetic energy operator in the different particles case with respect to the identical particles case.

The total angular momentum of the first n particle subsystem is defined as:

$$\hat{L}_n = \hat{L}_{n-1} + \hat{l}_n . \tag{2.44}$$

All the operators $\hat{K}_i^2$, $\hat{l}_j^2$, $\hat{L}_k^2$ and $\hat{L}_{t_z}^2$, with $i, j, k, t = 1, \ldots, N$, commute with each other and, as we see in the next section, form a complete set of operators defining the angular and hyperangular part of the states of an A-body system. The hyperspherical harmonics $\mathcal{Y}_{[K_n]}(\Omega_N)$ are the eigenfuntions of $\hat{K}_N^2$. We close this section by showing the grand angular momentum operator in the alternative hyperspherical scheme of eq. (2.40), where η_N and η_{N-1} are coupled by the relative $\phi_{N,N-1}$ hyperangle:

$$\hat{K}_N'^2 = -\frac{\partial^2}{\partial\tilde{\phi}_N^2} + \frac{3N - 9 - (3N - 5)\cos(2\tilde{\phi}_N)}{\sin(2\tilde{\phi}_N)}\frac{\partial}{\partial\tilde{\phi}_N}$$
$$+ \frac{1}{\cos^2(\tilde{\phi}_N)}\hat{K}_{N-2}^2 + \frac{1}{\sin^2(\tilde{\phi}_N)}\hat{K}_{N-1,N}^2 , \tag{2.45}$$

with the partial $\hat{K}_{N-1,N}^2$ defined as:

$$\hat{K}_{N-1,N}^2 = -\frac{\partial^2}{\partial\phi_{N-1,N}^2} - 4\cot(2\phi_{N-1,N})\frac{\partial}{\partial\phi_{N-1,N}}$$
$$+ \frac{1}{\cos^2(\phi_{N-1,N})}\hat{l}_{N-1}^2 + \frac{1}{\sin^2(\phi_{N-1,N})}\hat{l}_N^2 . \tag{2.46}$$
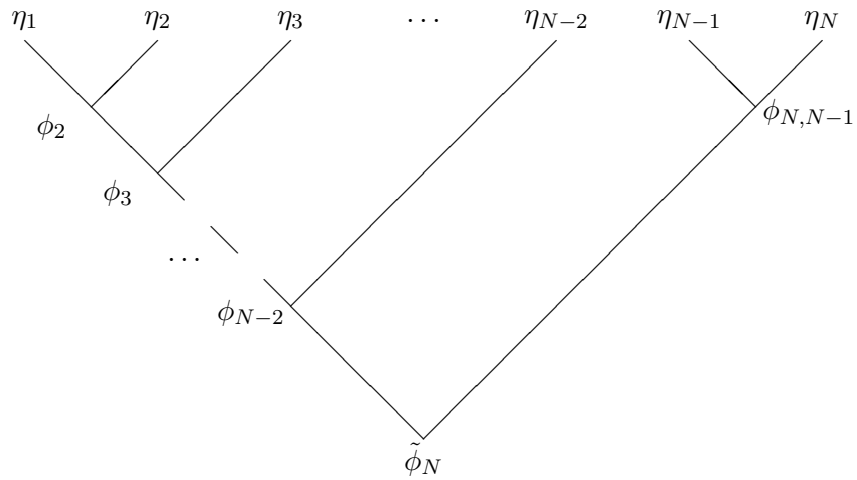
FIGURE 2.3: Tree diagram representing an alternative to the standard scheme of hyperangular coordinates. The explicit relations are shown in eq. (2.40).

In the section 2.3 we show how the HH functions change accordingly to the chosen hyperspherical scheme.

2.3 The Hyperspherical Harmonics Basis

The hyperspherical system of coordinates is directly related to the HH set of basis functions. Each tree diagram of the kind of fig. 2.2 and fig. 2.3 uniquely identifies the hyperspherical system and, consequently, the hyperangular coupling scheme of a given HH basis (the sequence of partial grand angular momentum quantum numbers K_i with $i = 1, \ldots, N$). This, combined with a given angular coupling scheme (the sequence of partial orbital angular momenta L_i), defines a complete basis of non-symmetrized hyperspherical harmonics defined on the angular and hyperangular domain.

We first derive the HH functions in the standard coupling scheme by following the iterative procedure shown in ref. [51] and first introduced in ref. [50] (we avoid technical details) and then we show their connection with the tree diagram of fig. 2.2. We also show an alternative HH set related to the tree of fig. 2.3. On this basis in chapter 2 we will show the transformations that allow to pass from one NSHH set to another and which constitute the core of the NSHH method.

We also define the hyperradial part of the A-body basis and the spin and isospin part, without assuming any particular feature on the particles composing the system.

2.3.1 The Hyperspherical Harmonics Functions

The $(n + 1)$-body hyperspherical harmonics functions are generated by the harmonic polynomials of the kind $h_{K_n}(\rho_n, \Omega_n) = \rho_n^{K_n} \mathcal{Y}_{[K_n]}$. The following

relation holds [52]:

$$\left[\Delta_{\rho_n} - \frac{\hat{K}_n}{\rho_n^2} \right] h_{K_n}(\rho_n, \Omega_n) = 0 \; . \tag{2.47}$$

By considering that:

$$\Delta_{\rho_n} h_{K_n}(\rho_n, \Omega_n) = K_n(K_n + 3n - 2) h_{K_n}(\rho_n, \Omega_n) \; , \tag{2.48}$$

from eq. (2.47) we can easily cancel the ρ_n dependence to obtain the eigenvalue equation for the $(n + 1)$-body HH functions:

$$\left[\hat{K}_n^2(\Omega_n) - K_n(K_n + 3n - 2) \right] \mathcal{Y}_{[K_n]}(\Omega_n) = 0 \; . \tag{2.49}$$

By exploiting the recursive structure of $\hat{K}_n^2(\Omega_n)$ in the index n, we introduce the explicit form of the standard A-body HH functions by adding one particle at a time, from the 3-body subset ($n = 2$) to the total A-body set ($n = N$). It is well known that the spherical harmonics functions, Y_l^m, constitute a good basis for the angular part of the relative motion of a two particle system, since they are the eigenfunctions of the angular momentum operator $\hat{l}_1$. The internal motion of a system of three particles is defined by six spatial coordinates, the 3-dimensional vectors $\boldsymbol{\eta}_1$ and $\boldsymbol{\eta}_2$ in the Jacobi set, or the four angular coordinates, $\hat{\boldsymbol{\eta}}_1 = (\theta_1, \varphi_1)$ and $\hat{\boldsymbol{\eta}}_2 = (\theta_2, \varphi_2)$, the hyperangle ϕ_2 and the 3-body hyperradius ρ_2. The kinetic operator in a partial 3-body hyperspherical set of coordinates looks:

$$\hat{T} \propto \left[\Delta_{\rho_2} + \frac{\hat{K}_2}{\rho_2^2} \right] + \Delta_{\eta_3} + \Delta_{\eta_4} + \dots \tag{2.50}$$

We now focus on the first term of the sum and look for the angular and hyperangular part of the 3-body eigenfunctions. The angular part is an eigenfunction of $\hat{l}_1$, the 2-body angular momentum, of $\hat{l}_2$, the relative angular momentum between the third particle and the CM of the preceding two and of $\hat{L}_2$ and $\hat{L}_{2_z}$, the total angular momentum and its projection. We have:

$$\Phi_{L_2 M_2}^{l_1 l_2}(\hat{\boldsymbol{\eta}}_1, \hat{\boldsymbol{\eta}}_2) = [Y_{l_1}(\hat{\boldsymbol{\eta}}_1) \otimes Y_{l_2}(\hat{\boldsymbol{\eta}}_2)]_{L_2 M_2} \; , \tag{2.51}$$

where the $[\dots \otimes \dots]_{LM}$ bracket is the usual two angular momenta coupling by means of the Clebsch-Gordan coefficients and M_2 is the $\hat{L}_{2_z}$ quantum number. By solving eq. (2.49) in ϕ_2 for $n = 2$ we obtain ${}^{(2)}\mathcal{P}_{K_2}^{l_2, l_1}(\phi_2)$, the hyperangular part of the wave function which, combined with the angular part, gives the 3-body hyperspherical harmonic function:

$$\mathcal{Y}_{[K_2]}(\Omega_2) = {}^{(2)}\mathcal{P}_{K_2}^{l_2, l_1}(\phi_2) \cdot \Phi_{L_2 M_2}^{l_1 l_2}(\hat{\boldsymbol{\eta}}_1, \hat{\boldsymbol{\eta}}_2) \; , \tag{2.52}$$

where we have introduced the 3-body hyperspherical polynomial [53]:

$$^{(2)}\mathcal{P}_{K_2}^{l_2,l_1}(\phi_2) = \mathcal{N}_2^{l_2+\frac{1}{2},l_1+\frac{1}{2}}(\sin\phi_2)^{l_2}(\cos\phi_2)^{l_1} P_{n_2}^{l_2+\frac{1}{2},l_1+\frac{1}{2}}(\cos 2\phi_2)\ . \quad (2.53)$$

The $\mathcal{N}$ factor is a normalization constant (we define it below for the general case) and $P_n^{a,b}$ denotes a Jacobi polynomial. The index n_2 is a positive integer which satisfies: $0 \leq n_2 = \frac{K_2-l_1-l_2}{2}$. The possible eigenvalues of $\hat{K}_2^2$ are $K_2(K_2+4)$ with:

$$0 \leq L_2 \leq l_1 + l_2 \leq K_2 < \infty\ . \quad (2.54)$$

In the tree formalism, the function $^{(2)}\mathcal{P}_{K_2}^{l_2,l_1}(\phi_2)$ is associated to the ϕ_2 node of the diagram in fig. 2.4.

With the addition of the 4-th particle, we transform the 3-body hyperspherical set combined with the spherical $(\eta_3, \theta_3, \varphi_3)$ set into the 4-body hyperspherical set. The Hamiltonian now looks:

$$\begin{aligned}
\hat{T} &\propto \left[\Delta_{\rho_3} + \frac{\hat{K}_3}{\rho_3^2}\right] + \Delta_{\eta_4} + \Delta_{\eta_5} + \dots \\
&= \left[\Delta_{\rho_3} + \frac{1}{\rho_3^2}\left(\Delta_{\phi_3} + \frac{\hat{K}_2}{\cos^2\phi_3} + \frac{\hat{l}_3^2}{\sin^2\phi_3}\right)\right] + \Delta_{\eta_4} + \dots\ ,
\end{aligned} \quad (2.55)$$

where Δ_{ϕ_3} is the sum of the first two terms of $\hat{K}_3^2$ [eq. (2.43)]. We first look for the 4-body angular part which, besides the 3-body set of angular operators $\hat{l}_1^2, \hat{l}_2^2, \hat{L}_2^2$, has to be eigenfunction of $\hat{l}_3^2, \hat{L}_3^2$ and $\hat{L}_{3_z}^2$. To this end we couple the angular eigenfuntion of $\hat{l}_3^2$ with the 3-body HH function:

$$\begin{aligned}
\Phi_{L_3 M_3}^{[K_2]l_3}(\hat{\boldsymbol{\eta}}_1, \hat{\boldsymbol{\eta}}_2, \hat{\boldsymbol{\eta}}_3, \phi_2) &= \left[\mathcal{Y}_{[K_2]}(\hat{\boldsymbol{\eta}}_1, \hat{\boldsymbol{\eta}}_2, \phi_2) \otimes Y_{l_3}(\hat{\boldsymbol{\eta}}_3)\right]_{L_3 M_3} \\
&= [Y_{l_1}(\hat{\boldsymbol{\eta}}_1) \otimes Y_{l_2}(\hat{\boldsymbol{\eta}}_2)|_{L_2} \otimes Y_{l_3}(\hat{\boldsymbol{\eta}}_3)]_{L_3 M_3}\ ^{(2)}\mathcal{P}_{K_2}^{l_2,l_1}(\phi_2)\ .
\end{aligned} \quad (2.56)$$

By solving eq. (2.49) in ϕ_3 we find the hyperspherical polynomial $^{(3)}\mathcal{P}_{K_3}^{l_3,K_2}$, associated to the ϕ_3 node in fig. 2.4. The 4-body HH function is then:

$$\mathcal{Y}_{[K_3]}(\Omega_3) = \ ^{(3)}\mathcal{P}_{K_3}^{l_3,K_2}(\phi_3) \cdot \Phi_{L_3 M_3}^{[K_2]l_3}(\hat{\boldsymbol{\eta}}_1, \hat{\boldsymbol{\eta}}_2, \hat{\boldsymbol{\eta}}_3, \phi_2)\ , \quad (2.57)$$

with $n_3 = \frac{K_3-K_2-l_3}{2}$. The eigenvalues are:

$$0 \leq K_2 + l_3 \leq K_3 < \infty\ . \quad (2.58)$$

To define the general recursive procedure we now calculate the A-body HH functions by assuming a well defined N-body HH set. The A-body hyperspherical parametrization leads to the kinetic operator in the form of eq. (2.42). By following the above procedure, we introduce the coupling

between the $\hat{l}_N$ eigenfuntion and the HH function of the preceding N particles:

$$\Phi_{L_N M_N}^{[K_{N-1}]l_N}(\Omega_{N-1}, \hat{\boldsymbol{\eta}}_N) = \left[\mathcal{Y}_{[K_{N-1}]}(\Omega_{N-1}) \otimes Y_{l_N}(\hat{\boldsymbol{\eta}}_N) \right]_{L_N M_N} . \qquad (2.59)$$

Eq. (2.49) for $n = N$ provides us the general form of the hyperspherical polynomial [15]:

$$^{(n)}\mathcal{P}_{K_n}^{l_n, K_{n-1}} = \mathcal{N}_{n_n}^{\alpha_{l_n}, \alpha_{K_n}} (\sin \phi_i)^{l_n} (\cos \phi_i)^{K_{n-1}} \cdot P_{n_n}^{\alpha_{l_n}, \alpha_{K_{n-1}}} (\cos 2\phi_n) , \qquad (2.60)$$

where we have introduced the α indices related to the structure of the hyperspherical tree diagram. In particular [50]:

$$\alpha_b = b + \mathcal{T}_b + \frac{1}{2}\mathcal{W}_b , \qquad (2.61)$$

where $\mathcal{T}_b$ is the number of nodes and $\mathcal{W}_b$ the number of terminations of the partial tree diagram generated by the b-th node of the hyperspherical tree diagram. In the standard HH set they become: $\alpha_{K_j} = K_j + 3j/2 - 1$ and $\alpha_{l_j} = l_j + 1/2$.

The A-body HH function in the standard hyperspherical set is then:

$$\mathcal{Y}_{[K_N]}(\Omega_N) = [Y_{l_1}(\hat{\boldsymbol{\eta}}_1) \otimes Y_{l_2}(\hat{\boldsymbol{\eta}}_2)|_{L_2} \otimes \ldots \otimes Y_{l_{N-1}}(\hat{\boldsymbol{\eta}}_{N-1}) \big|_{L_{N-1}}$$
$$\otimes Y_{l_N}(\hat{\boldsymbol{\eta}}_N)]_{L_N M_N} \left[\prod_{i=2}^{N} {}^{(i)}\mathcal{P}_{K_i}^{l_i, K_{i-1}}(\phi_i) \right] . \qquad (2.62)$$

The general definition of the normalization constant is:

$$\mathcal{N}_n^{ab} = \sqrt{\frac{2(2n + a + b + 1)n!\Gamma(n + a + b + 1)}{\Gamma(n + a + 1)\Gamma(n + b + 1)}} . \qquad (2.63)$$

The standard procedure just shown implies a sequential coupling of the angular momenta $\hat{l}_n$ analogue to the hyperangular one. However we stress that the angular coupling scheme does not necessarily have to reflect the hyperspherical scheme and it can be modifed at convenience.

As anticipated in the previous section, other hyperspherical tree diagrams exist besides the standard one. In fig. 2.3 one of the simplest alternative sets is shown and eq. (2.45), together with eq. (2.46), shows the corresponding form of the grand angular momentum. The HH construction procedure differs from the standard one by the last two iterations. One first solves eq. (2.49) with $\hat{K}_{N,N-1}$ instead of $\hat{K}_{N-1}$ and then proceeds by coupling the (N)-th hyperspherical polynomial, solution of eq. (2.49) with $\hat{K}_N'^2$ [eq. (2.45)]
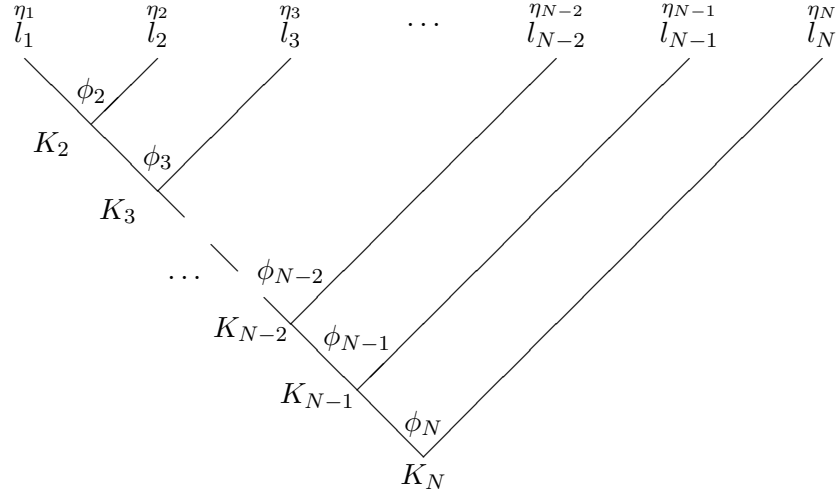
FIGURE 2.4: Tree diagram representing the standard scheme of non-symmetrized hyperspherical harmonic functions.

instead of $\hat{K}_N^2$. By choosing an analogue scheme of angular momenta coupling, the HH functions look:

$$\mathcal{Y}_{[K_N']}(\Omega_N) = [Y_{l_1}(\hat{\boldsymbol{\eta}}_1) \otimes Y_{l_2}(\hat{\boldsymbol{\eta}}_2)]|_{L_2} \otimes \ldots |_{L_{N-2}} \otimes [Y_{l_{N-1}}(\hat{\boldsymbol{\eta}}_{N-1})$$

$$\otimes Y_{l_N}(\hat{\boldsymbol{\eta}}_N)]_{L_{N,N-1}}]_{L_N M_N} \left[\prod_{i=2}^{N-2} {}^{(i)}\mathcal{P}_{l_i, K_{i-1}}(\phi_i) \right] \cdot \qquad (2.64)$$

$$\cdot \, {}^{(N-1)}\mathcal{P}_{l_i, K_{N,N-1}}(\phi_{N,N-1}) \, {}^{(N)}\mathcal{P}_{l_i, K_N}(\phi_N') \, .$$

In the next chapter we show the transformation that allow to pass from the HH set of the above equation to the set of eq. (2.62) as a starting point to define the transformations between any pair of HH sets of functions.

2.3.2   The complete A-body basis

The complete basis, besides the HH part, consists of the hyperradial part and of the spin and isospin bases:

$$|\Phi_i\rangle = \left|\mathcal{R}_{r_i}\mathcal{Y}_{[K_N]_i}\right\rangle \otimes \left|\chi_{[S_A]_i}\chi_{[T_A]_i}\right\rangle \, , \qquad (2.65)$$

where $\mathcal{R}_{r_i}$ are the hyperradial functions, $\chi_{[S_A]_i}$ and $\chi_{[T_A]_i}$ are the spin and isospin states.

The hyperradial part is based on a set of generalized Laguerre polynomials $L_n^\nu(\rho/\beta)$:

$$\mathcal{L}_n(\rho) = \sqrt{\frac{n!}{(n+\nu)!}} L_n^\nu(\rho/\beta) e^{-\frac{\rho}{2\beta}} \left(\frac{\rho}{\beta}\right)^{\frac{\nu-3A+4}{2}} \, , \qquad (2.66)$$

where β is a variational parameter with dimension of an inverse of a length and it has been studied in order to analyze the convergence of bound state

calculations in the maximum number of Laguerre polynomials (n_{max}). For most of our calculations we found that $n_{max} \approx 20$ with $\beta \approx 0.3$ is sufficient to entirely shift the dependence of the various convergence patterns into the HH part of the basis.

By using the properites of the Laguerre polynomials [54] we can calculate the analytical form of the matrix elements of the hyperradial part of the kinetic energy in eq. (2.42). The overlap of any power of ρ is obtained by:

$$
\begin{aligned}
R_{n,n'}^{\nu;a} &= \langle \mathcal{L}_n(\rho)| \rho^a |\mathcal{L}_{n'}(\rho)\rangle \\
&= \sqrt{\frac{n!n'!}{(n+\nu)!(n'+\nu)!}} \int_0^\infty e^{-\rho} \rho^\nu L_n^\nu(\rho) L_{n'}^\nu(\rho) \rho^a d\rho \\
&= \sqrt{\frac{n!(n+\nu)!}{n'!(n'+\nu)!}} \sum_{m=0}^n (-1)^m \frac{(\nu+p+m)!(-p-m)_{n'}}{(n-m)!(\nu+m)!m!} \ .
\end{aligned}
\tag{2.67}
$$

The radial part of the kinetic energy [51]:

$$
\begin{aligned}
\langle \mathcal{L}_n(\rho)| \Delta_\rho |\mathcal{L}_{n'}(\rho)\rangle &= \frac{1}{4}\delta_{n,n'} - \frac{3N-1+2n'}{2} R_{n,n'}^{\nu;-1} + (3N-\nu-2)\cdot \\
&\cdot \left[n' R_{n,n'}^{\nu;-2} - \sqrt{n'(n'+\nu)} R_{n,n'-1}^{\nu;-1} \right] \ .
\end{aligned}
\tag{2.68}
$$

The natural choice for the ν index is $\nu = 3N - 1$, since we recover the volume element dV_ρ defined in eq. (2.39), however, by choosing $\nu = 3N - 2$, the above matrix elements reduce to a simpler form.

The spin and the isospin basis are both defined on a reversed sequential coupling. By denoting as s_i and t_i, respectively, the spin and the isospin quantum numbers of the i-th particle, each spin and isospin state is identified by the following set:

$$
\begin{aligned}
[S_A] &= \{s_A, s_{A-1}, \dots, s_1; S_2, \dots, S_{A-1}, S_A; \} \\
[T_A] &= \{t_A, t_{A-1}, \dots, t_1; T_2, \dots, T_{A-1}, T_A; T_{A_z}\} \ ,
\end{aligned}
\tag{2.69}
$$

where the S_i number is the total spin quantum number of the system composed by particles from A to $A - i + 1$. The same notation holds for the isospin part. T_{A_z} is the projection on the z axis of the total isospin T_A. In fig. 2.5 the isospin coupling scheme is represented in the tree diagram form. Depending on the centrality of the interaction between particles, the orbital angular momentum L_N and the total spin S_N can or cannot be good quantum numbers for the eigenstates of $\hat{H}$. In the central case, L_N and S_N are conserved:

$$
[K_N; S_N]_c = [K_N] \otimes [S_A] \ ,
\tag{2.70}
$$

while in the non-central case, L_N and S_N are no longer good quantum numbers and only the total angular momentum J, toghether with T_A and T_{A_z}
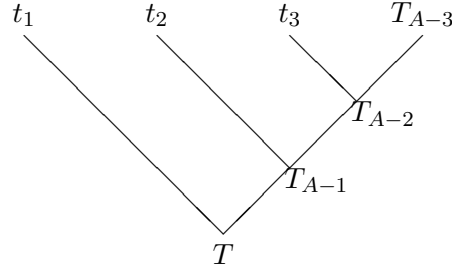
FIGURE 2.5: Tree diagram representing the sequential reversed-order A-body isospin coupling.
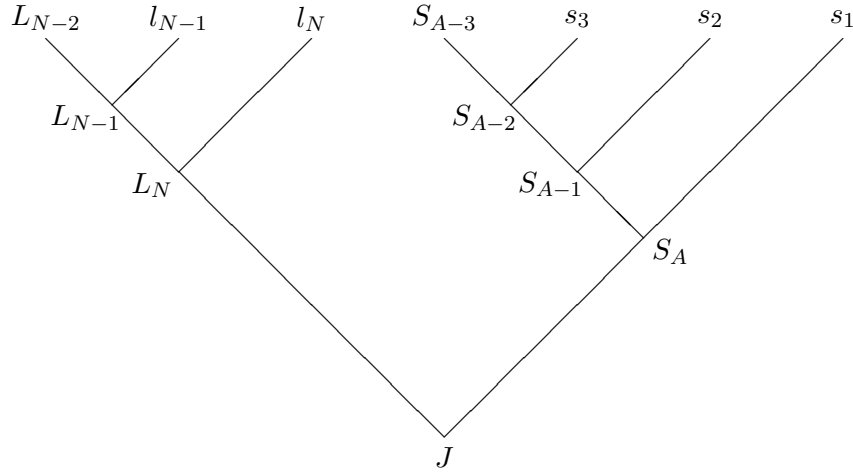

FIGURE 2.6: Tree diagram representing the coupling scheme between the orbital angular momentum L_N and the total spin S_A in a A-body non-central basis.

define the angular plus spin/isopin part of the wave function:

$$[K_N; S_N]_{\mathrm{nc}} = [[K_N]; [S_{A-2}]; [[L_{N-1}, l_N]_{L_N}; [S_{A-1}, s_A]_{S_A}]_J] \ , \qquad (2.71)$$

and this obviously leads to a larger basis. In fig. 2.6 the angular and spin coupling scheme in case of a non-central basis is shown in the tree notation.

Although the choice in the sequence of the spin and isospin coupling is arbitrary, some combinations might be more advantageus, depending on the physical system considered. For example, a 2-body interaction depends on the total spin of the couple of interacting particles and its extrapolation from the general A-body coupling scheme might result simpler depending on the chosen order of the single particle spins. The same consideration holds for the isospin part. In the next chapter we will show some simple tricks in order to reduce the computational weight in the calculation of the potential matrix elements.

2.3.3   The Symmetrized and the Non-Symmetrized HH Basis

The HH functions do not possess any particular symmetry under particle permutations. If for the 3- and 4-body case a direct symmetrization is still feasible, for systems with $A \geq 5$ it is not practicable and a more sophisticated procedure becomes necessary. One approach to the HH symmetrization consists in a recursive construction of HH functions by realizing irreducible representations not only of the orthogonal group $O(3N)$ but also of the group $O(N)$, accordingly to the chain $O(3N) \supset O(3) \otimes O(N)$:

$$
\begin{array}{ccccccccc}
O(3N-3) & \supset & O(3) & \otimes & O(N-1) & \supset & O(N-2) & \ldots & \supset & O(2) \\
& & & & \cup & & \cup & & & \cup \\
& & & & S_N & \supset & S_{N-1} & \ldots & \supset & S_3 & \supset & S_2
\end{array}
$$
$$(2.72)$$

Such approach has been developed through an efficient technique by N. Barnea about 20 years ago [51] and it led to the first 5-body calculation by means of the HH method. 6-body calculations have also been performed, but limited to central potentials [55].

An alternative HH approach to the few-body problem has been developed a few years ago by M. Gattobigio et al. in ref. [15] and it is based on the use of the Hyperspherical Harmonics basis without previous symmetrization. As it will be shown in the next chapter, the eigenvectors of the A-body Hamiltonian possess well defined symmetry under particle permutations, and this symmetry can be identified by means of the application of the Casimir operator of the group of permutations of A objects, $C(A)$. When the spatial part of the eigenstates is found and its symmetry determined, the spin and isospin parts are combined in order to obtain the desired total permutational symmetry.

A variation on the non-symmetrized HH (NSHH) approach has been later introduced by N. Barnea et al. [16] and it is based on the definition of a pseudo-Hamiltonian as a suitable combination of the A-body Hamiltonian and the $C(A)$ operator. The lowest eigenvectors of such operator possess the desired permutational symmetry and they can be calculated by means of fast diagonalization procedures (e.g. the Lanczos method). This last approach is the one adopted by the present work and it will be shown in detail in the next chapter. Here we just stress that the avoidance of the symmetrization procedure, however, is partly counterweighted by the larger dimension of the basis, which is not anymore constrained by the permutational symmetry.

In table 2.1 the dimension of the HH basis combined with the spin and isospin part is shown for $A = 4, 6$ systems and for different cuts in the total K_N quantum number (the hyperradial basis has not been considered).

TABLE 2.1: The number of HH plus spin and isospin states for systems with $A = 4, 6$.

$K_{\mathbf{max}}$	$^4\mathbf{He}$		$^6\mathbf{Li}$	
	c.	n.c.	c.	n.c.
2	24	54	675	2750
4	84	264	5400	40025
6	224	852	30600	315675
8	504	2172	137025	1728950
10	1008	4746	514215	7392960
12	1848	9269	1678950	26377350
14	3168	16776	-	-
16	5148	28404	-	-
18	8008	45694	-	-
20	12012	79488	-	-
22	17472	104988	-	-
24	24752	151788	-	-

Chapter 3

The Non-Symmetrized Hyperspherical Harmonics Method

In this chapter we expose the NSHH formalism generalized in order to treat systems composed by different species of particles. We start from the method developed by M. Gattobigio et al. in ref. [15] and later extended by N. Barnea et al. in ref. [16] and we add the basic extensions due to the presence of different particles and interactions.

The method is based on the employment of the NSHH basis introduced in the previous chapter, so it avoids the explicit symmetrization procedure and it provides an alternative way to select the physical states with the desired permutational symmetry. This is done by using one specific property of the transposition class sum operator $\hat{C}(n)$ of the permutation group S_n of n objects. In fact, in a quantum system that contains a subset of n_j identical particles, if the operator $\hat{C}(n_j)$ commutes with the Hamiltonian H, its largest and smallest eigenvalues correspond to the eigenfunctions of H symmetric and antisymmetric with respect to that subset. We show that by considering a pseudo-Hamiltonian defined as: $\tilde{H} = H + \sum_{i=1}^{N_s} \gamma_i \, \hat{C}(n_i)$, where N_s is the number of species of particles in our A-body system, and by setting properly the γ_i parameters, we obtain that the ground state (g.s.) of H coincides with the g.s. of $\tilde{H}$. The real energy E_0 is obtained by simply subtracting the sum of the eigenvalues of each Casimir operator $\hat{C}(n_i)$ multiplied by γ_i from the g.s. energy $\tilde{E}_0$ of $\tilde{H}$. In this way we do not need the exact diagonalization of $\tilde{H}$, but we can use much faster procedures to solve the eigenvalue problem only for the lowest values (e.g. the Lanczos algorithm).

An effective 2-body interaction procedure based on Lee-Suzuki theory [56] is also added and applied to multiple interactions in order to consider a

wide range of potentials which cannot be treated properly with a bare interaction approach.

The considerably larger size of the NSHH basis with respect to the symmetrized HH basis is compensated by the avoidance of the symmetrization procedure which is the main surce of computational effort in the standard HH method. By implementing a suitable parallelization procedure and by exploiting the power of the present super-computers, the NSHH method might result advantageus with respect to the symmetrized version [16]. Moreover its extra flexibility allows to pass from one physical model to another without spending anaytical and computational effort by applying every time a different symmetrization procedure.

In section 3.1 we define the permutation operators and in section 3.2 we show how to calculate the 2-body potential matrix elements. In section 3.3 we implement the Casimir operator in the pseudo-Hamiltonian $\tilde{H}$ in order to calculate the ground state of our A-body system. Finally, in section 3.4, we describe the incorporation of the Lee-Suzuki (L-S) effective interaction procedure, also in presence of different particles.

As interaction models we assume generic 2-body forces, which can be central or non-central, but we do not assume any other specific feature. In the next chapter we will introduce some specific extensions of the method in order to treat more sophisticated interactions.

3.1   Permutations in the NSHH Basis

In a system of A particles interacting through a 2-body force the Hamiltonian is given by the sum of the kinetic energy operator T with all the V_{ij} potential terms, where the (i, j) pair of indices runs over all the possible couples of particles composing the system:

$$
\begin{aligned}
\hat{H} &= \hat{T} + \sum_{i<j=2}^{A} \hat{V}_{ij}(\mathbf{r}_{ij}, \hat{S}_{ij}, \hat{T}_{ij}) \\
&= \hat{T} + \sum_{i<j=2}^{A} \hat{V}_{ij}(r_{ij}, \hat{l}_{ij}, \hat{S}_{ij}, \hat{T}_{ij}) \,,
\end{aligned}
\tag{3.1}
$$

where r_{ij} is the relative distance between particles i and j, $\hat{l}_{ij}$ is the relative angular momentum operator of the (i, j) couple and S_{ij} and T_{ij} are the total 2-body spin and isospin operators.

The only term of the potential involving a 2-dimensional integration in the calculation of its matrix elements is V_{12}. In fact the Jacobi vector $\boldsymbol{\eta}_N$, in the

standard set of eq. (2.1), is the only one proportional to the relative coordinate connecting two particles of the system, namely particle 1 and 2:

$$\mathbf{r}_{12} = \mathbf{r}_2 - \mathbf{r}_1 = \sqrt{\frac{m(m_1 + m_2)}{m_1 m_2}} \boldsymbol{\eta}_N \ . \tag{3.2}$$

In the standard hyperspherical set of eq. (2.34), the distance r_{12} is defined by only one hyperangle, ϕ_N, besides the hyperradius ρ:

$$r_{12} = \sqrt{\frac{m(m_1 + m_2)}{m_1 m_2}} \rho \sin \phi_N \ . \tag{3.3}$$

All the other V_{ij} terms, in general, imply multidimensional integrations in order to be evaluated since for any couple (i, j) different from $(1, 2)$ the relative vector $\mathbf{r}_{ij}$ is a combination of different Jacobi vectors and r_{ij} depends on more hyperangles. As a consequence, brute force calculations of the potential matrix elements become almost prohibitive already in the $A = 4$ case.

Moreover the 2-body spin and isospin quantum numbers related to the (i, j) couple, S_{ij} and T_{ij}, are not good quantum numbers in the standard coupling scheme of eq. (2.69), with the only exception of $S_{A,A-1} = S_2$.

To overcome these obstacles we define the operators $\mathcal{Q}_{12}^{ij}$, representing the composition of kinematic rotations, spin and isospin recouplings necessary in order to transform the starting scheme of Jacobi coordinates combined with the spin and isospin coupling schemes into another set where the coordinate $\boldsymbol{\eta}_N$ and the angular momentum number l_N, initially related to the couple of particles $(1, 2)$, refer to the (i, j) couple, and where S_{ij} and T_{ij} are good quantum numbers. If we denote as $V_{ij}^{[S_N][T_N]}[\mathbf{r}_{ij}(\boldsymbol{\eta}^{ab})]$ the 2-body potential operator between particles i and j and defined in a NSHH basis where the adopted Jacobi set of coordinates is $\boldsymbol{\eta}^{ab}$, we have:

$$\begin{aligned} V_{ij}^{[S_N][T_N]}[\mathbf{r}_{ij}(\boldsymbol{\eta}^{12})] &= V_{ij}'^{[S_N][T_N]}[\boldsymbol{\eta}^{12}] \\ &= V_{ij}'^{[S_N][T_N]}[p_{ij}^{12} \cdot \boldsymbol{\eta}^{ij}] \\ &= \mathcal{Q}_{ij}^{12} \cdot V_{ij}''^{[S_N]^{ij}[T_N]^{ij}}[\boldsymbol{\eta}_N^{ij}] \cdot \mathcal{Q}_{12}^{ij} \ , \end{aligned} \tag{3.4}$$

where $\boldsymbol{\eta}^{12}$ represents the Jacobi set in the standard order of coupling, as in eq. (2.1), while $\boldsymbol{\eta}^{ij}$ is the Jacobi set where the mass-position pairs $(m_1, \mathbf{r}_1)$

and $(m_2, \mathbf{r}_2)$ are replaced by $(m_i, \mathbf{r}_i)$ and $(m_j, \mathbf{r}_j)$ respectively:

$$\boldsymbol{\eta}_N^{ij} = \sqrt{\frac{m_i m_j}{m(m_i + m_j)}} (\mathbf{r}_j - \mathbf{r}_i) ;$$

$$\boldsymbol{\eta}_{N-1}^{ij} = \sqrt{\frac{m_3(m_i + m_j)}{m(m_i + m_j + m_3)}} \left(\mathbf{r}_3 - \frac{m_i \mathbf{r}_i + m_j \mathbf{r}_j}{m_i + m_j} \right) . \tag{3.5}$$

$$\vdots$$

The coordinate transformation p_{ij}^{12} is the composition of kinematic rotations of the kind of eq. (2.12) in order to pass from the $\boldsymbol{\eta}^{12}$ set to $\boldsymbol{\eta}^{ij}$. $[S_N]^{ij}$ and $[T_N]^{ij}$ denote a spin and an isospin basis where S_{ij} and T_{ij} are good quantum numbers.

The $\mathcal{Q}_{ab}^{ij}$ operators represent the combination of the coordinate transformations and spin and isospin recouplings needed in order to move particles i ans j in the a-th and b-th position of the spatial coupling scheme and to recouple the single particle spins and isospins in order to obtain the total 2-body spin and isospin S_{ij} and T_{ij}. They are given by the Kronecker products of the spatial, the spin and the isospin part:

$$\mathcal{Q}_{ab}^{ij} = \mathcal{P}_{ab}^{ij} \otimes \mathcal{S}_{ab}^{ij} \otimes \mathcal{I}_{ab}^{ij} . \tag{3.6}$$

In the following two subsections we define the $\mathcal{P}$, $\mathcal{S}$ and $\mathcal{I}$ operators. On this basis, besides the 2-body potential terms, in section (3.3), we are also able to define the explicit form of the Casimir operator $\hat{C}(n)$ of the permutation group S_n.

3.1.1 The HH Coupling Permutations

The operators $\mathcal{P}_{ab}^{ij}$ of eq. (3.6), in general, do not have a definite block-diagonal structure and their numerical evaluation could be demanding. However, due to the properties of the HH functions, the transformations related to any coupling permutation between two adjacent particles, j and $j+1$, couple only the $[K]^{(j)}$ subset of quantum numbers in the NSHH basis, with:

$$[K]^{(j)} = \{ K_i, l_i, l_{i-1}, L_i \} ; \qquad i = A - j . \tag{3.7}$$

Then the representation matrices $\mathcal{P}^{(j)}$ of the kinematic rotations $p_{j,j+1}$ in the NSHH basis do have a block structure and they can be calculated with resonable computational effort.

Eq. (2.18) proves the invariance of the hyperradius ρ with respect to kinematic rotations. However, the angular and hyperangular set Ω_N, in general, is not invariant and we have:

$$p_{j,j+1} \cdot \boldsymbol{\eta}(\rho, \Omega_N) = \boldsymbol{\eta}^{(j)}(\rho, \Omega_N^{(j)}) , \tag{3.8}$$

where $\Omega_N^{(j)}$ is the angular plus hyperangular set defined over the transformed Jacobi basis: $\boldsymbol{\eta}^{(j)} = \{\boldsymbol{\eta}_i^{(j)} = p_{j,j+1} \cdot \boldsymbol{\eta}_i ; \; i = 1, \ldots, N\}$.

Since the HH functions constitute a complete set for the angular and hyperangular part of the Hilbert space we can expand the HH functions that belong to one set into HH functions of another set:

$$\mathcal{Y}_{[K_N]}(\Omega_N) = \sum_{[K_N']} \mathcal{P}_{[K_N][K_N']}^{(j)} \mathcal{Y}_{[K_N']}(\Omega_N^{(j)}) \, . \tag{3.9}$$

The aim is to calculate the matrix elements:

$$\mathcal{P}_{[K_N][K_N']}^{(j)} = \int \mathcal{Y}_{[K_N]}^*(\Omega_N) \mathcal{Y}_{[K_N']}(\Omega_N^{(j)}) \, d\Omega_N \, . \tag{3.10}$$

The operator $\mathcal{P}^{(j)}$ is unitary and represents the kinematic rotation between the two mass-position pairs $(m_j, \mathbf{r}_j)$ and $(m_{j+1}, \mathbf{r}_{j+1})$ in the HH basis. Since it is a coupling permutation, it satisfies the permutational properties:

$$\left(\mathcal{P}^{(j)}\right)^2 = \mathbb{I} \; ; \qquad \mathcal{P}^{a,b} = \prod_{s=a}^{b-1} \mathcal{P}^{(s)} \prod_{s=b-2}^{a} \mathcal{P}^{(s)} \, , \, a < b \, , \tag{3.11}$$

where $\mathcal{P}^{a,b}$ is the coupling permutation between the a-th and the b-th mass-position pairs. We denote the double permutation $\mathcal{P}_{ab}^{ij}$ as:

$$\mathcal{P}_{ab}^{ij} = \mathcal{P}^{ia} \mathcal{P}^{jb} \, . \tag{3.12}$$

Any set of HH basis functions defined on a given coupling sequence in the Jacobi set can be expressed in terms of another set of HH functions defined on an arbitrarily permuted scheme. We have:

$$\mathcal{Y}_{[K]}^{LM}(\Omega_N) = \sum_{[K_N']} \mathcal{P}_{[K_N][K_N']}^{p} \mathcal{Y}_{[K_N']}^{LM}(\Omega_N^p) \, , \tag{3.13}$$

where the label p denotes a generic coupling permutation in the standard scheme of Jacobi coordinates. The total grand angular momentum K_N, the total angular momentum L and its projection M are always conserved by such transformations.

The elementary $\mathcal{P}^{(j)}$ transformations are compositions of three different kinds of transformation related, respectively, to:

1. angular recoupling;

2. hyperangular recoupling;

3. coupling permutation between $(m_j, \mathbf{r}_j)$ and $(m_{j+1}, \mathbf{r}_{j+1})$.
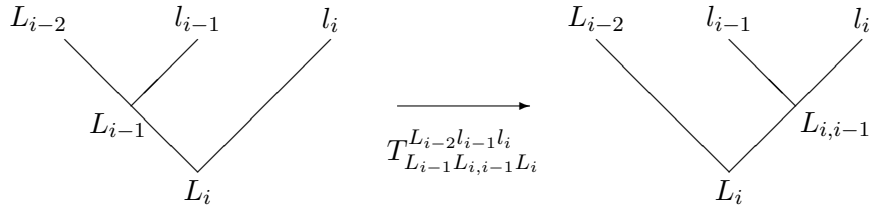
FIGURE 3.1: Recoupling scheme of the three angular momenta L_{i-2}, l_{i-1} and l_i by means of the T-coefficients defined in eq. (3.15).

Angular recoupling.   As anticipated in chapter 1, the choice of the angular coupling in the HH construction procedure is essentially arbitrary, although it is usually chosen to reflect the structure of the hyperspherical tree diagram, as in our case. By adopting the notation of ref. [15], we introduce the T-coefficients that relate two different coupling schemes of the $\{L_{i-2}, l_{i-1}, l_i\}$ triplet of angular momentum quantum numbers, as shown in fig. 3.1:

$$[[Y_{L_{i-2}}(\hat{\boldsymbol{\eta}}_{i-2}) \otimes Y_{l_{i-1}}(\hat{\boldsymbol{\eta}}_{i-1})]_{L_{i-1}} \otimes Y_{l_i}(\hat{\boldsymbol{\eta}}_i)]_{L_i} =$$
$$\sum_{L_{i,i-1}} T^{L_{i-2}l_{i-1}l_i}_{L_{i-1}L_{i,i-1}L_i}[Y_{L_{i-2}}(\hat{\boldsymbol{\eta}}_{i-2}) \otimes [Y_{l_{i-1}}(\hat{\boldsymbol{\eta}}_{i-1}) \otimes Y_{l_i}(\hat{\boldsymbol{\eta}}_i)]_{L_{i,i-1}}]_{L_i} \,,$$

$$(3.14)$$

where $i = A - j$ (we follow the reversed order convention). Explicitly:

$$T^{L_{i-2}l_{i-1}l_i}_{L_{i-1}L_{i,i-1}L_i} = (-1)^{L_{i-2}+l_{i-1}+l_i+L_i}\sqrt{2L_{i-1}+1}\cdot$$
$$\sqrt{2L_{i,i-1}+1} \left\{ \begin{array}{ccc} L_{i-2} & l_{i-1} & l_i \\ l_i & L_i & L_{i,i-1} \end{array} \right\} . \qquad (3.15)$$

The above transformation allows to extract the relative coupling between the l_{i-1} and l_i quantum numbers, $L_{i,i-1}$, from the standard sequential coupling of eq. (2.62). In case of $i = N$ eq. (3.14) reflects the angular coupling scheme of eq. (2.64).

Hyperangular recoupling.   In chapter 1 two different tree diagrams are shown, namely fig. 2.2 and fig. 2.3, representing two hyperspherical coupling schemes. They both define two alternative sets of HH functions built over the hyperspherical scheme of eq. (2.34) and (2.40) respectively. We now consider these two schemes, but in the generic case where $\boldsymbol{\eta}_i$ and $\boldsymbol{\eta}_{i+1}$ are recoupled together (and so l_i and l_{i+1}) instead of $\boldsymbol{\eta}_{N-1}$ and $\boldsymbol{\eta}_N$, and the relative hyperangle is $\phi_{i,i-1}$, as shown in fig. 3.2. The transformation connecting one set ($\mathcal{Y}_{[K_N]}$) to the other ($\mathcal{Y}^t_{[K_N]}$) is defined by the so called *Tree*
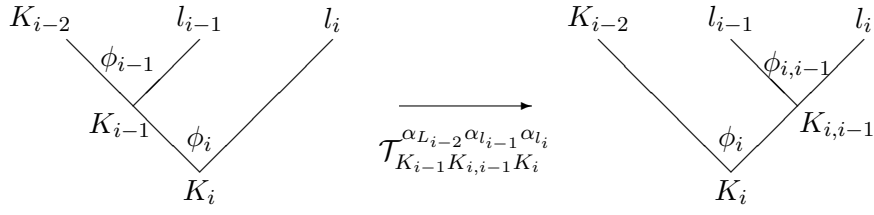
FIGURE 3.2: Hyperangular recoupling scheme of K_{i-2}, l_{i-1} and l_i by means of the $\mathcal{T}$-coefficients defined in eq. (3.16).

coefficients:

$$\left\langle \mathcal{Y}_{[K_N]} \middle| \mathcal{Y}_{[K'_N]}^t \right\rangle = \mathcal{T}_{K_{i-1}K_{i,i-1}K_i}^{\alpha_{K_{i-2}}\alpha_{l_{i-1}}\alpha_{l_i}} \cdot \delta_{[K_N]\backslash K_{i-1},[K'_N]\backslash K_{i,i-1}} , \qquad (3.16)$$

where the α indices are defined in eq. (2.61) and $\mathcal{Y}_{[K'_N]}^t = \mathcal{Y}_{[K'_N]}(\Omega'_N)$, with:

$$
\begin{aligned}
[K'_N] &= \{K_N, \dots, K_i, K_{i,i-1}, K_{i-2}, \dots, K_2; L_2, \dots; l_1, l_2, \dots\} ; \\
\Omega'_N &= \{\phi_2, \dots, \phi_{i-2}, \phi_{i,i-1}, \phi_i, \dots, \phi_N; \hat{\boldsymbol{\eta}}_1, \hat{\boldsymbol{\eta}}_2, \dots\} .
\end{aligned}
\qquad (3.17)
$$

The $\mathcal{T}$ coefficients are the analogue of the T coefficients defined in eq. (3.15), but for the grand angular momentum quantum numbers. In ref. [57] their explicit form is provided.

Kinematic Rotations. The matrix elements related to the kinematic rotations between two adjacent particles ($p_{i,i+1}$) in a 3-body HH basis are the Raynal-Revai (RR) coefficients. They are closely related to the Talmi-Moshinski transformations for two particles in an oscillator well and their analytical derivation follows this analogy, as shown in ref. [58].

However, they can also be used to define a kinematic rotation in a generic A-body HH basis with a partial 3-body coupling scheme for both angular momentum and grand angular momentum quantum numbers denoted as:

$$
\begin{aligned}
[K_N]_{(i)} = \{l_1, \dots, l_N; &L_2, \dots, L_{i-2}, L_{i,i-1}, L_i, \dots, L_N; \\
&K_2, \dots, K_{i-2}, K_{i,i-1}, K_i, \dots, K_N\} ,
\end{aligned}
\qquad (3.18)
$$

which can be always obtained by means of the T and the $\mathcal{T}$ coefficients described above, as shown in fig. 3.1 and fig. 3.2. As diagrammatically shown in fig. 3.3, we have:

$$\mathcal{Y}_{[K_N]_{(i)}}(\Omega_N) = \sum_{l'_{i-1}l'_i} \mathcal{R}_{l_{i-1}l_il'_{i-1}l'_i}^{L_{i,i-1}K_i}(\beta_j) \cdot \mathcal{Y}_{[K'_N]_{(i)}}(\Omega_N^{j,j+1}) . \qquad (3.19)$$
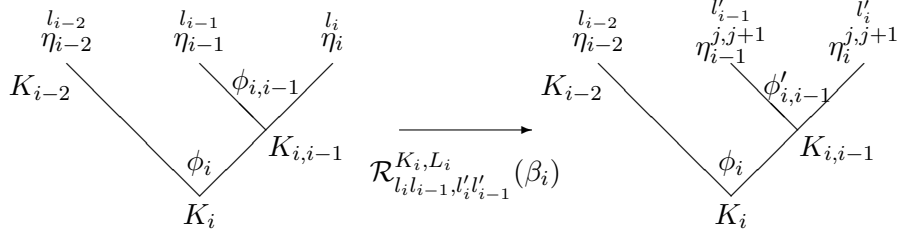
FIGURE 3.3: Transformation of the 3-body HH subset by
means of a kinematic rotation between particles j and $j+1$.
The RR coefficents define such transformation.

The set $[K'_N]_{(i)}$ differs from $[K_N]_{(i)}$ by the l_{i-1} and l_i quantum numbers, since a kinematic rotation acts on the $\boldsymbol{\eta}_{i-1}$ and $\boldsymbol{\eta}_i$ Jacobi vectors, and β_j is the kinematic angle defined in eq. (2.14) which contains the dependence on the first $j+1$ masses of the system. The RR coefficients are defined as:

$$
\mathcal{R}^{K_{i,i-1},L_{i,i-1}}_{l_{i-1}l_i,l'_{i-1}l'_i}(\beta_j) = \int (\cos\phi_{i,i-1}\sin\phi_{i,i-1})^2 d\phi_{i,i-1}\ {}^2\mathcal{P}^{l_i,l_{i-1}}_K(\phi_{i,i-1}) \int d\hat{\boldsymbol{\eta}}_{i-1} d\hat{\boldsymbol{\eta}}_i
$$

$$
\cdot\, [Y_{l_{i-1}}(\hat{\boldsymbol{\eta}}_{i-1}) \otimes Y_{l_i}(\hat{\boldsymbol{\eta}}_i)]^*_{LM}\ {}^2\mathcal{P}^{l'_i,l'_{i-1}}_K[\phi'_{i,i-1}(\phi_{i,i-1},\beta_j)]\cdot
$$

$$
\cdot\, [Y_{l'_{i-1}}(\hat{\boldsymbol{\eta}}^{(j)}_{i-1}) \otimes Y_{l'_i}(\hat{\boldsymbol{\eta}}^{(j)}_i)]_{LM}\ .
$$

$$(3.20)$$

Their analytical form is provided in ref. [58].

By combining the above three kinds of transformations we can calculate explicitly the matrix elements of eq. (3.10) that belong to $\mathcal{P}^{(i)}$ in the standard HH basis.

Of course if the coordinates $\boldsymbol{\eta}_{i-1}$ and $\boldsymbol{\eta}_i$ are already coupled in both grand angular and angular space, as in the case of $j = N$, the transformation $\mathcal{P}^{(j)}$ reduces to the RR coefficients:

$$
\mathcal{P}^{(N)}_{[K][K']} = \delta_{K_N K'_N} \left[\prod_{i=3}^{N} \delta_{l_i l'_i}\delta_{L_{i-1}L'_{i-1}}\delta_{K_{i-1}K'_{i-1}} \right] \mathcal{R}^{K_2,L_2}_{l_2 l_1,l'_2 l'_1}(\beta_N)\ ,
\qquad (3.21)
$$

otherwise we have the block diagonal transformation:

$$
\mathcal{P}^{(j)}_{[K][K']} = \left[\prod_{\alpha=1}^{i-2} \delta_{l_\alpha,l'_\alpha} \prod_{k=2}^{i-2} \delta_{L_k,L'_k}\delta_{K_k,K'_k} \right]\ {}^{(i)}\mathcal{B}^{L_{i-2}K_{i-2},L_i K_i}_{l_{i-1}l'_{i-1}l_i l'_i L_{i-1}K_{i-1}L'_{i-1}K'_{i-1}}
$$

$$
\cdot \left[\prod_{\alpha=i+1}^{N} \delta_{l_\alpha,l'_\alpha} \prod_{k=i+1}^{N} \delta_{L_k,L'_k}\delta_{K_k,K'_k} \right]\ .
$$

$$(3.22)$$

The $\mathcal{B}$ matrices represent the blocks of the $\mathcal{P}$ matrix and are combinations recouplings by means of the Tree, the T and the RR coefficients [57]:

$$
\begin{aligned}
^{(i)}\mathcal{B}^{L_{i-2}K_{i-2},L_iK_i}_{l_{i-1}l'_{i-1}l_il'_iL_{i-1}K_{i-1}L'_{i-1}K'_{i-1}} &= \sum_{L_{i,i-1}} T^{L_{i-2}l_{i-1}l_i}_{L_{i-1}L_{i,i-1}L_i} T^{L_{i-2}l'_{i-1}l'_i}_{L_{i-1}L_{i,i-1}L_i} \cdot \\
&\cdot \sum_{K_{i-1,i}} \mathcal{T}^{\alpha_{K_{i-2}}\alpha_{l_{i-1}}\alpha_{l_i}}_{K_{i-1}K_{i,i-1}K_i} \mathcal{T}^{\alpha_{K_{i-2}}\alpha'_{l_{i-1}}\alpha'_{l_i}}_{K'_{i-1}K_{i,i-1}K_i} \cdot \mathcal{R}^{K_{i,i-1},L_{i,i-1}}_{l_{i-1}l_i,l'_{i-1}l'_i}(\beta_j) \, .
\end{aligned}
\tag{3.23}
$$

We conclude by noting that the simplest case of such transformations corresponds to $j = 1$, where the permutation matrix elements reduce to a phase factor:

$$
\mathcal{P}^{(1)}_{[K][K']} = (-1)^{l_N}\delta_{[K_N][K'_N]} \, ,
\tag{3.24}
$$

in fact the action of $p_{1,2}$ on the Jacobi basis vectors is simply given by $\boldsymbol{\eta}^1_N = -\boldsymbol{\eta}_N$.

3.1.2 The Spin and the Isospin Matrix Elements

A 2-body potential term V_{ij}, in general, depends on the total spin S_{ij} and on the total isospin T_{ij} of the (i, j) couple of particles that, except for the $(A, A-1)$ case, is not one of the quantum numbers defining the basis in eq. (2.69). Moreover it may depend on the single particle spin or isospin projection numbers. For these reasons it is necessary to introduce recoupling transformations that allow to change the coupling scheme of the basis in order to obtain the desired quantum numbers.

By means of recoupling transformations we can also define spin and isospin permutation operators between particles having the same total spin or isospin quantum number.

The spin permutation between two particles, i and j, with identical spin s is defined as:

$$
P_{ij}\,|i : s, m_i\rangle\,|j : s, m_j\rangle = |i : s, m_j\rangle\,|j : s, m_i\rangle \, .
\tag{3.25}
$$

In case of spin $s = 1/2$ fermions we recover the spin exchange operator:

$$
\begin{aligned}
P_{ij}\,|1/2, m_i\rangle\,|1/2, m_j\rangle &= \frac{1}{2}(\boldsymbol{\sigma}_i \cdot \boldsymbol{\sigma}_j + \mathbb{I})\,|1/2, m_i\rangle\,|1/2, m_j\rangle \\
&= \sum_{S_{ij}} C^{m_im_j}_{S_{ij}M_{ij}}(2S_{ij} - 1)\,|S_{ij}M_{ij}\rangle \, ,
\end{aligned}
\tag{3.26}
$$

Where the $C^{m_im_j}_{S_{ij}M_{ij}}$ are the usual Clebsch-Gordan coefficients. If the spins are not identical, permutations are not defined, however one can always exchange the order of coupling of the single spins by exploiting the general

phase relation [59]:

$$\langle j_i j_j m_i m_j | J_{ij} M_{ij} \rangle = (-1)^{j_i + j_j - J_{ij}} \langle j_j j_i m_j m_i | J_{ij} M_{ij} \rangle \ . \tag{3.27}$$

In a certain analogy to the masses in the spatial kinematic rotations, in case of identical spins the above operation coincides with a true spin permutation, in fact $2S_{ij} - 1 = (-1)^{s_i + s_j - S_{ij}}$ for $s_i = s_j = 1/2$, otherwise it represents a change in the coupling order.

In an A-body spin state, the usual three momenta recoupling is made by means of $6j$ coefficients, as shown in fig. 3.4:

$$
\begin{aligned}
S_{S_i S_{i,i-1}}^{S_{i-2} S_i} &= \left\langle [[S_{i-2}, s_{i-1}]_{S_{i-1}}, s_i]_{S_i} \big| [S_{i-2}, [s_{i-1}, s_i]_{S_{i,i-1}}]_{S_i} \right\rangle \\
&= \sqrt{(2S_{i-1} + 1)(2S_{i,i-1} + 1)} (-1)^{1 + S_{i-2} + S_i}
\left\{
\begin{array}{ccc}
s_{i-1} & s_i & S_{i,i-1} \\
S_{i-2} & S_i & S_{i-1}
\end{array}
\right\} \ .
\end{aligned}
\tag{3.28}
$$

A coupling permutation between two adjacent spins in the A-body basis of eq. (2.69) is defined as:

$$\mathcal{S}^{i,i+1} = \sum_{S_{i,i-1}} S_{S_{i-1} S_{i,i-1}}^{S_{i-2} S_i} (-1)^{s_{i-1} + s_i - S_{i,i-1}} S_{S'_{i-1} S_{i,i-1}}^{S_{i-2} S_i} \tag{3.29}$$

Any given order of single particle spins can be obtained by compositions of the above transformations. In particular, in case of a potential term that depends on the spin projection of a couple of particles i and j (or of a single particle), the most convenient coupling scheme is the one where the s_i and s_j spins are in the last positions, which can be obtained by means of the transformation $\mathcal{S}_{12}^{ij}$, given, in analogy to eq. (3.12) together with eq. (3.11), by the product of coupling transpositions between adjacent spins defined in eq. (3.29). The two coupling schemes connected by $\mathcal{S}_{12}^{ij}$:

$$\left| S_2 \dots [S_{i-1}, s_i]_{S_i} \dots [S_{j-1}, s_j]_{S_j} \dots \right\rangle \xrightarrow[\mathcal{S}_{12}^{ij}]{} \left| S_2 \dots [[S'_{A-2}, s_i]_{S'_{A-1}}, s_j]_{S_A} \right\rangle \ . \tag{3.30}$$

and by means of the S recoupling of eq. (3.28) and Clebsch-Gordan coefficients one can easily extract the whole information on the (s_i, s_j) couple of spins:

$$\left| [S_{i-2}, [s_i, s_j]_{S_{i,j}}]_{S_i} \right\rangle = \sum_{S_{ij}} C_{M_{i-1} M_{ij}}^{S_i M_i} \left| [S_{i-2}, M_{i-2}] \right\rangle \left| S_{i,j}, M_{ij} \right\rangle \ . \tag{3.31}$$

Do to the independence of the spin and isospin basis from the spatial part, one is free to choose a suitable starting sequence in the spin and isospin coupling in order to reduce the number of recoupling operations needed to
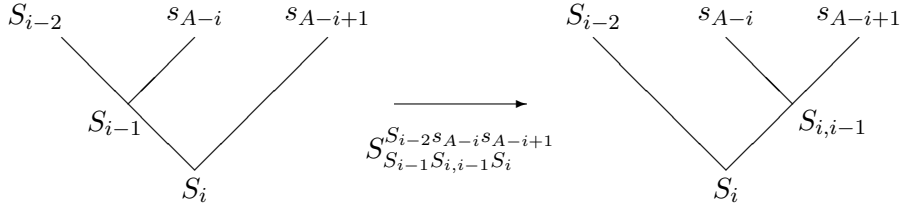
FIGURE 3.4: Recoupling scheme of the three spins S_{i-2}, s_{i-1} and s_i by means of the S-coefficients defined in eq. (3.28).
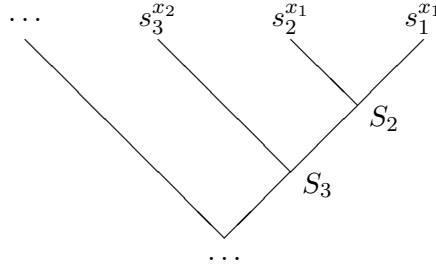

FIGURE 3.5: Tree diagram representing a sequence of spin coupling where the spins of the particles of species x_1 are at the bottom so that S_2 is already the total spin of the couple.

calculate a given matrix element. For example, in a system with two particle of one species, x_1, and $A - 2$ particles of another species, x_2, and with a 2-body potential V_{x_1} for the first species that depends on the total spin of the couple, one can put the two spins of the particles belonging to x_1 at the bottom of the coupling sequence so that each basis state is already an eigenstate of the total spin of that couple and the use of recoupling transformations can be limited the subset of particles of the species x_2, as shown in fig. 3.5.

If the two particles of species x_1 occupy the i-th and the j-th position respectively in the spatial part, the operator of eq. (3.6) employed to calculate the 2-body potential V_{x_1} as in eq. (3.4) becomes:

$$\mathcal{Q}_{12}^{ij} = \mathcal{P}_{12}^{ij} \otimes \mathbb{I}_s \otimes \mathcal{I}_{12}^{ij} . \tag{3.32}$$

Of course the above machinery is applicable exactly in the same way to the isospin part of the basis.

We conclude by showing the recoupling coefficients to extract the total angular momentum $J_{A,A-1}$ of the couple of particles A and $A - 1$ from the standard coupling scheme of a non central basis, where the total orbital angular momentum L_N and the total spin S_A are coupled to the total A-body

angular momentum J:

$$
\begin{aligned}
\mathcal{J}^{L_N S_A J}_{J_{A,A-1} S_{A,A-1}} &= \langle [[L_{N-1}, L_N]_{L_N}, [S_{A-2}, S_{A,A-1}]_{S_A}]_J | \\
&\quad \overline{[[L_{N-1}, S_{A-2}]_{J_{A-2}}, [l_N, S_{A,A-1}]_{J_{A,A-1}}]_J} \rangle \\
&= \sqrt{(2L_N + 1)(2S_A + 1)(2J_{A-2} + 1)(2J_{A,A-1} + 1)} \cdot \\
&\quad \cdot \left\{ \begin{array}{ccc} L_{N-1} & S_{A-2} & J_{A-2} \\ l_N & S_{A,A-1} & J_{A,A-1} \\ L_N & S_A & J \end{array} \right\} .
\end{aligned}
\tag{3.33}
$$

3.2 Calculation of the potential matrix elements

We consider the general case of an A-body system with a number n_x of different species of particles, each one including N_s particles. We have:

$$
\sum_{s=1}^{n_x} N_s = A .
\tag{3.34}
$$

The number of 2-body interactions in such system is $n_x + C_{n_x,2}$, where $C_{n_x,2}$ is the number of pairs in a set of n_x elements. Eq. (3.1) expressed in terms of the n_x subsets of particles becomes:

$$
\begin{aligned}
H &= T + V_{\text{id}} + V_{\text{diff}} \\
&= T + \sum_{s=1}^{n_x} \sum_{i<j=1}^{N_s} V_s(\mathbf{r}_{ij}, S_{ij}, T_{ij}) + \sum_{s'<s=2}^{n_x} \sum_{i=1}^{N_{s'}} \sum_{j=1}^{N_s} V_{s's}(\mathbf{r}_{ij}, S_{ij}, T_{ij}) ,
\end{aligned}
\tag{3.35}
$$

where V_{id} is the sum of the 2-body potetial terms between identical particles and V_{diff} between different ones.
By recalling eq. (3.4), we have:

$$
V^{[S_N][T_N]}_{ss'}(\mathbf{r}_{ij}) = \mathcal{Q}^{12}_{ij} \cdot V''^{[S_N]^{ij}[T_N]^{ij}}_{ss'}(\boldsymbol{\eta}^{ij}_N) \cdot \mathcal{Q}^{ij}_{12} ,
\tag{3.36}
$$

where, in case of $s = s'$ the spatial part of the $\mathcal{Q}^{12}_{ij}$ operator, $\mathcal{P}^{12}_{ij}$, is a true spatial permutation that exchanges particles i and j with 1 and 2. In this case, the couple of particles is subjected to the exchange symmetry:

$$
V''^{[S_N]^{ij}[T_N]^{ij}}_{s,\text{symm}}(\boldsymbol{\eta}^{ij}_N) = \frac{1}{2} \left[(-1)^{l_N + S_{ij} + T_{ij}} + I_s \right] V''^{[S_N]^{ij}[T_N]^{ij}}_{s}(\boldsymbol{\eta}^{ij}_N) ,
\tag{3.37}
$$

with $I_s = -1$ if the species s is fermionic and $I_s = 1$ if bosonic. In the case $s \neq s'$ the $\mathcal{Q}^{12}_{ij}$ operator is a coupling permutation that moves the two interacting particles in the last Jacobi coordinate and changes the spin and isospin bases so that S_{ij} and T_{ij} are good quantum numbers. We note that the dependence on the masses is contained in the scaling parameter shown in eq. (3.3) and in the kinematic angles β in the RR coefficients defining the

coupling permutations, as shown in eq. (3.23).

The matrix elements of the 2-body potential between the i and j particles in the HH basis after the application of $\mathcal{Q}_{12}^{ij}$ are given by:

$$
\begin{aligned}
V''^{[S_N]^{ij}[T_N]^{ij}}_{ss',[K_N][K'_N]}\left[\boldsymbol{\eta}_N^{ij}\right] =& \delta_{[K_{N-1}][K'_{N-1}]}\delta_{[S_{N-1}]^{ij}[S'_{N-1}]^{ij}}\delta_{[T_{N-1}]^{ij}[T'_{N-1}]^{ij}} \\
& \sum_{S_{i,i-1}} S^{S_{i-2}S_i}_{S_{i-1}S_{i,i-1}}\, T^{T_{i-2}T_i}_{T_{i-1}T_{i,i-1}} \cdot \\
& \cdot V^{K_{N-1}j}_{K_N l_N s t T_z, K'_N l'_N s' t' T_z}(\rho)\, T^{T_{i-2}T_i}_{T'_{i-1}T_{i,i-1}}\, S^{S_{i-2}S_i}_{S'_{i-1}S_{i,i-1}}
\end{aligned}
\tag{3.38}
$$

where $s = S_{ij}$ and $t = T_{ij}$. Differently from the permutation operators, the 2-body potential matrix $V''^{[S_N]^{ij}[T_N]^{ij}}_{ss',[K_N][K'_N]}(\boldsymbol{\eta}_N^{ij})$ couples different values of K_N, but it is diagonal in the quantum numbers related to the residual $(A-3)$-body system. The 2-body matrix element in term of the radial part $W(\rho)$ and of the operator part O is dfined as:

$$
V^{K_{N-1}j}_{K_N l_N s t t_z, K'_N l'_N s' t' t_z}(\rho) = \sum_p W^{(p)K_{N-1}}_{K_N l_N, K'_N l'_N}(\rho) O^{(p)j}_{l_N s t t_Z, l'_N s' t' t_z}\,.
\tag{3.39}
$$

The radial function is the result of the hyperangular integration:

$$
W^{(p)K_{N-1}}_{K_N l_N, K'_N l'_N}(\rho) = \int d\Omega_N \mathcal{Y}^*_{[K_N]} V^{(p)}\left(\sqrt{\frac{mM_2}{m_1 m_2}}\rho\sin\phi_N\right)\mathcal{Y}_{[K'_N]}\,,
\tag{3.40}
$$

and the operator part of the 2-body matrix element:

$$
O^{(p)j}_{l_N s t t_z, l'_N s' t' t_z} = \langle(l_N; s)jtt_z|\,\hat{O}^p\,|(l'_N; s')jt't_z\rangle\,.
\tag{3.41}
$$

3.3 Calculations of Bound State Energies and Wave Functions

The NSHH basis has no definite behaviour under particle permutations and the physical states with good permutational symmetry constitute a subset of the entire Hilbert space. Only in case of an A-body system where each particle is different from the others the physical states cover the whole space.

In a system of A identical particles the selection of the physical states is done by using one specific property of the Casimir operator $\hat{C}(A)$ which corresponds to the transposition class sum operator $[(2)]_A$ of the group of permutations of A objects S_A. We refer to ref. [60] for mathematical details, here we are just interested in the property that, as shown in table 3.1 for the cases $A = 3 \div 5$, the symmetric representation (labeled by the Young diagram $[A]$) and the antisymmetric one (labeled by $[1, 1, \ldots, 1]$) correspond to the highest and lowest eigenvalues of $[(2)]_A$ respectively. The Casimir

TABLE 3.1: Eigenvalues of the class sums in the permutation groups S_3, S_4 and S_5. The highest and lowest eigenvalues belong to the symmetric and antisymmetric irreps respectively [60].

S_3	$[(2)]_3$	S_4	$[(2)]_4$	S_5	$[(2)]_5$
$[3]$	3	$[4]$	6	$[5]$	10
$[2,1]$	0	$[3,1]$	2	$[4,1]$	5
$[1,1,1]$	-3	$[2,2]$	0	$[3,2]$	2
		$[2,1,1]$	-2	$[3,1,1]$	0
		$[1,1,1,1]$	-6	$[2,2,1]$	-2
				$[2,1,1,1]$	-5
				$[1,1,1,1,1]$	-10

operator in the NSHH basis is defined as:

$$\hat{C}(A) = \sum_{j>i=1}^{A} \hat{P}_{ij} \, , \qquad (3.42)$$

where $\hat{P}_{ij}$ is the transposition operator for two identical particles, i and j, and it can be defined by means of the $\mathcal{Q}$ recoupling operators:

$$\hat{P}_{ij} = \mathcal{Q}_{ij}^{12} \cdot (-1)^{l_N + S_{ij} + T_{ij}} \cdot \mathcal{Q}_{12}^{ij} \, . \qquad (3.43)$$

As shown in the previous section, permutations among identical particles do not affect the total grand angular momentum quantum number K_N nor the hyperradial part of the wave function, so they commute with the kinetic energy operator T, defined in eq. (2.42). It can be easily verified that the total 2-body potential operator of a system of A identical particles commutes with $\hat{C}(A)$, so:

$$\left[H, \hat{C}(A) \right] = 0 \, . \qquad (3.44)$$

By denoting with Ψ_s, Ψ_m, Ψ_a three generic eigenfunctions symmetric, with mixed symmetry and antisymmetric respectively, we have [60]:

$$\hat{C}(A)\Psi_s = \lambda_s \Psi_s = \frac{A(A-1)}{2} \Psi_s \, ;$$
$$\hat{C}(A)\Psi_m = \lambda_m \Psi_m \, ; \qquad (3.45)$$
$$\hat{C}(A)\Psi_a = \lambda_a \Psi_a = -\frac{A(A-1)}{2} \Psi_a \, ,$$

with $\lambda_a < \lambda_m < \lambda_s$. We then consider the pseudo-Hamiltonian $\tilde{H}$ [16]:

$$\tilde{H} = H + \gamma \hat{C}(A) \, , \qquad (3.46)$$

whose eigenvalues are:

$$\tilde{E}_n^x = E_n^x + \gamma \lambda_x \, , \tag{3.47}$$

where γ is a real parameter and $x = s, m, a$ is the symmetry label. E_n^x is the n-th eigenvalue of H with symmetry x. A proper choice of the parameter γ can make $\tilde{E}_0^a$ or $\tilde{E}_0^s$ the lowest eigenvalue of $\tilde{H}$ so that E_0^a or E_0^s, namely the ground state energy of a fermionic or bosonic system, is easily obtained by subtracting the quantity $\gamma \lambda_a$. In this way there is no need to perform the exact diagonalization of $\tilde{H}$ because the new eigenvalue problem can be solved only for the lowest values using much faster procedures, e.g. the Lanczos algorithm.

The choice of γ in the antisymmetric case is done by imposing the relation:

$$\tilde{E}_0^a = E_0^a + \gamma \lambda_a < E_n^x + \gamma \lambda_x \ , \ n = 0, 1, \dots \ , \ x = s, m \, , \tag{3.48}$$

which gives:

$$\gamma > \frac{E_0^a - E_n^x}{\lambda_x + \lambda_a} \tag{3.49}$$

By assuming that $E_0^a < 0$ and by noting that $\lambda_x - \lambda_a \geq A$ we obtain:

$$\gamma > \frac{|E_{\min}|}{A} \tag{3.50}$$

where $E_{\min}$ is the lowest eigenvalue of the Hamiltonian. If the lowest symmetric eigenstate is desired instead of the antisymmetric one, it is easy to see that we reach the same conclusion by introducing a -1 factor in eq. (3.48):

$$\tilde{E}_0^s = E_0^s - \gamma \lambda_s < E_n^x + \gamma \lambda_x \ , \ n = 0, 1, \dots \ , \ x = a, m \, . \tag{3.51}$$

In this case our pseudo-Hamiltonian:

$$\tilde{H} = H - \gamma \hat{C}(A) \, . \tag{3.52}$$

We note that such approach is somehow analogous to the Lawson method for the removal of the spurious center of mass motion in Shell Model calculations.

With systems made by n different species of particles, the symmetrization operator, which for identical particle systems is the Casimir operator of the permutation group for A elements, splits into a sum of n operators, each one being the Casimir operator for a set of N_s elements, namely the number of identical particles in the subset of species s. The operator has now the more general form:

$$\hat{C}(N_1, \dots, N_n) = \sum_{s=1}^n b_{\Lambda_s} \hat{C}_s(N_s) \ ; \ \hat{C}_s(N_s) = \sum_{j>i=1}^{N_s} \hat{P}_{ij} \, , \tag{3.53}$$

where:

$$b_{\Lambda_s} = \begin{cases} 1 & \Lambda_s = A, M \\ -1 & \Lambda_s = S \end{cases} \quad ; \quad \sum_{s=1}^{n} N_s = A \; . \tag{3.54}$$

Of course if $N_s = 1$ then $\hat{C}_s(N_s) = 0$. The b_{Λ_s} coefficients are related to the different symmetries of each species. The $\hat{C}(N_1, \ldots, N_n)$ operator still commutes with the Hamiltonian, in fact, each single permutation commutes with the kinetic energy operator and each $\hat{C}_s(N_s)$ commutes with the total potential of the N_s subsystem and, of course, with all the remaining terms since they refer to different particles.

By diagonalizing the matrix $\tilde{H}$, the eigenvalues for a given symmetry configuration Λ are:

$$\tilde{E}_{k,\Lambda} = E_{k,\Lambda} + \gamma \sum_{s=1}^{n} b_s \lambda_{\Lambda_s} \quad ; \quad k = 0, 1, 2, ..., N_{\max}(\Lambda) \; . \tag{3.55}$$

If Γ is the symmetry configuration of our physical system, we choose $\gamma > 0$ large enough so that $\tilde{E}_{0,\Gamma}$ is by far the lowest eigenvalue of $\tilde{H}$. Thus one imposes the relations:

$$\tilde{E}_{0,\Gamma} = E_{0,\Gamma} + \gamma \sum_{s=1}^{n} b_{\Gamma_s} \lambda_{\Gamma_s} < E_{k,\Lambda} + \gamma \sum_{s=1}^{n} b_{\Lambda_s} \lambda_{\Lambda_s} \quad ; \; \forall \, k, \Lambda \neq \Gamma \; . \tag{3.56}$$

By following the above scheme we impose the relation:

$$\gamma > \frac{E_{0,\Gamma} - E_{0,\Lambda}}{\sum_{s=1}^{n} \left(b_{\Lambda_s} \lambda_{\Lambda_s} - b_{\Gamma_s} \lambda_{\Gamma_s} \right)} \; , \tag{3.57}$$

and we obtain a condition analogue to eq. (3.50):

$$\gamma > \frac{|E_{\min}|}{\sum_{s=1,(N_s \neq 1)}^{n} N_s} \; . \tag{3.58}$$

3.4   Incorporation of the Lee-Suzuki Effective Interaction Procedure

Since the A-body potential operator acts on the whole Hilbert space, in general, the convergence of ab-initio calculations, which are necessarily done in a finite subspace, is not guaranteed. With the employment of a soft potential, like the Minnesota NN interaction or the V_{lowk}, convergent results can be obtained with simple variational calculations, where the truncation parameters act as variational ones.

However, when realistic standard NN (and/or YN) potentials that generate strong short-range correlations are used, as it is the case for the AV18, the CD-Bonn 2000 or most of the modern YN interactions, the reaching of
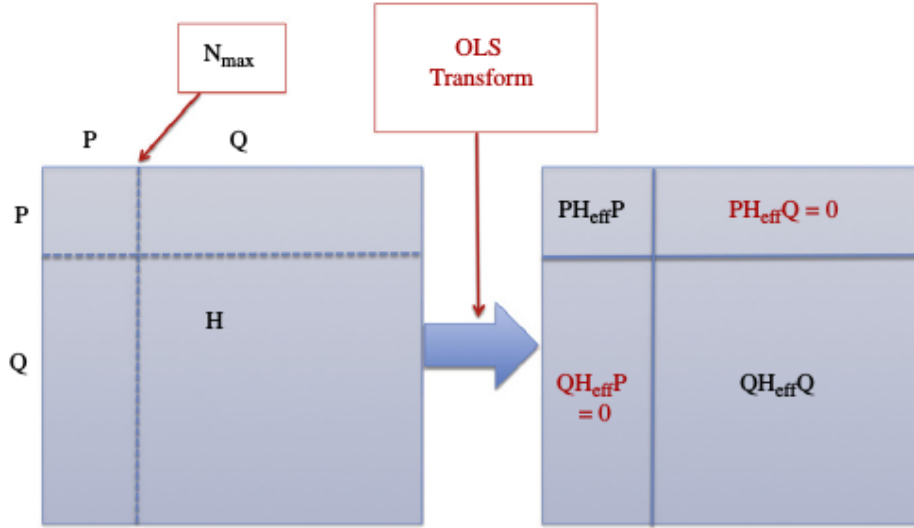
FIGURE 3.6: Schematic illustration of the action of the Lee-Suzuki similarity transformation which produces an effective Hamiltonian $H_{\mathbb{P}}$ defined in the model space $\mathbb{P}$ decoupled from the complementary $\mathbb{Q}$. Figure taken from ref. [63].

convergence is not ensured.

To overcome this problem we incorporate in the NSHH method a renormalization procedure, the Lee-Suzuki (L-S) one [61, 62], that softens the interactions and generates effective operators for all observables, while preserving all the experimental quantities in the low-energy domain. The resulting effective interaction still acts among all A nucleons and preserves all the symmetries of the bare interactions [63].

We define the projectors $\hat{\mathbb{P}}$ and $\hat{\mathbb{Q}}$ respectively on the model space $\mathbb{P}$ and on its complementary $\mathbb{Q}$, with the total Hilbert space $\mathbb{H} = \mathbb{P} \oplus \mathbb{Q}$, and we look for an effective potential in the model space. The effective Hamiltonian is defined as:

$$H_{\mathbb{P}} = \hat{\mathbb{P}} \left[\sum_{i=1}^{A} T_i \right] \hat{\mathbb{P}} + \hat{\mathbb{P}} \left[\sum_{i<j}^{A} V_{ij} \right]_{\text{eff}} \hat{\mathbb{P}} . \tag{3.59}$$

The effective interaction, as shown in the above equation, is an A-body interaction that allows to obtain a subset of exact eigenvalues of the original Hamiltonian H by limiting their calculation to the model space. The latter results decoupled from the complementary $\mathbb{Q}$, as shown in fig. 3.6. Of course, in practical applications, the transformation from the bare interaction model to the effective one must act on a finite space, so the complement space $\mathbb{Q}$ is chosen finite, but big enough to significantly improve convergence of the lowest eigenvalues.

However, the determination of an A-body effective interaction does not provide any computational advantage with respect to the calculation of the

eigenvalues of the bare Hamiltonian, therefore we look for a simpler effective interaction model with the following features [56]:

$$
\begin{aligned}
V_{\text{eff}} &\xrightarrow[\hat{\mathbb{P}}\to\mathbb{I}]{} V \\
\left| E_i^{\text{eff}}(\mathbb{P}) - E_i \right| &\underset{\hat{\mathbb{P}}\to\mathbb{I}}{<} \left| E_i^{\text{bare}}(\mathbb{P}) - E_i \right| ,
\end{aligned}
\tag{3.60}
$$

where $E_i^{\text{eff}}(\mathbb{P})$ and $E_i^{\text{bare}}(\mathbb{P})$ are the i-th eigenvalues of respectively H_{eff} and H_{bare} both limited to the $\mathbb{P}$ space, while E_i is the exact i-th eigenvalue of H_{bare} defined in the full $\mathbb{H}$ space.

A natural choice is the approximation of V^{eff} with a sum of 2-body effective interaction terms, one for each couple of particles of the system:

$$
V^{\text{eff}} = \sum_{i<j} V_{ij}^{\text{eff}} = \sum_{i<j} \mathcal{Q}_{ij}^{12} \, V_{s_i s_j}^{\text{eff}} \, \mathcal{Q}_{12}^{ij} ,
\tag{3.61}
$$

where s_i is the species of the i-th particle and s_j the species of the j-th one. Due to their block diagonal structure in the grand angular momentum quantum number K_N, the $\mathcal{Q}$ operators do not affect the structure of the effective interaction terms, where the $\mathbb{P}$ space is decoupled from $\mathbb{Q}$. The determination of an effective interaction is then turned into a quasi 2-body problem that is computationally manageable. For each kind of interaction we define a "pseudo" 2-body Hamiltonian:

$$
H_{ss'}(\rho, \phi_N, \hat{\boldsymbol{\eta}}_N, S_{ij}, T_{ij}) = T_{K_N} + V_{ss'} \left(a_{ij}\rho\sin\phi_N, \hat{\boldsymbol{\eta}}_N, S_{ij}, T_{ij}\right) ,
\tag{3.62}
$$

where T_{K_N} is the hyperspherical term of the A-body kinetic energy operator and a_{ij} is the mass scale constant:

$$
T_{K_N} = \frac{1}{2m}\frac{\hat{K}_N^2}{\rho^2} ; \qquad a_{ij} = \sqrt{\frac{m(m_i + m_j)}{m_i m_j}} .
\tag{3.63}
$$

Due to its dependence on the collective coordinate ρ and due to the fact that T_{K_N} is an A-body term of the total kinetic energy, $H_{ss'}$ is an A-body Hamiltonian. Since the hyperradial part of the basis is a complete set, it is not necesssary to include the hyperradial term of the kinetic energy in the effective interaction procedure.

The matrix elements of $H_{ss'}$ are:

$$
\begin{aligned}
\langle [K_N] | \, H_{ss'}(\rho) \, | [K_N'] \rangle =& \delta_{[K_N][K_N']} \frac{1}{2m} \frac{K_N(K_N + 3N - 2)}{\rho^2} + \\
& \delta_{[K_{N-1}][K_{N-1}']} V_{K_{N-1}L_{N-1}}^{K_N L_N l_N, K_N' L_N' l_N'}(\rho) .
\end{aligned}
\tag{3.64}
$$

We note the dependence on K_{N-1} and, for non-central forces, on L_{N-1}. By consequence the effective interaction includes a dependence on the state of

the residual $A - 2$ particle subset of the system which can be interpreted as sort of a "medium correction" [64]. We solve the effective interaction problem on a hyperradial grid, diagonalizing $H_{ss'}$ on each grid point ρ_i and for all the possible values K_{N-1} in the model space.

As shown in section 2.3, the Hilbert space of the spatial part of our A-body porblem is a product of the hyperradial subspace with the HH-generated space. The hyperradial set is complete, so the EI transformation is applied only to the HH part and we identify $\mathbb{P}_{\text{cut}}$ with $K_{\max}$ and $\mathbb{Q}_{\text{cut}}$ with $K_{\max}^{\text{eff}}$.

If we call $|p\rangle$ and $|q\rangle$ the elements of the HH basis belonging, respectively, to $\mathbb{P}$ and to $\mathbb{Q}$ we define the Lee-Suzuki (L-S) effective two body Hamiltonian:

$$\hat{\mathbb{P}} \, H_{ss'}^{\text{L-S}} \, \hat{\mathbb{P}} = \hat{\mathbb{P}} \, H_{ss'} \, \hat{\mathbb{P}} + \hat{\mathbb{P}} \, H_{ss'} \, \hat{\mathbb{Q}} \omega \hat{\mathbb{P}} \,, \tag{3.65}$$

where $\omega = \hat{\mathbb{Q}} \omega \hat{\mathbb{P}}$ is the transformation operator defined by:

$$\langle q | \epsilon_i \rangle = \sum_p \langle q | \, \omega \, | p \rangle \, \langle p | \epsilon_i \rangle \,. \tag{3.66}$$

The $|\epsilon_i\rangle$ are the eigenstates of $H_{ss'}^{K_{N-1} L_{N-1}}(\rho)$. If we consider the set of $n_p = \dim(\mathbb{P})$ eigenvectors with the lowest eigenvalues ϵ_i, we can invert the matrix $\langle p | \epsilon_i \rangle$ to solve eq. (3.66) and find the matrix ω. The effective 2-body Hamiltonian results [64]:

$$\langle p | \, H_{ss'}^{\text{L-S}}(K_{N-1}, \rho) \, | p' \rangle = \\ \sum_i^{n_p} \left[\langle p | \epsilon_i \rangle \, \epsilon_i \, \langle \epsilon_i | p' \rangle + \sum_q \langle p | \epsilon_i \rangle \, \epsilon_i \, \langle \epsilon_i | q \rangle \, \langle q | \, \omega \, | p \rangle \right] \,, \tag{3.67}$$

and for each of the chosen eigenvectors $|\epsilon_i\rangle$ we have:

$$H_{ss'}^{\text{L-S}} \, \hat{\mathbb{P}} \, |\epsilon_i\rangle = \epsilon_i \, |\epsilon_i\rangle \,. \tag{3.68}$$

The $H_2^{\text{L-S}}$ operator is, in general, non-hermitian, but it can be hermitized using the following transformation [56]:

$$H_{ss'}^{\text{eff}} = \left[\hat{\mathbb{P}}(1 + \omega^\dagger \omega) \hat{\mathbb{P}} \right]^{\frac{1}{2}} H_{ss'}^{\text{L-S}} \left[\hat{\mathbb{P}}(1 + \omega^\dagger \omega) \hat{\mathbb{P}} \right]^{-\frac{1}{2}} \,. \tag{3.69}$$

The effective interaction then is given by:

$$V_{ss'}^{\text{eff}} = H_{ss'}^{\text{eff}} - T_{K_N} \,. \tag{3.70}$$

As pointed out in ref. [64] we stress the following facts:

1. the hyperradius ρ acts as a parameter rather than a coordinate, and $V_{ss'}^{\text{eff}}$ is calculated for various values of ρ on the hyperradial grid. So $V_{ss'}^{\text{eff}}$ is a 2-body interaction, but it contains a dependence on the whole

A-body system via this collective coordinate;

2. an additional dependence of $V_{ss'}^{\text{eff}}$ on the residual $(N-1)$-body system is highlighted by the presence of the K_{N-1} quantum number in eq. (3.64);

3. for $\hat{\mathbb{P}} \to \mathbb{I}$ we have $V_{ss'}^{\text{eff}} \to V_{ss'}$. By consequence the energies converge to the exact ones;

4. the effective interaction $V_{ss'}^{\text{eff}}$ contains information on the $\mathbb{Q}$ space, besides the model space, so the convergence to the exact energy spectrum is accelerated with respect to the use of the bare interaction;

5. in presence of multiple interactions, the L-S procedure has to be applied separately for each potential. By considering the starting assumptions, nothing prevents the use of different $K_{\text{max}}^{\text{eff}}$ for each potential, depending on the specific features of each $V_{ss'}$ interaction model.

3.5   Implementation of the NSHH Method

The large dimension of the NSHH basis is partly balanced by the possibility to use fast diagonalization procedures to calculate the lowest eigenvalues of the pseudo-Hamiltonian. One of the most used is based on the Lanczos algorithm, which is an adaptation of the power method, thought to find the lowest eigenvalues of a matrix by successive matrix-vector multiplications, starting from a random vector.

We briefly describe our implementation of the NSHH method and we provide a number of benchmark results of binding and separation energies for systems with simple interactions.

3.5.1   The Algorithm

The total pseudo-Hamiltonian operator $\tilde{H}$ is:

$$
\begin{aligned}
\tilde{H} &= -\frac{\hbar^2}{\beta^2 m}\left(T_\rho^1 \otimes \mathbb{I} + T_\rho^2 \otimes \hat{K}_N^2\right) + \sum_{ij} \mathcal{Q}_{ij}^{12} \cdot V_{s_i s_j} \cdot \mathcal{Q}_{12}^{ij} + \gamma \hat{C}(N_1 \dots, N_n) \\
&= -\frac{\hbar^2}{\beta^2 m}\left(T_\rho^1 \otimes \mathbb{I} + T_\rho^2 \otimes \hat{K}_N^2\right) + \sum_{ij} \mathcal{Q}_{ij}^{12} \cdot \left[V_{s_i s_j} + \gamma \delta_{s_i s_j} \hat{P}_{12}\right] \cdot \mathcal{Q}_{12}^{ij} \,,
\end{aligned}
\tag{3.71}
$$

where T_ρ^1 is the hyperradial term of the kinetic energy whose matrix elements in the Laguerre basis are shown in eq. (2.68), and T_ρ^2 is the $1/\rho^2$ term, whose analytical form is obtained by means of eq. (2.67). Of course $\hat{K}_N^2 = K_N(K_N + 3N - 2)\delta_{[K_N][K_N']}$ in the HH basis.

We adopt the stabilized Lanczos algorithm [65] in order to calculate the lowest eigenvalues and eigenvectors of the pseudo-Hamiltonian matrix. The algorithm is based on an iterative scheme where at each step the vector (Lanczos vector) resulting from the previous step is multiplied by the matrix to diagonalize. Iterations are computed until convergence in the lowest eigenvalue and eigenvector is reached, starting from a random vector.

The largest part of the computational weight is due to the matrix-vector multiplication and the larger is the matrix, the longer is the computation time at each step. However, the sparse structure of the permutation matrices and the block diagonal structure of the potential in the permuted basis constitute a big advantage in the application of this method since they drastically reduce the number of numerical computations.

The main loop is the one related to the total potential matrix vector multiplication, and it runs over all the possible couples of particles, from $(1,2)$ to $(A-1,A)$. For each 2-body term involving an (i,j) couple, the Lanczos vector is transformed by means of the $\mathcal{Q}$ operator before and after the multiplication of the potential matrix in the reference Jacobi set, whose matrix elements are stored on file. So for each (i,j) term the two particles involved in the interaction are temporarily moved in the first two positions of the Jacobi set. This means that at each step the total potential matrix is built "on flight" starting from the 2-body potential matrix elements and the $\mathcal{Q}$ ones.

The application of the potential matrix is done by means of the Lagrange Mesh Method (LMM) [66]. The Lanczos vector is first converted into the hyperradial grid basis and, for each value of ρ on the grid, the potential matrix is computed by running all over the HH basis. Then the conversion to the hyperradial Laguerre basis is applied.

3.5.2 Numerical tests: Nuclei

In general, the convergence in the K_{max} number in the NSHH method is the same with respect to the symmetrized version, since the subspace composed by the physical states with the correct symmetry does not change.

In fig. 3.7 the convergence patterns of two 4-body NSHH calculations are shown with the employment of the semi-realistic soft-core NN Minnesota potential [67] and of the realistic hard-core Argonne V8' NN potential [68]. In the first case a treatment with bare interaction is possible and convergence to the third digit is obtained with a reasonable K_{max} number, namely $K_{\mathrm{max}} = 20$ (12012 states for a central HH basis). With the use of the Lee-Suzuki transformation, however, we observe a consistent improvement and the third digit convergence is reached already with $K_{\mathrm{max}} = 14$ (3168 basis states) and with a relatively low value of $K_{\mathrm{max}}^{\mathrm{eff}}$, namely $K_{\mathrm{max}}^{\mathrm{eff}} = 60$.

In the second case the hard-core features of the AV8' potential and its non central character makes hard to reach convergence with a bare interaction
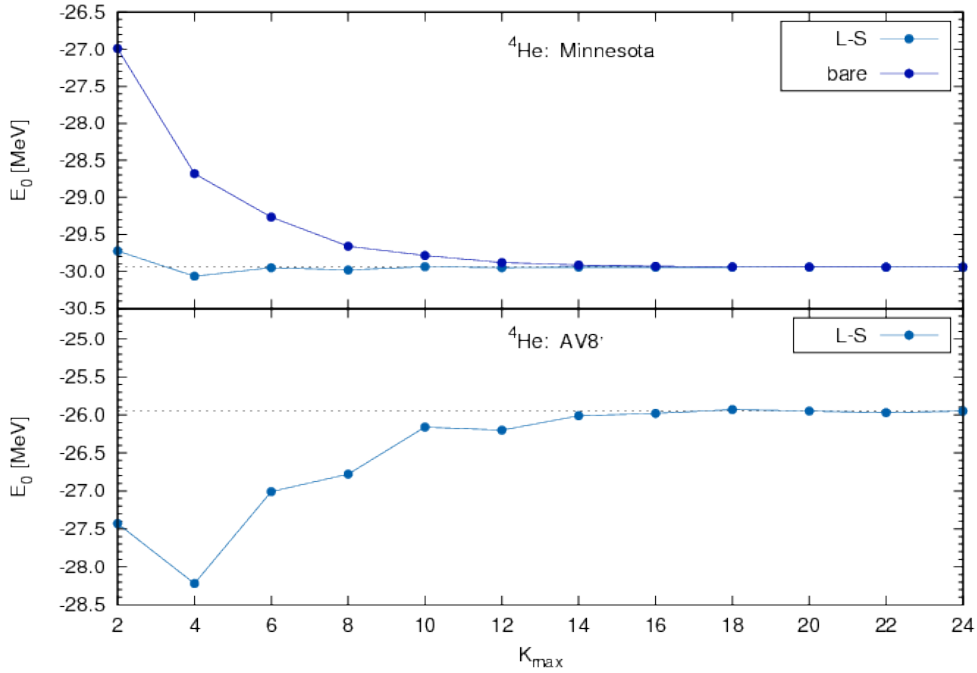
FIGURE 3.7: Convergence patterns of ^{4}He binding energies calculated with the NSHH method. In the first graph the central soft-core Minnesota potential has been used both with bare and Lee-Suzuki effective interaction. In the second graph the AV8' potential has been employed with the Lee-Suzuki Effective Interaction.

approach and the inclusion of the L-S effective interaction becomes important. We observe convergence at the second digit at $K_{max} = 18$ (45694 states for a non-central HH basis) with an effective interaction cut of $K_{max}^{eff} = 120$. Without Lee-Suzuki the binding energy at the same K_{max} is far away from the expected value, being still less than 10 MeV.

In ref. [69] the same 4-body calculation with AV8' potential has been performed and benchmarked among seven different ab-initio methods, namely Faddeev Yakubovski equations (FY), coupled-rearrangement-channel Gaussian-basis variational method (CRCGV), stochastic variational method (SVM), HH variational method (HH), Green's function Monte Carlo Method (GFMC), no-core shell model method (NCSM) and the effective interaction HH method (EIHH). In table 3.2 results for the binding energy and for the potential and kinetic energy expectation values are shown [69].

As expected EIHH and NS-EIHH are almost coincident. The binding energy E_b is convergent to a high precision while the expectation values $\langle T \rangle$ and $\langle V \rangle$ are still not in full convergence, with variations of the order of 1% on the last three values of K_{max}. To obtain faster convergence also for the

TABLE 3.2: Expectation values of kinetic and potential energies and binding energies in MeV for ^{4}He with AV8' NN interaction calculated with seven different ab-initio methods and compared with the EI-NSHH ones. The results of the first seven methods are taken from ref. [69].

Method	$\langle T \rangle$	$\langle V \rangle$	E_b
FY	102.39(5)	-128.33(10)	-25.94(5)
CRCGV	102.30	-128.20	-25.90
SVM	102.35	-128.27	-25.92
HH	102.44	-128.34	-25.90(1)
GFMC	102.3(1.0)	-128.25(1.0)	-25.93(2)
NCSM	103.35	-129.45	-25.80(20)
EIHH	100.8(9)	-126.7(9)	-25.944(10)
EI-NSHH	100(1)	-126(1)	-25.94(1)

expectation values one should employ effective operators, which becomes necessary when observables that contain short-range information have to be calculated. However, in the present framework, we focus on the calculation of binding and separation energies of hypernuclei and we postpone the treatment of such operators to future developments.

3.5.3 Numerical tests: Hypernuclei

Several numerical tests by means of unrealistic interactions have been performed in order to set the whole program. In particular binding energies of 3- and 4-body systems mainly with gaussian potentials were provided from of AFDMC [70] and NCSM calculations [71]. In table 3.3 a restricted selection of such benchmark results is shown for $A = 3 \div 5$.

In table 3.3 the label "MN" denotes the gaussian Minnesota potential:

TABLE 3.3: Binding and separation energies in MeV for different systems with $A = 3 \div 5$. The NN potential is the Minnesota one (no Coulomb force) and the YN potential is the Minnesota $T = 0$ channel multiplied by a factor 0.9.

Interaction	System	NSHH	AFDMC	NCSM
MN+0.9MN(T=0)	$^3_\Lambda$H	-2.27(1)	-2.38(12)	-2.29(2)
	B_Λ	0.05(1)	0.21(13)	0.07(1)
MN+0.9MN(T=0)	$^4_\Lambda$H	-17.694(3)	-18.12(15)	-17.9(3)
	B_Λ	9.304(3)	10.07(17)	9.51(30)
MN+0.9MN(T=0)	$^5_\Lambda$He	-70.54(1)	-70.41(25)	-
	B_Λ	39.92(1)	39.67(25)	-

$$V_{S=0}(r) = V_1 e^{-\mu_1 r^2} + V_2 e^{-\mu_2 r^2} \ ;$$
$$V_{S=1}(r) = V_1 e^{-\mu_1 r^2} + V_3 e^{-\mu_3 r^2} \ .$$

(3.72)

where: $V_1 = 200\,\mathrm{MeV}$, $V_2 = -91\,\mathrm{MeV}$, $V_3 = -178\,\mathrm{MeV}$ and $\mu_1 = 1.487\,\mathrm{fm}^{-2}$, $\mu_2 = 0.465\,\mathrm{fm}^{-2}$ and $\mu_1 = 0.639\,\mathrm{fm}^{-2}$. As YN interaction the isospin $T = 0$ channel ($V_{S=1}$) of the total Minnesota potential multiplied by a factor 0.9 has been used. The NSHH results are compatible with NCSM ones. In the 4- body case a shift in the AFDMC energy is present, but this is not unexpected, due to the technical limits of the method when open shell systems are considered. In fact, the binding and separation energies for the closed shell system $^{5}_{\Lambda}\mathrm{He}$ are fully compatible with our NSHH results. The NCSM results are compatible with the NSHH ones, although the matching is not optimal. However such calculations were performed in a preliminary testing phase and more precise benchmark results will be provided in chapter 5.

In appendix C more results are provided. In line with all the preceding EIHH calculations performed in the nuclear sector [16, 56], we adopted the Lee-Suzuki approach with $K_{\mathrm{max}}^{\mathrm{eff}} = 60$ for soft-core potentials, like the Minnesota one, and $K_{\mathrm{max}}^{\mathrm{eff}} = 120$ for hard-core interactions, like the Argonne vn potentials and the YN interactions that will be employed in chapter 5.

As part of a Master Thesis of the student C.A. Manzata the NSHH method has been applied to α-cluster models for $^{12}\mathrm{C}$ and $^{9}\mathrm{Be}$ with simple local $\alpha\alpha$ and αn potentials, obtaining agreement of the same order of the above results with the expected energies [72].

Chapter 4

Extensions of the NSHH Method

We introduce a number of extensions of the NSHH method that allow to include most of the hypernuclear interaction models defined in configuration space. However we define them in a general way so that they can be applied to any few-body system whose interactions can be treated by means of such extensions.

In section 4.1 we apply 3-body forces both for the NNN and NNΛ sector. We just adopt the approach of ref. [73] (and relative code) for the incorporation of the NNN force and we include minor extensions in order to take into account the presence of a Λ particle and of two different types of 3-body potentials.

In section 4.2 we introduce a new extension of the method in order to treat interaction models based on particle mixing. In particular we start by showing how to treat systems where the masses of the particles differ from the mass parameters of the adopted Jacobi set of coordinates. Such extension is not trivial since the use of the hyperspherical system of coordinates creates a strong correlation between the HH basis and the mass parameters, and a change in one or more of them causes a change in the whole structure of the HH basis. We overcome this problem by acting on the kinetic energy operator. We then apply such extension in order to include interactions that couple different species for one or more particles by introducing new single-particle degrees of freedom. By exploiting the same formalism we also show how to define spatial permutations between different particles.

Finally in section 4.3 we briefly describe the work done and the adopted approach for the parallelization of the NSHH calculations, but we avoid any technical detail.

4.1   Implementation of 3-Body Forces

With the inclusion of the 3-body forces, the total Hamiltonian of a Λ-hypernucleus is given by:

$$
\begin{aligned}
H &= T + V_{NN} + V_{N\Lambda} + V_{NNN} + V_{NN\Lambda} \\
&= T + \sum_{i<j=2}^{N} V_{ij} + \sum_{j=1}^{N} V_{jA} + \sum_{i<j<k=3}^{N} V_{ijk} + \sum_{i<j=2}^{N} V_{ijA} \,,
\end{aligned}
\tag{4.1}
$$

where we assumed the Λ particle being in the last position of the Jacobi set. Of course if $A = 3$ the V_{NNN} term is not present.

Analogously to eq. (3.4) for the 2-body case, each 3-body term of the potential is calculated by means of the $\mathcal{Q}$ transformations:

$$
\begin{aligned}
V_{ijk}^{[S_N][T_N]}[\mathbf{r}_{i,j,k}(\boldsymbol{\eta}^{123})] &= V_{ijk}^{\prime[S_N][T_N]}[\boldsymbol{\eta}^{123}] \\
&= V_{ijk}^{\prime[S_N][T_N]}[p_{ijk}^{123} \cdot \boldsymbol{\eta}^{ijk}] \\
&= \mathcal{Q}_{ijk}^{123} \cdot V_{ijk}^{\prime\prime[S_N]^{ijk}[T_N]^{ijk}}[\boldsymbol{\eta}_N^{ijk}, \boldsymbol{\eta}_{N-1}^{ijk}] \cdot \mathcal{Q}_{123}^{ijk} \,,
\end{aligned}
\tag{4.2}
$$

where $\boldsymbol{\eta}^{ijk}$ denotes the Jacobi set of coordinates where, besides particles i and j moved in the first two positions of the coupling scheme, a third particle, k, is moved to the third position. The transformation $\mathcal{Q}_{123}^{ijk}$ is analogue to $\mathcal{Q}_{12}^{ij}$, but for the triplet of particles ijk instead of the couple ij.

The inclusion of 3-body terms implies additional coordinates involved in the calculation of the potential matrix elements with respect to the 2-body case. In order to separate the interacting 3-body part from the rest of the system, we perform a change of coordinates by passing from the standard set of angles and hyperangles Ω_N defined in eq. (2.35) to the new one of fig. 4.1:

$$
\Omega_{3,A-3} = (\tilde{\phi}_N, \Omega_{(3)}, \Omega_{A-3}) \,,
\tag{4.3}
$$

where $\Omega_{(3)}$ represents the angles and hyperangles of the 3-body interacting subsystem:

$$
\Omega_{(3)} = (\phi_{N,N-1}, \hat{\boldsymbol{\eta}}_{A-2}, \hat{\boldsymbol{\eta}}_{A-1}) \,,
\tag{4.4}
$$

and Ω_{A-3} represents those of the residual system:

$$
\Omega_{A-3} = (\phi_2, \ldots, \phi_{A-3}, \hat{\boldsymbol{\eta}}_1, \ldots, \hat{\boldsymbol{\eta}}_{A-3}) \,.
\tag{4.5}
$$

The hyperangle $\phi_{N,N-1}$ is related to the 3-body subsystem and $\tilde{\phi}_N$ is associated to the lower vertex in the hyperspherical tree diagram shown in fig. 4.1.
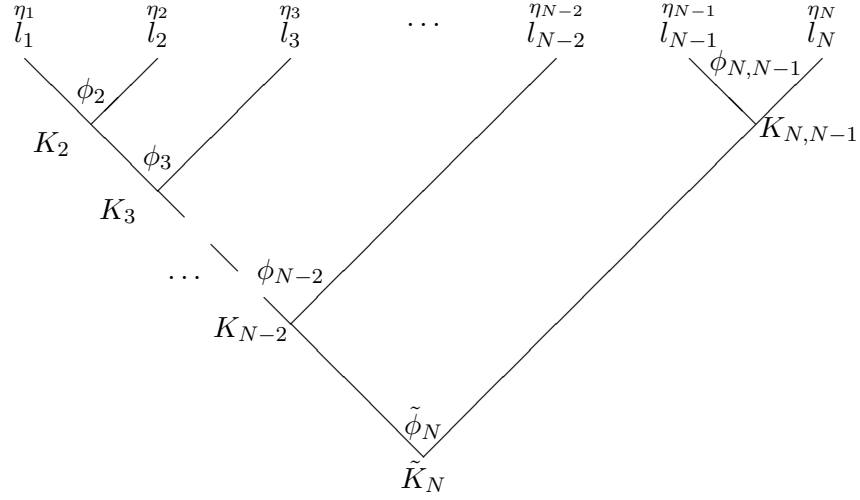
The following relations hold:

FIGURE 4.1: Tree diagram representing the non-symmetrized hyperspherical harmonic functions in the 3- plus $(A-3)$-body scheme.

$$\rho_{(3)} = \sqrt{\eta_{A-1}^2 + \eta_{A-2}^2} = \rho \sin \tilde{\phi}_N$$
$$\rho_{A-3} = \sqrt{\eta_1^2 + \ldots + \eta_{A-3}^2} = \rho \cos \tilde{\phi}_N \ . \tag{4.6}$$

The coordinates $\rho_{(3)}$ and $\Omega_{(3)}$ form a complete set for the 3-body subsystem and allow to calculate the matrix elements of the 3-body potential without involving spurious degrees of freedom related to the residual system.

The radial dependence of each 3-body term of the potential is related to the relative vectors connecting each couple of the particles composing the triplet. For the NNΛ triplet we have:

$$\mathbf{r}_{31/32} = \sqrt{\frac{2m + m_\Lambda}{2m_\Lambda}} \boldsymbol{\eta}_1 \pm \frac{1}{\sqrt{2}} \boldsymbol{\eta}_2 \ . \tag{4.7}$$

The spatial integration of the matrix elements is performed by employing the technique described in ref. [74]. By considering the last two Jacobi vectors:

$$\boldsymbol{\eta}_{A-1} = \rho_{(3)} \sin \phi_{N,N-1} \hat{\boldsymbol{\eta}}_{A-1} \ , \ \ \boldsymbol{\eta}_{A-2} = \rho_{(3)} \sin \phi_{N,N-1} \hat{\boldsymbol{\eta}}_{A-2} \ , \tag{4.8}$$

we can choose a reference frame where $\hat{\boldsymbol{\eta}}_{A-1}$ lies on the z axis and $\hat{\boldsymbol{\eta}}_{A-2}$ on the $(x-z)$ plane. Then the five coordinates $\phi_{N,N-1}$, $\hat{\boldsymbol{\eta}}_{A-1}$ and $\hat{\boldsymbol{\eta}}_{A-2}$ are replaced with:

$$x = \cos(2\phi_{N,N-1}) \ , \ \ y = \hat{\boldsymbol{\eta}}_{A-1} \cdot \hat{\boldsymbol{\eta}}_{A-2} \ , \tag{4.9}$$

plus the three Euler angles ω. The three body volume element turns into:

$$d\boldsymbol{\eta}_{A-1}d\boldsymbol{\eta}_{A-2} = \frac{1}{8}[\rho_{(3)}]^5 d\rho_{(3)} \sqrt{1 - x^2} dx dy d\omega \ . \tag{4.10}$$

The three body HH function becomes [73]:

$$
\begin{aligned}
\mathcal{Y}_{[K_2]M}(\Omega_2) &= {}^{(2)}\mathcal{P}_{K_2}^{l_2,l_1}(x)[Y_{l_1m_1}(\hat{\boldsymbol{\eta}}_{A-1}) \otimes Y_{l_2m_2}(\hat{\boldsymbol{\eta}}_{A-2})]_{LM} \\
&= {}^{(2)}\mathcal{P}_{K_2}^{l_2,l_1}(x)\sum_{M'} D_{M'M}^{(L)}(\omega)[Y_{l_1m_1}(\hat{\boldsymbol{\eta}}_{A-1}) \otimes Y_{l_2m_2}(\hat{\boldsymbol{\eta}}_{A-2})]_{LM'} \\
&= \sum_{M'} D_{M'M}^{(L)}(\omega)\mathcal{Y}_{[K_2]M'}(x,y) \ .
\end{aligned}
$$

$$(4.11)$$

The above expression allows to reduce the integration of the potential matrix elements from 5- to 3-dimensional, in fact, with simple manipulation one finds the reduced matrix elements for a coordinate space operator $V_{\lambda\mu}$ of rank λ and projection μ [73]:

$$
\begin{aligned}
\langle KLl_1l_2 \, ||V_\lambda(\rho_{(3)},\Omega_{(3)})||\, K'L'l_1'l_2'\rangle &= \sum_{MM'\mu} (-1)^{L+M} \begin{pmatrix} L & \lambda & L' \\ -M & \mu & M' \end{pmatrix} \\
&\cdot \pi^2 \int dx\sqrt{1-x^2}dy\mathcal{Y}_{[K_2]M}(x,y)V_{\lambda\mu}(\rho_{(3)},x,y)\mathcal{Y}_{[K_2']M'}(x,y) \ .
\end{aligned}
$$

$$(4.12)$$

The V_{NNN} matrix elements can be fully symmetrized. However, in the hypernuclear terms, only two particles obey symmetry constrictions and the above matrix element combined with the spin and isospin part can be set as null if the exchange condition $(-1)^{l_1+S_{NN}+T_{NN}} = -1$ is not satisfied.

4.2   Inclusion of Particle Mixing Extensions and Space-Exchange Operators

As anticipated in chapter 2, in case of different particle systems, spatial permutations cannot be described as compositions of kinematic rotations, since the association between mass and cartesian positon (m_i, r_i) inside the coordinate system is no longer conserved (see section 2.1.2). It is thus necessary to define the $\hat{P}_{ij}$ operators of eq. (2.19) in the HH basis in order to treat potentials with space-exchange terms as the one shown in eq. (2.21).

Moreover some interaction models are based on the explicit treatment of particle resonances or excitations degrees of freedom. In these cases the mass of a particle could depend on some of the quantum numbers defining a given state (for example the isospin of the particle itself). Examples of such models are the *Argonne v28* NN potential [75], which takes the $\Delta(1232)$ degree of freedom explicitly into account, and most of the modern hypernuclear YN interactions, based on the inclusion of the explicit $\Lambda - \Sigma$ coupling (see section 1.2).

We start from the simplest case of a single particle resonance inside an *A*-body system and we show how to extend it to the case of an arbitrary number of resonance degrees of freedom for one or more particles in the *A*-body system.

The aim is then to incorporate in the Hyperspherical Harmonics formalism the interaction models that explicitly include these kind of degrees of freedom.

We start by showing how to treat an *A*-body system in a HH basis where the mass parameters of the Jacobi set of coordinates are chosen different from the physical ones and then we show how to implement the above mentioned interaction models in the NSHH framework.

As simple application of the transformatios between different sets of mass parameters we also show how to include space-exchange operators between different particles.

4.2.1 HH Basis with Mass Parameters Different from the Physical Ones

By adopting the standard Jacobi set, where the mass parameters defining the coordinates coincide with the physical masses, the total Hamiltonian is given by:

$$H_{\text{tot}} = H_{\text{CM}}(\boldsymbol{\eta}_0) + H_{\text{int}}(\boldsymbol{\eta}_1, \dots, \boldsymbol{\eta}_N) \,, \tag{4.13}$$

where $\boldsymbol{\eta}_0$ is the rescaled CM coordinate defined in eq. (2.4). The separation of the CM part is trivial in this case since the CM part of the Hamiltonian and the internal one depend on the CM coordinate and on the internal Jacobi vectors respectively.

If the internal coordinates $\boldsymbol{\eta}_1, \dots, \boldsymbol{\eta}_N$ are not defined on the physical set of mass parameters, we have:

$$\begin{aligned} H_{\text{tot}} &= H_{\text{CM}} \left[\boldsymbol{\eta}_0(\boldsymbol{\eta}_0', \boldsymbol{\eta}_1', \dots, \boldsymbol{\eta}_N') \right] + H_{\text{int}} \left[\boldsymbol{\eta}_1(\boldsymbol{\eta}_1', \dots, \boldsymbol{\eta}_N'), \dots, \boldsymbol{\eta}_N(\boldsymbol{\eta}_N') \right] \\ &= H_{\text{CM}}' \left(\boldsymbol{\eta}_0', \boldsymbol{\eta}_1', \dots, \boldsymbol{\eta}_N' \right) + H_{\text{int}}' \left(\boldsymbol{\eta}_1', \dots, \boldsymbol{\eta}_N' \right) \,, \end{aligned} \tag{4.14}$$

where $\boldsymbol{\eta}_0', \dots, \boldsymbol{\eta}_N'$ are defined on a non physical set of masses. In this case H_{CM} and H_{int} depend both on the internal Jacobi coordinates. However, due to the invariance of the internal subspace $\langle \boldsymbol{\eta}_1, \dots, \boldsymbol{\eta}_N \rangle$ with respect to any change of mass parameters, one can always substitute the $\boldsymbol{\eta}_0$ coordinate with $\boldsymbol{\eta}_0'$ to obtain:

$$H_{\text{tot}} = H_{\text{CM}}(\boldsymbol{\eta}_0) + H_{\text{int}}'(\boldsymbol{\eta}_1', \dots, \boldsymbol{\eta}_N') \,, \tag{4.15}$$

where H_{CM} is separable as in eq. (4.13). By considering the two different internal Jacobi sets $\boldsymbol{\eta}$ and $\boldsymbol{\eta}'$, two different HH bases are defined, but the

transformation from one to another is not trivial since it involves both the hyperradial and the hyperangular coordinates, as shown in section 2.2.

The problems due to the use of a Jacobi system of coordinates based on a set of mass parameters different from the physical ones are related to the calculation of the kinetic energy operator T'_{int}:

$$T'_{\text{int}}(\boldsymbol{\eta}) = T_{\text{int}}\left[\boldsymbol{\eta}'(\boldsymbol{\eta})\right] = T_{\text{int}}\left(W_{\zeta\zeta'} \cdot \boldsymbol{\eta}\right) , \qquad (4.16)$$

where $W_{\zeta\zeta'}$ is the coordinate transformation defined in eq. (2.29) and ζ and ζ' are the mass parameter sets related to the Jacobi sets $\boldsymbol{\eta}$ and $\boldsymbol{\eta}'$ respectively. In fact the kinetic energy operator in the hyperspherical set of coordinates has no longer the form of eq. (2.42) and the hyperradial term is not separable from the hyperangular term.

If one builds the T'_{int} operator by adopting the NSHH basis defined on the $\boldsymbol{\eta}$ set instead of the natural one $\boldsymbol{\eta}'$, two alternatives are allowed: the explicit calculation of T'_{int} in the chosen HH basis or the calculation of T'_{int} in the natural HH basis followed by the application of a suitable transformation to pass to the HH basis defined over the $\boldsymbol{\eta}$ Jacobi set:

$$|\mathcal{L}_{n'}(\rho, \Omega_N)\rangle\, |\mathcal{Y}_{[K'_N]}(\Omega_N)\rangle = \sum_{[K_N],n} \mathcal{W}_{[K_N],n}^{[K'_N],n'}\, |\mathcal{L}_n(\rho)\rangle\, |\mathcal{Y}_{[K_N]}(\Omega_N)\rangle , \quad (4.17)$$

where we have stressed the fact that the dependence on ρ and Ω_N is no longer separate in the HH basis built over $\boldsymbol{\eta}$. If we denote with hh the HH basis defined on the Jacobi set $\boldsymbol{\eta}$ and with hh' the HH basis built over $\boldsymbol{\eta}'$, we have:

$$T'_{\text{int},hh} = \mathcal{W}^{\dagger}\, T'_{\text{int},hh'}\, \mathcal{W} , \qquad (4.18)$$

where the $\mathcal{W}$ operator represents the transformation of eq. (2.29) in the HH basis. A new formalism to treat such transformations in the HH framework and beyond is under development and it will be introduced in the near future. However, in order to perform hypernuclear bound state calculations, we look for an alternative approach. The adopted one is the direct calculation of the kinetic energy operator in the HH basis defined over the $\boldsymbol{\eta}$ Jacobi set. So we consider the operator $T'_{\text{int},hh}$ in the $\boldsymbol{\eta}$ set and calculate the matrix elements directly in the starting HH basis.

The simplest case is when only the last mass parameter m_A in the Jacobi set of coordinates is different from the corresponding physical mass. In this case the coordinate transformation of the Jacobi set is given by $W_{(A)}$, defined in eq. (2.27). By denoting $T' = T'_{\text{int}}$, the kinetic energy operator

becomes:

$$
\begin{aligned}
T' &= \frac{\hbar^2}{2m}\left(\Delta_{\eta_1'} + \Delta_{\eta_2'} + \ldots + \Delta_{\eta_N'}\right) \\
&= \frac{\hbar^2}{2m}\left(\frac{1}{a_A^2}\Delta_{\eta_1} + \Delta_{\eta_2} + \ldots + \Delta_{\eta_N}\right) \\
&= T + \Delta_T \,,
\end{aligned}
\tag{4.19}
$$

where the constant a_A is the proportionality constant between $\boldsymbol{\eta}_1$ and $\boldsymbol{\eta}_1'$:

$$
a_A = \sqrt{\frac{m_A}{M_A}\frac{M_A'}{m_A'}} \,.
\tag{4.20}
$$

The operator Δ_T is then given by:

$$
\Delta_T = \frac{\hbar^2}{2m}\left(\frac{a_A^2 - 1}{a_A^2}\Delta_{\eta_1}\right) = \frac{\hbar^2}{2m}\frac{M_{A-1}(m_A' - m_A)}{M_A m_A'}\Delta_{\eta_1} \,.
\tag{4.21}
$$

By calculating explicitly the Δ_{η_1} operator one can solve the A-body problem in the HH basis with $m_A \neq m_A'$. In appendix A the explicit form of the generic Δ_{η_i} operator in the A-body NSHH basis is provided.

In fig. 4.2 we observe a comparison between the convergence patterns of the binding energies for a 3-body Λ-hypernucleus interacting via the Argonne V4' [68] NN and the 2-body Bodmer-Usmani [46] (no space exchange term) ΛN potentials first in the case where the mass parameters of the Jacobi set of coordinates coincide with the physical masses and, in the second case, where the mass parameter related to the Λ particle is set equal to the nucleon mass and the operator ΔT of eq. (4.21) is added to the Hamiltonian (we remind the ratio of the two masses: $m_N \approx 0.84\, m_\Lambda$).

We observe a convergence a bit slower in the case with unphysical mass parameters, due to the fact that the quality of the adopted basis is lower with respect to the former case. In fact, the HH functions are not anymore the eigenfunctions of the total hyperangular kinetic energy operator, but they are eigenfunctions of the analogue operator in a system with the Λ particle having the mass equal to the nucleon one. Moreover, due to the fact that the ΔT operator in eq. (4.19) cannot be splitted into an hyperradial and an hyperangular term as the T operator, when the Lee-Suzuki effective interaction is applied, it does not involve such operator. This means that the "medium correction" effect mentioned in section 3.4 is reduced. Finally, the hyperradius is defined over an unphysical set of mass parameters, so the confinement due to this collective coordinate is not optimal anymore.

The binding energy in the two cases calculated for $K_{\text{max}} = 30$:

$$E^{3b}_{\Delta T} = -2.524(2) \text{ MeV}$$
$$E^{3b} = -2.530(3) \text{ MeV} .$$

(4.22)

We see that the compatibility is not optimal, due to fact that $E^{3b}_{\Delta T}$ is still not in full convergence. In the 4-body case, the convergence patterns are closer with respect to the 3-body case, due to the fact that the total mass ratio:

$$r_M = \frac{(A-1)m_N + m_\Lambda}{Am_N}$$

(4.23)

is smaller. We have:

$$E^{4b}_{\Delta T} = -12.015(2) \text{ MeV}$$
$$E^{4b} = -12.025(3) \text{ MeV} .$$

(4.24)

In both 3- and 4-body cases the system with all nucleon masses and without the addition of ΔT does not bind.

It is clear that, the bigger is r_M, the less advantageus is such approach. However, as it will be shown in section 4.2.3, the aim is to introduce particle mixing extensions, in particular the $\Lambda - \Sigma$ hyperons mixing in hypernuclei with $A \geq 3$. In this case the mass ratio between the system with the Λ and the system with the Σ is sufficiently close to one.

If the mass parameters different from the physical masses are more than one, mixed derivative terms appear in the kinetic energy operator. However, they can be calculated by means of kinematic rotations. By recalling eq. (2.10) we have:

$$T' = -\frac{\hbar^2}{2m} \nabla^T_\eta \cdot S' \cdot \mathcal{M}' \cdot (\mathcal{M}^{-1})^2 \cdot \mathcal{M}' \cdot S'^T \cdot \nabla_\eta - T_{CM}$$
$$= -\frac{\hbar^2}{2m} \left[\sum_{i=1}^{N} c_i \Delta_{\eta'_i} + \sum_{i<j} d_{ij} \nabla_{\eta'_i} \cdot \nabla_{\eta'_j} \right] ,$$

(4.25)

where $\mathcal{M}'$ is the matrix of eq. (2.6) with the mass parameters of the adopted Jacobi set instead of the physical masses, contained in $\mathcal{M}$. S' is the matrix related to the change of coordinates from the Jacobi set $\boldsymbol{\eta'}$ to the cartesian set. The c_i and the d_{ij} coefficients are determined from the application of the $\mathcal{M}$ and the S' matrices.

From eq. (2.12) and followings one can arrange the mixed derivative term of two consecutive Jacobi vectors as:

$$\nabla_{\eta_i} \cdot \nabla_{\eta_{i+1}} = \frac{1}{a_i b_i} \left(-\Delta_{\eta^p_i} + a_i^2 \Delta_{\eta_i} + b_i^2 \Delta_{\eta_{i+1}} \right) ,$$
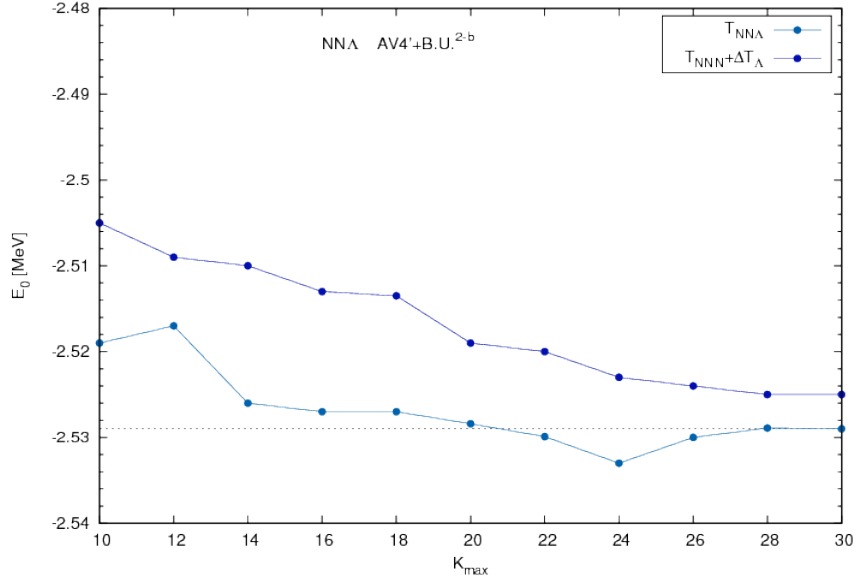
(4.26)

FIGURE 4.2: Convergence patterns of the binding energy for the $^3_\Lambda$H hypernucleus with the AV4' NN interaction combined with the Bodmer-Usmani ΛN potential for two different HH bases built on two different Jacobi sets. The convergence is slower when the mass parameter of the Λ particle is set equal to the nucleon mass (upper line). Lee-Suzuki EI is applied.

where:

$$a_i = \cos\beta_{A-i} \; ; \qquad b_i = \sin\beta_{A-i+1} \, , \tag{4.27}$$

and $\Delta_{\eta_i^p}$ is the laplacian term related to the transformed $\boldsymbol{\eta}_i$ coordinates after the application of the $p_{i,i+1}$ kinematic rotation:

$$\boldsymbol{\eta}_i^p = p_{A-i,A-i+1} \cdot \boldsymbol{\eta}_i \tag{4.28}$$

If two Jacobi vectors are not consecutive and the difference between their indices is n, the corresponding mixed derivative term can be expressed in terms of mixed derivative terms between Jacobi vectors with indices different by a number smaller that n. By applying a sequence of n kinematic rotations, with some manipulation the following iterative rule holds:

$$\nabla_{\eta_i} \cdot \nabla_{\eta_{i+n}} = \frac{1}{a_i b_i \ldots b_{i+n}} \left[-\Delta_{\eta_i^{p^n}} + \sum_{j=1}^{n+1} a_j (b_i \ldots b_{i+n}) \Delta_{\eta_{i+j-1}} + \right.$$
$$\left. + \sum_{\alpha < \beta}^{n} (b_i \ldots b_{i+\alpha})(b_i \ldots b_{i+\beta}) a_{i+\alpha} a_{i+\beta} \nabla_{\eta_{i+\alpha}} \cdot \nabla_{\eta_{i+\beta}} \right]$$

$$\tag{4.29}$$

where $\Delta_{\eta_i^{p^n}}$ is the laplacian term related to the $\boldsymbol{\eta}_i$ vector transformed by p_i^n, where:

$$p_i^n = p_{(i,i+1)} \cdot p_{(i+1,i+2)} \cdot \ldots \cdot p_{(i+n-1,i+n)} \, . \tag{4.30}$$

In this way one can calculate the kinetic energy operator in a set of Jacobi coordinates with mass parameters different from the physical masses. We have:

$$\begin{aligned} T' &= \sum_i \left[c_i \Delta_{\eta_i} + \sum_{n=1}^{N-i} d_i \Delta_{\eta_i^{p^n}} \right] \\ &= T + \sum_i \left[(c_i - 1) \Delta_{\eta_i} + \sum_{n=1}^{N-i} d_i \Delta_{\eta_i^{p^n}} \right] \end{aligned} \tag{4.31}$$

where the c_i and d_i coefficients have to be determined by means of the above iterative scheme. The above equation allows to calculate the kinetic energy operator in the HH basis with different mass parameters by avoiding multidimensional integrations, since the matrix elements of each Δ_{η_i} operator can be calculated by means of one dimensional integrals, as shown in appendix A.

The general form of the Δ_T operator in the HH basis:

$$\Delta T = \sum_i \left[(c_i - 1) \Delta_{\eta_i} + \sum_{n=1}^{N-i} d_{i,i+n} \left(\prod_{j=i+n-1}^{i} \mathcal{P}^{(j)} \right) \Delta_{\eta_i} \left(\prod_{j=i}^{i+n-1} \mathcal{P}^{(j)} \right) \right] \, , \tag{4.32}$$

where the $\mathcal{P}^{(j)}$ operators are defined in section 3.1.

We show the explicit form of the ΔT operator in case of two particles with masses different from the corresponding Jacobi mass parameters (for simplicity we assume the two mass parameters in the last positions of the Jacobi scheme):

$$\Delta T_{m_N, m_A} = (c_1 - 1) \Delta_{\eta_1} + (c_2 - 1) \Delta_{\eta_2} + d_{1,2} \mathcal{P}^{(N)} \Delta_{\eta_1} \mathcal{P}^{(N)} \, , \tag{4.33}$$

with $N = A - 1$. In fig. 4.3 the convergence pattern of the binding energy of an unrealistic 3-body system with two particles with mass m_Λ interacting through AV4' potential and one particle with mass m_N interacting through the Bodmer-Usmani interaction is shown. The aim is to test the implementation of the operator of eq. (4.33) and compare the obtained result with the energy calculated in the usual way, where the mass parameters coincide with the physical masses. As expected, the bigger mass ratio:
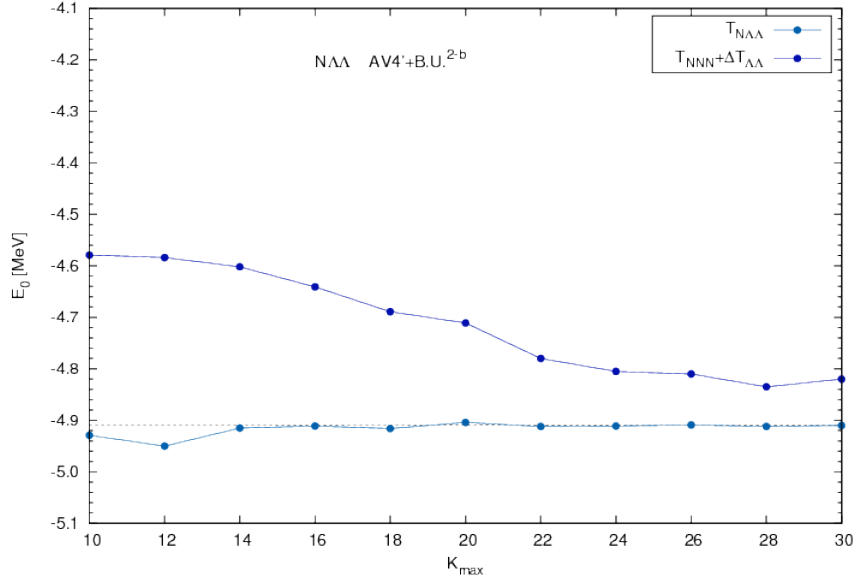
$$r_M = \frac{m_N + 2m_\Lambda}{3m_N} \tag{4.34}$$

FIGURE 4.3: Convergence patterns of the binding energy of an unrealistic 3-body system with two particles with mass m_Λ interacting through AV4' potential and one particle with mass m_N interacting through the Bodmer-Usmani interaction. Again the convergence is slower when the mass parameter of the Λ particle is set equal to the nucleon mass (upper line). Lee-Suzuki EI is applied.

leads to a slower convergence pattern in the first case. The energies in the two cases:

$$E_{\Delta T}^{3b} = -4.810(10) \text{ MeV}$$
$$E^{3b} = -4.911(1) \text{ MeV} .$$

(4.35)

4.2.2 Spatial Permutation Operators

A first direct application of the above extension is the treatment of spatial permutations for different particles. As explained in section 2.1.2, when different particles are involved, the kinematic rotations no longer coincide with spatial permutations. A spatial permutation, in general, is a composition of kinematic rotations and transformations of the mass parameters. The action of a generic spatial transposition between particles i and j on the Jacobi set is given by [we recall eq. (2.30)]:

$$
\begin{aligned}
P_{ij}\,\boldsymbol{\eta} &= W_{ij} \cdot p_{i,j} \cdot \boldsymbol{\eta}\left[(m_1, \mathbf{r}_1), \ldots, (m_i, \mathbf{r}_i), \ldots, (m_j, \mathbf{r}_j), \ldots\right] \\
&= \boldsymbol{\eta}\left[(m_1, \mathbf{r}_1), \ldots, (m_j, \mathbf{r}_j), \ldots, (m_i, \mathbf{r}_i), \ldots\right] .
\end{aligned}
$$

(4.36)

However, if the mass parameters related to the particles to permute, m_i and m_j, are both equal to m, then the permutation coincides with the sequence

of kinematic rotations needed to exchange $(m, \mathbf{r}_i)$ and $(m, \mathbf{r}_j)$:

$$P_{ij} = p_{i,j} \ . \tag{4.37}$$

The price to pay is that the kinetic energy is not diagonal anymore in the hyperangular part of the basis and the operator ΔT defined in the previous section has to be explicitly evaluated.

As example we consider a Λ-hypernucleus and the 2-body Bodmer Usmani potential of eq. (2.21) as ΛN interaction. By choosing a HH basis where the mass parameter related to the Λ hyperon, m_Λ, is equal to the nucleon mass, m_N, the Hamiltonian looks:

$$H = T + \Delta T_\Lambda + \sum_{i<j=1}^{A-1} V_{ij} + \sum_{i=1}^{A-1} V_{iA} \ , \tag{4.38}$$

where we assumed the Λ particle in the last position of the Jacobi set. The spatial exchange operator $\hat{P}_{N_i\Lambda}$ of eq. (2.21) included in each V_{iA} term is given by:

$$\hat{P}_{N_iA} = \mathcal{P}^{i,A} \ . \tag{4.39}$$

However, in the specific case of spatial permutations, one can also explicitly calculate the space exchange operator $\hat{P}_{N_iA}$ defined in the natural HH basis where the mass parameters coincide with the physical masses. If we denote as T_b the kinetic energy operator in the HH basis defined on the natural Jacobi set and as T_a the kinetic energy operator in the basis where particles N_i and Λ are spatially permuted (which can be calculated by means of kinematic rotations and the iterative scheme described in the previous section), one can solve the following equation:

$$\hat{P}_{N_iA} \, T_b \, \hat{P}_{N_iA} = T_a \ , \tag{4.40}$$

which is a second order algebraic Riccati equation with analytical solution [76]:

$$\hat{P}_{N_iA} = T_b^{-1}(T_b \cdot T_a)^{1/2} \ . \tag{4.41}$$

However this last approach has not been implemented and the computational weight due to the calculation of the above operator could become significant by increasing the dimension of the basis.

4.2.3 Particle Mixing

When an interaction model that couples different particles is adopted, in general, the mass of the involved particles is related to a given quantum number defining the basis states (for example the isospin in the case of $\Lambda - \Sigma$

coupling). We call it t. The complete A-body Hamiltonian is then:

$$H = T_{CM}(t) + H_{\text{int}}(t) .$$ (4.42)

Since we are looking for a translationally invariant state that minimizes $\langle H_{\text{int}} \rangle$, we consider a generic total wave function:

$$\Psi = \Psi_{\text{CM}}(\boldsymbol{\eta}_0) \cdot \Psi_{\text{int}}(\rho, \Omega_N, t) ,$$ (4.43)

and we look for Ψ_{int} such that:

$$\delta \frac{\langle \Psi_{\text{int}} | H_{\text{int}} | \Psi_{\text{int}} \rangle}{\langle \Psi_{\text{int}} | \Psi_{\text{int}} \rangle} = 0$$ (4.44)

by solving the eigenvalue problem related to H_{int} (from now on we denote H_{int} with H).

We first consider the simplest case of an A-body system with $A - 1$ particles of a given species, q, and one particle, p_A, of a different species, p, and we include a potential V_{qp} that couples p to a third species, p^*.
As already mentioned, we define a label, $t = 0, 1$, related to the p^* degree of freedom induced by the interaction V_{qp}. If $t = 0$ then p_A belongs to the species p, otherwise to p^*.
The Hamiltonian is:

$$H = T + \Delta M + \sum_{i<j=1}^{A-1} V_{q_i q_j} + \sum_{i=1}^{A-1} V_{q_i p_A} .$$ (4.45)

In the following we consider the block structure of each term of the Hamiltonian in the quantum number t:

$$H = \begin{pmatrix} H^{00} & H^{01} \\ H^{10} & H^{11} \end{pmatrix} .$$ (4.46)

where $H^{ab} = \langle t = a | H | t = b \rangle$. The ΔM term is the matrix related to the mass difference between p and p^* in energy units:

$$\Delta M = \begin{pmatrix} 0 & \\ & \Delta M_{p,p^*} \end{pmatrix} .$$ (4.47)

In this case the block $\Delta M_{p,p^*}$ is diagonal and proportional to the identity matrix through $(m_{p^*} - m_p)$ in energy units. In the next chapter, however, we will see the slightly more complex case of the $\Lambda - \Sigma$ coupling (with $q = N$, $p = \Lambda$ and $p^* = \Sigma$), where $m_p = m_\Lambda$ and m_{p^*} depends on the isospin projection t_z of the Σ particle, being m_{Σ^-} if $t_z = -1$, m_{Σ^0} if $t_z = 0$ and m_{Σ^+} if $t_z = 1$. In this case $\Delta M_{p,p^*}$ is not diagonal in the total A-body isospin

basis of eq. (2.69).

Due to the difference between the masses of p and p^*, we apply the procedure described in section 4.2.1 to calculate the kinetic energy difference related to the difference between the p^* mass and the p mass. We choose the mass parameter of the particle p_A in the Jacobi set of the adopted HH basis equal to m_p. The T operator is then:

$$T = \begin{pmatrix} T & \\ & T + \Delta T_{p_A} \end{pmatrix} , \tag{4.48}$$

where ΔT_{p_A} is derived by means of eq. (4.21):

$$\Delta T_{p_A} = \frac{\hbar^2}{2m} \frac{N m_q (m_{p^*} - m_p)}{(N m_q + m_p) m_{p^*}} \Delta_{\eta_1} . \tag{4.49}$$

In this way each term of the total potential in eq. (4.45) can be calculated by means of the usual procedure through the application of the $\mathcal{Q}$ transformations as shown in eq. (3.4). The block structure in t of the V_{qp} potential is:

$$V_{qp} = \begin{pmatrix} V_{qp-qp} & V_{qp^*-qp} \\ V_{qp-qp^*} & V_{qp^*-qp^*} \end{pmatrix} , \tag{4.50}$$

where:

$$V_{qp-qp^*} = \langle t = 0 | V_{qp} | t = 1 \rangle \tag{4.51}$$

and V_{qp^*-qp} are the coupling blocks providing the mixing between the p and the p^* species. Of course, since V_{qq} does not depend on t, we have:

$$V_{qq} = \begin{pmatrix} V_{qq-qq} & \\ & V_{qq-qq} \end{pmatrix} . \tag{4.52}$$

By implementing the above extensions, the NSHH method can be applied without particular complications to systems with mixing interactions. The Casimir operator simply splits in t:

$$\hat{C} = \begin{pmatrix} C(A-1) & \\ & C(A-1) \end{pmatrix} . \tag{4.53}$$

However one particular possibility is $p^* = q$. In this specific case the Casimir operator becomes:

$$\hat{C} = \begin{pmatrix} C(A-1) & \\ & C(A) \end{pmatrix} . \tag{4.54}$$

since the $t = 1$ part of the basis must be symmetric with respect to A particles of species q instead of $A - 1$.

The above scheme can be easily generalized (net of computational weight)

to an arbitrary number of mixing degrees of freedom for a single particle and to an arbitrary number of particles subjected to an interaction that couples different species.

For simplicity we only show the case of two particles of species p (p_1 and p_2) in an A-body system of particles of species q and we consider the previous potentials V_{qq} and V_{qp}.

In this case the block structure of the Hamiltonian is:

$$
H = \begin{pmatrix}
H^{00-00} & V^{00-10} & V^{00-01} & V^{00-11} \\
V^{10-00} & H^{10-10} & V^{10-01} & V^{10-11} \\
V^{01-00} & V^{01-10} & H^{01-01} & V^{01-11} \\
V^{11-00} & V^{11-10} & V^{11-01} & H^{11-11}
\end{pmatrix} ,
\tag{4.55}
$$

with $H^{ab-cd} = \langle t_{p_1} = a, t_{p_2} = b | H | t_{p_1} = c, t_{p_2} = d \rangle$. The non diagonal blocks are the mixing parts of the potential V_{qp}. The kinetic energy, in this case, needs an additional ΔT term due to the change of the two mass parameters related to the two particles of species p:

$$
T = \begin{pmatrix}
T & & & \\
& T + \Delta T_{q_2} & & \\
& & T + \Delta T_{p_2} & \\
& & & T + \Delta T_{p_2 q_2}
\end{pmatrix} ,
\tag{4.56}
$$

where $\Delta T_{p_2 q_2}$ is obtained by means of eq. (4.33). The Casimir operator in this case must take into account the symmetry in the $t_{p_1} = 1$ and $t_{p_2} = 1$ part of the basis:

$$
\hat{C} = \begin{pmatrix}
C(A-2,2) & & & \\
& C(A-2) & & \\
& & C(A-2) & \\
& & & C(A-2,2)
\end{pmatrix} .
\tag{4.57}
$$

The natural application of such scheme are of course $\Lambda\Lambda$-hypernuclei. However, the lightest known hypernuclear system is the $^{6}_{\Lambda\Lambda}\text{He}$ and more work is needed in the parallelization of the NSHH code in order to be able to treat such system. In the next chapter we show how such calculation has been set, but without providing results.

4.3   Parallelization of the NSHH Method

The serial approach to the NSHH calculations is rather efficient when dealing with systems up to $A = 4$, depending on the complexity of the interaction models. However, already in the 5-body case like, for example, the hyperhelium $^{5}_{\Lambda}\text{He}$ with a combination of central potentials like the Argonne

V4′ NN and the Usmani ΛN ones, the serial computation time grows considerably approaching to the order of months for an average laptop processor. Moreover, the use of more realistic non central interaction models, 3-body forces or particle mixing interactions, make the serial approach to 4-body calculations highly time consuming too.

For these reasons the implementation of a parallelization procedure becomes necessary when the physical investigation is intended to go beyond the 4-body and, in some cases, the 3-body sector.

In the following subsection we first present a variation on the NSHH method (whose idea was proposed to the author by Nir Barnea [77]), that has been used as a testing tool. In section 4.3.2 we briefly show the adopted parellel scheme by avoiding technical details. We stress that, although some results have been obtained, this part of the work is still partial, and further analysis is necessary.

4.3.1 A Variation on the NSHH Method

In a system of A identical particles, by adopting a symmetrized HH basis, the Hamiltonian looks:

$$H^{12} = T + \frac{A(A-1)}{2}V(\mathbf{r}_{12}) \ . \tag{4.58}$$

If we keep the same definition, but in the NSHH basis, the above operator is no longer a good Hamiltonian for the system, however, if Ψ_0 is the lowest antisymmetric eigenstate of H with the relative eigenvalue E_0, and Ψ_0^γ the lowest eigenstate of $\tilde{H}^{12}$, the following relation holds:

$$\lim_{\gamma\to\infty} \tilde{H}^{12}\,|\Psi_0^\gamma\rangle = \lim_{\gamma\to\infty} [H^{12} + \gamma(C(A) - \lambda\mathbb{I})]\,|\Psi_0^\gamma\rangle = E_0\,|\Psi_0\rangle \ . \tag{4.59}$$

In fact, although H^{12} does not commute with $C(A)$ and it has not a block diagonal structure in a basis with definite symmetry, in the limit $\gamma \to \infty$ the second term in eq. (4.59) forces the lowest eigenstates of $\tilde{H}^{12}$ to be antisymmetric, therefore the dominant part of H^{12} becomes the block made of antisymmetric states.

Of course the same reasoning can be applied to any other kind of systems with a given permutational symmetry. In case of an hypernuclear system with n_N nucleons and n_Y hyperons, assuming that the first two hyperons are in the i-th and $(i+1)$-th position of the Jacobi set, eq. (4.59) becomes:

$$\lim_{\gamma\to\infty} \left[T + \frac{n_N(n_N+1)}{2}V_{NN}(\mathbf{r}_{12}) + \frac{n_Y(n_Y+1)}{2}V_{YY}(\mathbf{r}_{i,i+1}) \right.$$
$$\left. + V_{\mathrm{mix}} + \gamma(C(n_N,n_Y) - \lambda\mathbb{I}) \right] |\Psi_0^\gamma\rangle = E_0\,|\Psi_0\rangle \ , \tag{4.60}$$

where V_{mix} is the part of the potential involving pairs of different particles, as shown in eq. (3.35).

The advantage of such procedure is the reduction of the number of matrix-vector multiplications in a single Lanczos iteration. In fact, as explained in subsection 3.5.1, the large dimension of the H matrix impedes the direct calculation and memorization of the whole matrix, therefore each single term is rebuilt "on flight" each time it has to be employed. By reducing the number of such operations, the computation time of a single iteration is reduced too. In particular, for an A identical particle system, the potential matrix in the standard Hamiltonian H is computed a number of times n_V:

$$n_V(H) = \frac{A!}{2(A-2)!} ,$$ (4.61)

which is the number of combinations of two in a set of A elements. By using the modified NSHH approach clearly the potential matrix is computed one single time. The total number of computations of the matrices of transpositions between adjacent particles in the standard NSHH aproach is given by:

$$n_P(H) = 2 \sum_{i<j=2}^{A} (i+j-3) ,$$ (4.62)

while, in the second case, the requested number is only due to the Casimir operator $C(A)$:

$$n_P(H^{12}) = \frac{A!}{2(A-2)!} + 2 \sum_{i<j=2}^{A} (j-i-1) .$$ (4.63)

In table 4.1 the numbers n_V and n_P are shown in a number of cases from $A=3$ to $A=5$.

In systems made of identical particles the number of computations of the V

TABLE 4.1: Number of matrix-vector multiplications with the potantial operator V (n_V) and with transpositions operators $P_{i,i+1}$ (n_P) for a single Lanczos computation in the NSHH case (H) and in the modified NSHH case (H^{12}).

System	$n_V(H)$	$n_V(H^{12})$	$n_P(H)$	$n_p(H^{12})$
^{3}H	3	1	6	5
$^3_\Lambda$H	3	3	6	6
^{4}H	6	1	24	14
$^4_\Lambda$H	6	4	24	23
$^5_\Lambda$He	10	5	60	50

and of the P matrices is significatively reduced when A grows starting from

$A = 4$. However, in presence of different particles the situation is different, due to the V_{mix} potential of eq. (3.35) which is not subjected to permutational symmetry constraints and which has to be explicitly computed in the entire form, as shown in eq. (4.60). It is clear that the more different species are involved, the less advantages this modified NSHH method provides, especially considering that the target for few-body calculations up to now in most of the cases is $A \leq 7$. Already in presence of a single different particle, as shown in table 4.1 we see that $n_V(H^{12})$ and $n_P(H^{12})$ approaches to $n_V(H)$ and $n_P(H)$ respectively.

However, also in the identical particles case the gain in the computation of each Lanczos step is partially lost by a significative increase (about one order of magnitude in most of the cases) in the total number of Lanczos steps necessary in order to reach convergence.

4.3.2   The Parallel Scheme

We do not treat technical details, rather we briefly show the adopted parallelization scheme and some simple additional modifications to the method which, in some cases, result advantageus.

We decided to employ an hybrid MPI+OpenMP approach in order to better exploit the architecture of most of the modern supercomputers where each of the $\mathcal{N}$ nodes is composed by a number $\mathcal{C}$ of CPUs with shared memory. In the previous chapter we saw the implementation of the method, where the lowest bound state energies and the relative eigenvectors are calculated through the Lanczos algorithm. The latter is a fundamentally sequential algorithm where each iteration involves the multiplication of the whole H matrix with a normalized vector and the resulting vector is employed in the next iteration. This means that the parallelization is applicable only into each single iteration, while the general sequential structure of the algorithm remains unchanged.

However, due to the non-symmetric character of the basis, the Hamiltonian is a sum of more terms, one for each couple of particles composing the system as shown in eq. (3.35), or, in presence of a 3-body force, one more for each triplet involved, as in eq. (4.1). Moreover each term is a product of more operators, namely the operator $\mathcal{Q}_{12}^{ij}$ [defined in eq. (3.6) and followings], the 2-body potential and the reversed order operator $\mathcal{Q}_{ij}^{12}$. The $\mathcal{Q}$ operator, in turn, is a product of all the needed exchange operators between adjacent particles in order to move particle i and j in the first coupling position and vice versa. This means that there is a non-parallelizable structure also inside each iteration of the Lanczos algorithm, namely the sequence of matrix-vector multiplication due the different operators composing each term of the total potential operator.

By denoting as Ψ the Lanczos vector, each matrix-vector multiplication is

parallelized with the following scheme:

$$\Phi_i^{n(i)c(i)} = \sum_j H_{ij}\Psi_j \quad ; \quad i,j = 1,2,\ldots,\dim[H(\rho)] \qquad (4.64)$$

where the index $n(i)$ and $c(i)$ denote the node label and the CPU label associated to the i-th HH basis state respectively:

$$n(i) = \mathrm{mod}\left(\frac{i-1}{\mathcal{N}}\right) \quad ; \quad c(i) = \frac{1}{\mathcal{C}}\left(\frac{i}{\mathcal{N}}+1\right) . \qquad (4.65)$$

We performed tests mainly on a 5-body system with $K_{\max} = 16 \div 20$. By means of such approach we obtained an almost linear time scaling until a number of 40 nodes, where a scale factor of 30 is obtained in the MPI part. After this threshold the gain start to slow down. A deeper technical analysis is needed in order to fully exploit the parallel structure of the algorithm.

Chapter 5

Application of NSHH to Hypernuclei

In this last part of the work we apply the formalism developed in the previous chapters to provide a number of selected benchmark results for binding an separation energies of systems up to $A = 5$ (part of the results is present in ref. [78]). We also set up new calculations to be performed in the near future as natural continuations of the present work.

As anticipated in chapter 1, quite a variety of potential models involving hyperons exist and ab initio calculations allow to test the quality of these interactions by providing a comparison of experimental and theoretical results for given observables, mostly binding and separation energies of hypernuclei. In fact the result of an ab initio calculation only depends on the chosen interaction model, thus one is led to a clearcut conclusion about its validity when comparing to experimental data. On the other hand, since any calculation is made with a finite accuracy, one may ask for the precision of the obtained ab initio results. Of course one can try to make error estimates, but it is more instructive to benchmark various ab initio methods for a few selected observables. An extensive benchmark test has been made, for example, in the non-strange sector of nuclear physics for the [4]He case [69] about fifteen years ago, involving seven different ab-initio methods. It is not the present aim to replicate such analysis with hypernuclei, rather we calculate a selected number of binding and separation energies for systems with $A = 3 \div 5$ and compare them with results from three other ab-initio methods. The aim is then to test and introduce the Non-Symmetrized Hyperspherical Harmonics method as new ab-initio approach to study light hypernuclei. The three other considered methods are the Auxiliary Field Diffusion Monte Carlo (AFDMC) method, the Faddeev-Yakubovski (FY) approach and the Gaussian Expansion Method (GEM). In particular we note that, due to the limited diffusion of the Bodmer-Usmani

interaction model, no benchmark tests have been made with AFDMC cal-
culations in the hypernuclear sector. In fact an almost independent line of
research based on the application of the AFDMC method on hypernuclear
systems with the phenomenological Bodmer-Usmani interaction model has
been developed in the last few years, with significative results both for hy-
pernuclei and hypermatter [12, 47]. Because of this, we retain useful to ex-
ploit the NSHH method as a benchmark instrument to compare the range
of accuracy of the AFDMC results and, in a future study, to work on a possi-
ble reduction of the uncertainties on the fitted parameters of the interaction.
In order to test the mixing extensions introduced in the previous chapter,
we also perform 3- and 4-body calculations by considering a second YN in-
teraction, namely the NSC97f simulated gaussian YN potential [14], which
simulates the scattering phase shifts given by NSC97f [79].

As landmarks we will refer to results from the well tested Faddeev-Yakubovski
(FY) method in the 3-body sector and from the Gaussian Expansion Method
(GEM) in the 3- and 4-body sector. As nuclear NN interactions we employ
the phenomenological 2-body Argonne V4' and V8' potentials [68].

Finally we show how we set up a 6-body calculation for the binding en-
ergy of the lightest $^{6}_{\Lambda\Lambda}$He hypernucleus by implementing the extensions
described in the previous chapter. However, more work on the paralleliza-
tion is needed in order to obtain results.

5.1   The Hamiltonians

As shown in chapter 1 the hypernuclear Hamiltonian is composed by a
nuclear part, an hyperonic part and the mix potential. In the following
calculations we consider Λ-hypernuclei and the last section we set up a
calculation for the lightest $\Lambda\Lambda$-hypernucleus, namely the $^{6}_{\Lambda\Lambda}$He, but we do
not provide results since more work on the parallelization procedure is still
required. So in the next benchmark calculations the Hamiltonian does not
contain the YY potential term.

5.1.1   Nuclear Potentials

As nuclear interactions we employ the 2-body potentials Argonne V4' and
V8' [68], obtained with a reprojection of the Argonne V18 potential that
preserves the phase shifts of the lower partial waves. The general definition
of the Argonne Vn potential:

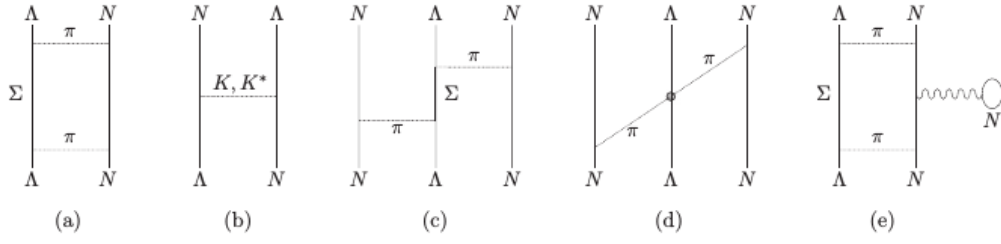$$V_{ij} = \sum_{p=1}^{n} v_p(r_ij)\mathcal{O}_{ij}^p \, , \qquad\qquad (5.1)$$

FIGURE 5.1: Meson exchange processes between nucleons
and hyperons at the ΛN and ΛNN level. Figure taken from
ref. [12].

where n is the number of operators and $v_p(r_{ij})$ are radial functions of Yukawa
and Woods-Saxon type. The first eight operators mainly come from the one-
pion exchange (OPE) between nucleons and read:

$$\mathcal{O}_{ij}^{p=1,8} = \{\mathbb{I}, \boldsymbol{\sigma}_i \cdot \boldsymbol{\sigma}_j, S_{ij}, \mathbf{L}_{ij} \cdot \mathbf{S}_{ij}\} \otimes \{\mathbb{I}, \boldsymbol{\tau}_i \cdot \boldsymbol{\tau}_j\} \ , \tag{5.2}$$

where S_{ij} is the usual tensor operator. The AV4' is purely central since
it contains only the first four operators in the above set. Details on AVn'
potentials can be found in ref. [68].

Of course the AVn' potentials do not provide the accuracy of the original
AV18, moreover in the following calculations we do not consider the 3-
body NNN forces. However, the aim is to provide benchmark results and
we postpone realistic calculations to near future developments.

5.1.2 Hypernuclear Potentials

The first hypernuclear interaction model we consider is the phenomenolog-
ical Bodmer-Usmani [46] model, which consists in an Argonne-like poten-
tial and has been employed exclusively in quantum Monte Carlo calcula-
tions for hypernuclei and hypermatter [3, 12, 47], due to its specific features
that make it manageable by such approaches. The complete model includes
2- and 3-body terms associated to the ΛN and ΛNN couplings at the two
pion exchange level, as shown in fig. 5.1.

The ΛN interaction has been modeled with an Urbana type potential with
spin-spin and a two-pion exchange tail consistent with the available Λp
scattering data, with explicit space exchange term:

$$v_{\Lambda N}(r) = v_0(r)(1 - \epsilon + \epsilon \hat{P}_{\Lambda N}) + \frac{v_\sigma}{4} T_\pi^2(r) \boldsymbol{\sigma}_\Lambda \cdot \boldsymbol{\sigma}_N \ , \tag{5.3}$$

where the short-range contributions are included, as in the Argonne inter-
actions, by means of a Wood-Saxon repulsive potential:

$$v_0(r) = \frac{W_c}{1 + e^{\frac{r-\bar{r}}{a}}} - \bar{v}T_\pi^2(r) \tag{5.4}$$

where $T_\pi(r)$ is the usual regularized OPE tensor operator:

$$T_\pi(r) = \left[1 + \frac{3}{\mu_\pi r} + \frac{3}{(\mu_\pi r)^2}\right] \frac{e^{-\mu_\pi r}}{\mu_\pi r}(1 - e^{-cr^2})^2 \tag{5.5}$$

where μ_π is the pion reduced mass. Further details can be found in ref. [12].
Constants are shown in appendix B.

The 3-body terms of the Bodmer-Usmani potential are related to the $c)$ $d)$
and $e)$ diagrams of fig. 5.1. The first two correspond to P-wave and S-wave
2π exchange. The last one represents a dispersive contribution associated
with the medium modifications of the intermediate-state potentials for Σ,
N and Δ due to the presence of a second nucleon. In ref. [12] the explicit
expressions and parameters are provided.

The second adopted YN interaction is a 2-body potential based on the ex-
plicit $\Lambda - \Sigma$ coupling therefore including the additional Σ degree of free-
dom. We consider the phenomenological interaction of ref. [14], which is
an hard-core type gaussian potential that simulates the NSC97f scattering
phase shifts. It is defined as:

$$^{2S,2T}V_{NY-NY'}(r) = \sum_{i=1}^{2} \left({}^{2S,2T}V_{NY-NY'}^{C}e^{-(r/\beta_i)^2} + \right.$$
$$\left. + {}^{2S,2T}V_{NY-NY'}^{T}e^{-(r/\beta_i)^2} + {}^{2S,2T}V_{NY-NY'}^{LS}e^{-(r/\beta_i)^2} \right), \tag{5.6}$$

where C, T, LS denote central, tensor and spin-orbit terms. Details can be
found in ref. [14]. Parameters are listed in appendix B.

5.2   The NSHH Approach for Λ-Hypernuclei

In the following section we briefly show how to set the extended NSHH
method for the application to Λ-hypernuclei. Such systems contain two dif-
ferent species of particles with different masses. We define the parameter:

$$\mu = \frac{m_N}{m_\Lambda} \approx 0.84 \ . \tag{5.7}$$

When a 2-body potential term V_{ij} has to be calculated, the sequence of kine-
matic rotations needed to move particles i and j in the first two positions of

the Jacobi coupling scheme involve four different types of kinematic angles, depending on the masses of the two particles involved and on the mass of the particle placed in the first position of the Jacobi scheme. Assuming that the hyperons are initially placed in the last positions of the Jacobi coupling sequence, we have

$$\cos \beta_i = \begin{cases} 1/i \; ; & NN - N \\ 1/\sqrt{i[1 + \mu(i - 1)]} \; ; & N\Lambda - N \\ 1/[\mu(A - n_\Lambda) + i - (A - n_\Lambda)] \; ; & \Lambda\Lambda - N \\ 1/\sqrt{(1 + \mu(i - 1))(2/\mu + i - 2)} \; ; & N\Lambda - \Lambda \end{cases} \tag{5.8}$$

where NN-N denotes a kinematic rotation between two nucleons with a nucleon in the first position of the Jacobi sequence, NΛ-N a kinematic rotation between a nucleon and a Λ with a nucleon in the first position and so on. Obviously if only one hyperon is present in the A-body system, only the first two definitions of β_i are necessary.

The relation between the relative coordinate of two interacting particles, i and j, in an hypernucleus after the application of the $\mathcal{Q}_{12}^{ij}$ permutation:

$$\mathbf{r}_{N_i N_j} = \frac{1}{\sqrt{2}} \, \boldsymbol{\eta}_N \; ;$$

$$\mathbf{r}_{N_i \Lambda_j} = \frac{1}{\sqrt{\mu + 1}} \, \boldsymbol{\eta}_N \; ; \tag{5.9}$$

$$\mathbf{r}_{\Lambda_i \Lambda_j} = \frac{1}{\sqrt{2\mu}} \, \boldsymbol{\eta}_N \; .$$

If n_Λ is the number of hyperons and $n_N = A - n_\Lambda$ the number of nucleons, we define the operator $\hat{C}(n_N, n_\Lambda)$ as the sum of the Casimir operators $\hat{C}(n_N)$ and $\hat{C}(n_\Lambda)$ associated, respectively, to the permutation groups S_{n_N} and S_{n_Λ}:

$$\hat{C}(n_N, n_\Lambda) = \hat{C}(n_N) + \hat{C}(n_\Lambda) = \sum_{j>i=1}^{n_N} \mathcal{Q}^{ij} + \sum_{j>i=n_N+1}^{A} \mathcal{Q}^{ij} \; , \tag{5.10}$$

where $\hat{Q}_{ij}$ is the usual permutation operator for particles i and j.

By recalling eq. (1.7), the Hamiltonian for a Λ-hypernucleus with a $\Lambda - \Sigma$

mixing interaction model is defined as:

$$
H = \begin{pmatrix} T & \\ & T + \Delta T_{m_\Sigma} \end{pmatrix} + \begin{pmatrix} 0 & \\ & \Delta M \end{pmatrix}
$$
$$
+ \begin{pmatrix} V_{NN} & \\ & V_{NN} \end{pmatrix} + \begin{pmatrix} V_{N\Lambda-N\Lambda} & V_{N\Sigma-N\Lambda} \\ V_{N\Lambda-N\Sigma} & V_{N\Sigma-N\Sigma} \end{pmatrix}
$$

$$(5.11)$$

In this case the ΔM matrix is not diagonal in the isospin basis because of the different mass of the three different isospin states of the Σ particle: Σ^0 for $t_z = 0$, Σ^- for $t_z = -1$ and Σ^+ for $t_z = 1$. Each matrix element has to be explicitly evaluated by means of Clebsch-Gordan recouplings. The same consideration holds for the calculation of the ΔT_{m_Σ} matrix.

5.3   Benchmark Results of Binding and Separation Energies

As mentioned in the introduction, we considered two different cases, adopting two versions of the Argonne NN potential in combination with the two aforementioned interaction models for the YN sector. We computed the total binding energies of Λ-hypernuclei and corresponding core nuclei and the Λ separation energies B_Λ.

In the first case the adopted NN potential is the Argonne V4′ (AV4′). We omit the electromagnetic part. The YN interaction is the Bodmer-Usmani 2-body ΛN potential with exchange parameter ϵ set to zero due to technical complications in its treatment with AFDMC method. We denote it with B.U.$^{2b'}$ to distinguish from the complete ΛN force (B.U.^{2b}) employed in the 3-body calculation in the next section. As explained in ref. [47], the omission of the 3-body hyperon-nucleon force in this framework produces over-estimated hyperon separation energies, as can be seen in table 5.1. However our aim is to compare the accuracy of NSHH for hypernuclear systems with other ab-initio methods for a given interaction model, rather than reproducing the experimental results. In Tab. 5.1 we report the complete comparison between NSHH and AFDMC for 3- to 5-body systems, and an additional comparison with FY results in the 3-body case [80].
 The uncertainties of NSHH results are calculated as the standard deviation on the last three to four data in the convergence pattern. Due to the larger computational effort in reaching full convergence in the 4- and 5-body case, the error bar is about one order of magnitude larger than in the 3-body case. In particular we have an error estimate of few KeV for both NSHH and FY calculations for $^3_\Lambda$H and of 10 keV for $^4_\Lambda$H and $^5_\Lambda$He. We believe that more

Interaction	System	J^π	NSHH	AFDMC	FY	exp
AV4'	^{2}H	1^+		-2.245(15)	-2.245(1)	-2.225
AV4'+B.U.$^{2b'}$	$^3_\Lambda$H	$1/2^+$	-2.539(2)	-2.42(6)	-2.537(1)	
	B_Λ		0.294(2)	0.18(6)	0.292(1)	0.13(5)
AV4'	^{3}H	$1/2^+$	-8.98(1)	-8.92(4)		-8.482
AV4'+B.U.$^{2b'}$	$^4_\Lambda$H	0^+	-12.02(1)	-11.94(6)		
	B_Λ		3.04(1)	3.02(7)		2.04(4)
AV4'	^{4}He	0^+	-32.89(1)	-32.84(4)		-28.30
AV4'+B.U.$^{2b'}$	$^5_\Lambda$He	$1/2^+$	-39.54(1)	-39.51(5)		
	B_Λ		6.65(1)	6.67(6)		3.12(2)

precise calculations with error bars reduced by about a factor ten will be calculated in the near future with the help of an improved parallelization. AFDMC uncertainties are typically larger due to the statistical nature of the method.

The 5-body results, both binding and separation energies, are in very good agreement between NSHH and AFDMC. For lighter systems good agreement is found for B_Λ, while AFDMC binding energies are $50 \div 100$ keV higher than the corresponding NSHH. This is due to technical complications in the AFDMC implementation of the many-body wavefunction for open-shell systems. A new way to treat 2- and 3-body correlations in AFDMC is under study.

Due to the central character of the potentials, the NSHH basis is constrained by the total orbital angular momentum L and the spin S of the system, besides the isospin numbers T and T_z. The resulting order of magnitude of the basis employed to reach the accuracy of the values shown in Tab. 5.1 is 10^2 for the three-body, 10^4 for the four-body and 10^6 for the five-body case. These dimensions would not be sufficient to reach convergence within a simple variational approach, due to the strong short-range repulsion of the potential. The Lee-Suzuki procedure generates softer effective interactions, allowing for the efficient computation of the NSHH results shown in Tab. 5.1.

In the second case the NN potential is the Argonne V8' (AV8') [68] with no Coulomb force combined with the simulated NSC97f YN interaction of ref. [4, 14] which contains a central, a tensor and a spin-orbit term. As shown in the previous section it includes the $\Lambda - \Sigma$ coupling by taking into account the Σ degree of freedom. The AFDMC method has not been

extended yet to deal with explicit Σ. The comparison is then carried out among three methods, namely NSHH, FY [80] and GEM. Results are shown in tab. 5.2 for 3- and 4-body systems. The GEM values are taken from ref. [14].

The agreement is optimal both in the 3- and 4-body case. We expect to

TABLE 5.2: Binding and separation energies in MeV for different systems with $A = 3 - 4$. The NN potential is the Argonne V8' (no Coulomb force). The YN potential is the NSC97f.

Interaction	System	J^π	NSHH	FY	GEM	exp
AV8'	$^2\mathrm{H}$	1^+		-2.226(1)		-2.225
AV8'+NSC97f	$^3_\Lambda\mathrm{H}$	$1/2^+$	-2.413(3)	-2.415(1)	-2.42(1)	
	B_Λ		0.187(3)	0.189(1)	0.19(1)	0.13(5)
AV8'	$^3\mathrm{H}$	$1/2^+$	-7.76(0)	-7.76(0)	-7.77(1)	-8.43(1)
AV8'+NSC97f	$^4_\Lambda\mathrm{H}$	0^+	-10.05(7)		-10.10(1)	
	B_Λ		2.29(7)		2.33(1)	2.04(4)

reduce the error bar in the 4-body case soon by applying the parallellized version of the code. Since both the NN and YN potentials are not central and the Σ is treated as explicit degree of freedom, the NSHH Hilbert space is much bigger compared to the previous test based on the Bodmer-Usmani interaction. The basis dimension is one order of magnitude larger and therefore the convergence in this case requires additional computational effort.

We conclude that the accuracy of the NSHH approach for 3-body hypernuclear systems is good in comparison to other ab-initio methods such as AFDMC, FY and GEM and it has not been compromised by the addition of the considered extensions. Its applicability goes beyond $A = 3$ systems and it has been tested for $A = 4$ and $A = 5$. The potentiality of the method, however, is expected to be completely exploited by combining an efficient parallelization procedure in order to deal with larger basis dimensions. As pointed out in the previous chapter, this has partially been achieved and we hope that, with some more optimization work, the aim of studying systems with $5 \leq A \leq 7$, including cases with strangeness $S = -2$, belongs to the near future. This benchmark calculation is then intended to be the starting point for the application of the NSHH method to the physical study of hypernuclear systems.

5.4 Application of the ΛNN Potential and Perspectives on the $^{6}_{\Lambda\Lambda}$He Calculation

As described in section 4.1, the ΛNN force has been implemented in the NSHH framework. However, for technical reasons, the addition of this term makes the computation time grow considerably. Moreover the symmetrization of the matrix elements is limited to the NN particles only, so the number of elements to store and read is much bigger than in the NNN symmetrized case. An optimization of this part of the code is in progress. For these reasons we provide only the 3-body result for the hypertritium $^{3}_{\Lambda}$H with the AV4′ NN potential combined with the ΛN+ΛNN Bodmer-Usmani interaction.

In this way we provide a result that AFDMC calculations could not provide in ref. [12] due to technical limits (the separation energy results negative as shown in ref. [12]). However updated versions of AFDMC are now available and more precise results in the 3- and 4-body sector will be provided soon. In addition, we consider the same 3-body system with the inclusion of the space-exchange term (denoted with the label 2b'). As shown in table 5.3

TABLE 5.3: Binding and separation energy in MeV for $^{3}_{\Lambda}$H with Argonne V4′ NN potential (no Coulomb force) and Bodmer-Usmani(B.U.) ΛN+ΛNN force. In the second case the AV18 potential is employed with the complete B.U. potential including space-exchange term (label 2b).

Interaction	System	J^{π}	NSHH
AV4′+B.U.$^{2b'+3b}$	$^{3}_{\Lambda}$H	$1/2^{+}$	-2.44(2)
	B_{Λ}		0.19(2)
AV4′+B.U.$^{2b+3b}$	$^{3}_{\Lambda}$H	$1/2^{+}$	-2.45(2)
	B_{Λ}		0.20(2)

the separation energy is in line with the result from the calculation with the simulated NSC97f potential. The contribution of the space-exchange term, as expected, is very small [46, 81]. A more detailed analysis on the effect of such term on the $^{5}_{\Lambda}$He separation energy is presented in ref. [81]. It would be interesting by means of the NSHH method to extend this analysis by studying such an effect on other systems, especially light open-shell hypernuclei, which Monte Carlo approach could not treat with high precision up to now. We postpone such analysis to a possible future study.

Up to now no 6-body ab-initio calculations have been performed in the hypernuclear sector, with the only exception of Monte Carlo ones. The main reason is of course the large dimension of the basis needed to obtain convergent results. In fact, besides the already large dimensions of an ordinary

6-body basis, the presence of hyperons and relative mixing degrees of freedom enlarge the basis of one-to-two orders of magnitude. Moreover the most recent YY interaction models for the $S = -2$ sector, besides $\Lambda - \Sigma$ coupling, include additional coupling channels involving $\Xi - N$ mixing too. Our attempt has been to consider the above mentioned NSC97f simulated YN potential combined with the phenomenological $\Lambda\Lambda$ interaction from ref. [82]. No $\Sigma\Sigma$ channel has been included. However, additional work on the parallelization procedure is needed and no results have been obtained up to now.

Conclusions

We conclude with a general recap of the present work and we highlight the objectives achieved and the ones that still need work to be reached. Finally we focus on the perspectives and future applications.

Extended NSHH Method: Recap

The main objective was the extension of the Non-Symmetrized Hyperspherical Harmonics method in order to treat few-body hypernuclear systems. The contribution of this work has then been focused on the method more than on the physics of hypernuclei.

We first focused on the basic extensions of the HH formalism in order to treat systems with different species of particles.
Due to the absence of permutational symmetry in the NSHH basis, permutation operators have to be defined explicitly. When identical particles are involved, they coincide with the HH coupling permutation operators defined in ref. [15] and described in chapter 3. In case of different particles a distinction between permutations and coupling permutations is needed, as stressed in section 2.1.3. Coupling permutations are formally analogue to permutation operators for identical particles, and when 2- or 3-body potential operators involving different particles have to be evaluated, the procedure remains basically the same as the identical particles case, described in ref. [15], however, attention has to be paid to the presence of different masses and different single particle quantum numbers (like spins or isospins). True spatial permutations between different particles are employed in particular cases and have a more complex action involving both the hyperradial and the hyperangular part of the HH basis, as shown in chapter 4. They are needed only in specific cases, mainly when potentials with space-exchange terms are involved.
When no particular interaction models containing permutation operators

are involved, the formalism of the coupling transformations among different particles has no substancial differences with respect to the case of identical particles, as shown in chapter 3. By consequence the main difference in the calculation of the potential operator is the presence of multiple interactions, which have to be implemented separately and, when an effective interaction procedure is applied, it has to be applied to each kind of interaction separately, as shown in section 3.4.

Of course, when different species of particles are present, the permutational symmetry is limited to each subset of identical particles so the Casimir operator, which selects the physical eigenstates of the Hamiltonian, splits into as many terms as the present species, as shown in section 3.3.

In chapter 4 we introduced a number of extensions in order to treat interaction models with specific features that are present in most of the hypernuclear interactions, as 3-body or particle mixing terms.

In the first case we have adapted the implementation of the 3-body NNN force described in ref. [73] to the specific case of the ΛNN force. This allowded us to use the phenomenological Bodmer-Usmani ΛN+ΛNN interaction model.

In the second case we have extended the NSHH formalism in order to take into account additional degrees of freedom due to the presence of particle mixing. Attention has been paid to the management of the masses, which are not fixed anymore, but could depend on some of the quantum numbers defining a given state, like the isospin in the $\Lambda - \Sigma$ coupling case. In fact, due to the fact that the HH basis is built over a mass dependent set of coordinates, the calculation of the mixing potential matrix elements leads to technical complications. They are due to the need of a transformation that allows to pass from one HH basis set built over a given set of masses to another HH set based on a different set of masses. We have circumvented such a problem by keeping fixed only one set of mass parameters for the whole HH basis functions and calculating explicitly the kinetic energy difference related to the blocks of states where the mass parameters of the Jacobi set are different from the physical ones.

By adopting the same principle, in section 4.2.2 we have also shown how to implement permutation operators between different particles.

Part of the work has also been devoted to the parallelization of the NSHH method with the aim of reaching the possibility to treat systems with $A \geq 5$. An hybrid MPI+OpenMP scheme has been implemented, but still with partial results. On this basis a deeper and more systematic study still has to be done, especially by means of some of the modern profiling softwares in order to better define the dependence of the time scaling on the input parameters.

Results

Since the general aim was to introduce a new tool for the study of few-body hypernuclei, our applications have been focused on such systems. We have performed benchmark calculations of binding and separation energies of systems with $A = 3 \div 5$ involving different ab-initio methods, namely the Auxiliary Field Diffusion Monte Carlo (AFDMC) method, the Faddeev Yakubovski equations (FY) and, by reference, the Gaussian Expansion Method (GEM).

In particular, we have provided results for Λ-hypernuclei by adopting the 2-body ΛN Bodmer-Usmani interaction and compared them to the AFDMC results, showing an acceptable agreement, especially considering the precision limits of the Monte Carlo calculations for open shell systems, like the $^3_\Lambda$H and the $^4_\Lambda$H. In fact the agreement for the $^5_\Lambda$He, which is a closed shell system, is optimal. In the 3-body case we have also provided an additional comparison with FY results, showing a difference in the calculated binding energy of the order of 0.1%.

The mixing extensions introduced in chapter 4 have been used in the benchmark calculations of the $^3_\Lambda$H and the $^4_\Lambda$H systems with the employment of the simulated NSC97f interaction and the results have been compared with the GEM results from ref. [14] and, in the 3-body sector, with FY results, showing a general agreement of the same order of the previous calculations. We conclude that the introduced NSHH extensions, in general, preserve the accuracy of the HH-based approaches.

Finally we have performed a 3-body calculation by adding the 3-body ΛNN Bodmer-Usmani potential to the already used 2-body ΛN part with no space exchange, and compared the result with the value obatained with the addition of the space-exchange term. We observed a small difference of the order of 10 keV, in line with the analysis in ref. [81]. However, we postpone a deeper study on a possible future development. Calculations with 4- and 5-body systems and with the 3-body NNN and NNΛ forces are still in progress, due to technical difficulties in the management of the 3-body operators in our NSHH code.

A 6-body calculation of the $\Lambda\Lambda$-hypernucleus $^6_{\Lambda\Lambda}$He has been set up, however it is still in the preliminary phase of testing and no significative results have been obtained. More work on the parallelization procedure is needed, due to the very large dimension of the basis which, besides the number of particles, is determined by the multiple mixing degrees of freedom in the $S = -2$ sector.

In conclusion, the NSHH method (combined with the Lee-Suzuki effective interaction) shows quite a promising versatility, allowing the treatment of

a variety of systems and interaction models. Such a versatility, however, is expected to be completely developed when the included parallelization procedure will be fully optimized.

Perspectives

The NSHH method has been adapted for the treatment of few-body hypernuclear systems and tested for systems up to 5-body. The idea is that, by implementing a suitable parallelization procedure, one could go beyond the 5-body sector. In fact, up to now, almost no ab-initio methods have been able to treat 6- or more body hypernuclear systems like, for example, the $^{6}_{\Lambda\Lambda}$He without cluster approximations (except Monte Carlo ones and NCSM for single Λ-hypernuclei [9]). However, as explained, some work still has to be done in this sense, in particular the optimization of the shared memory openMP part in the parallelized scheme of the NSHH code.

In chapter 4 we solved the particle mixing problem by calculating explicitly the operator of the difference in kinetic energy due to the difference of the masses in the coupled particles. However we have recently defined the representation in the HH basis of the set of transformations $W_{\zeta\zeta'}$ that allow to pass from one Jacobi set defined on a given set of masses ζ to another set defined on a different one, ζ'. The aim is to introduce a new set of coefficients that define the passage from an HH basis defined over a ζ set to another HH basis defined over a different ζ' set. First numerical tests have been performed for 3-body systems and we expect to fully develop the formalism in the near future.

One limit of the present method is the fact that it is defined in coordinate space, precluding the employment of the most recent YN interactions coming from χEFT theory. A conversion of the method in momentum space is in progress, and once it will be completed, the implementation of the extensions introduced in this work should be almost straightforward. The possibility to adopt interactions coming from χEFT or meson-theoretical models is not a secondary aspect because, due to the lack of experimental data in the hypernuclear sector, interaction models whith a non purely-phenomenological basis constitute the fundamental line of investigation, opening the possiblity of improvements that are not fully dependent on the lacking experimental database.

Appendix A

Matrix Elements of Δ_{η_1} in the NSHH Basis

We derive the explicit form of the Δ_{η_1} operator in the NSHH basis. We have:

$$\Delta_{\eta_1} = \frac{\partial^2}{\partial \eta_1^2} + \frac{2}{\eta_1}\frac{\partial}{\partial \eta_1} + \frac{\hat{l}_1}{\rho^2} \ . \tag{A.1}$$

By expliciting the derivation in the complete HH set, we decompose the operator in its hyperradial and hyperangular parts:

$$\frac{\partial^2}{\partial \rho^2}\Delta_\Omega^a + \frac{2}{\rho}\frac{\partial}{\partial \rho}\Delta_\Omega^b + \frac{1}{\rho^2}\Delta_\Omega^c \ . \tag{A.2}$$

The matrix elements of the Δ_Ω^a operator:

$$
\begin{aligned}
\Delta_\Omega^a = &-l_1(l_1+1)\prod_{\alpha=2}^N P_{1/c^2}^\alpha \\
&- 2\sum_{i=i+1}^N \left(\prod_{\alpha=i+1}^N P_{1/c^2}^\alpha\right)\left(\prod_{\alpha=2}^{i-1}\delta_\alpha^{KK}\right)\left[(l+k)\delta_i^{KK} - KP_{1/c^2}^i - 4P_{s^2}^\partial\right] \\
&- 2\sum_{i=2}^{i-1}\left(\prod_{\alpha=2}^{i-1}P_{c^2}^\alpha\right)\left(\prod_{\alpha=i+1}^N\delta_\alpha^{KK}\right)\left[(l+k)P_{c^2}^i - K\delta_i^{kk} - 4P_{s^2c^2}^\partial\right] \\
&+ \sum_{i=2}^N\left(\prod_{\alpha=2}^{i-1}P_{c^2}^\alpha\right)\left(\prod_{\alpha=i+1}^N P_{1/c^2}^\alpha\right)\Big[(l+K+(l+K)^2)P_{c^2}^i \\
&\qquad + K(K-1)P_{1/c^2}^i - (2K^2 + l(2K+1))\delta_i^{KK} + \\
&\qquad (8(K+l)-4)P_{s^2}^\partial - (8(k+l)+12)P_{s^2c^2}^{i\partial} + 16P_{s^2c^2}^{i\partial^2}\Big]
\end{aligned}
\tag{A.3}
$$

$$+ \sum_{i>j} \left(\prod_{\alpha=2}^{j-1} P_{c^2}^\alpha \right) \left(\prod_{\alpha=j-1}^{i+1} \delta_\alpha^{KK} \right) \left(\prod_{\alpha=i+1}^{N} P_{1/c^2}^\alpha \right) \left[(l+K)P_{c^2}^j - K\delta_j^{KK} - 4P_{s^2c^2}^{j\partial} \right]$$

$$\left[(1-K)P_{1/c^2}^i + \delta_i^{KK}(l+K-1) - 4P_{s^2}^{i\partial} \right]$$

$$+ \sum_{i<j} \left(\prod_{\alpha=2}^{i-1} P_{c^2}^\alpha \right) \left(\prod_{\alpha=i+1}^{j-1} \delta_\alpha^{KK} \right) \left(\prod_{\alpha=j+1}^{N} P_{1/c^2}^\alpha \right) \left[-(K+1)\delta_i^{KK} \right.$$

$$\left. + (l+K+1)P_{c^2}^i - 4P_{s^2c^2}^{i\partial} \right]$$

$$\left[(l+K)\delta_j^{KK} - KP_{1/c^2}^j - 4P_{s^2}^{j\partial} \right] .$$

$$\text{(A.4)}$$

The Δ_Ω^b operator:

$$\Delta_\Omega^b = 2\delta_T^{KK}$$

$$- 2\sum_{i=2}^{N} \left(\prod_{\alpha=2}^{i-1} P_{c^2}^\alpha \right) \left(\prod_{\alpha=i+1}^{N} \delta_\alpha^{KK} \right) \left[(l+k)\delta_i^{KK} - KP_{1/c^2}^i - 4P_{s^2}^\partial \right] \qquad \text{(A.5)}$$

$$+ \sum_{i=2}^{N} \left(\prod_{\alpha=2}^{i-1} P_{c^2}^\alpha \right) \left(\prod_{\alpha=i+1}^{N} \delta_\alpha^{KK} \right) \left[\delta_i^{KK} - P_{c^2}^i \right] .$$

The Δ_Ω^c part:

$$\Delta_\Omega^c = \prod_{\alpha=2}^{N} P_{c^2}^i . \qquad \text{(A.6)}$$

We adopted the following notation:

$$P_f^i = \int d\phi_i \, {}^{(i)}\mathcal{P}_{K_{i-1}}(\phi_i) f(\phi_i) \, {}^{(i)}\mathcal{P}_{K'_{i-1}}(\phi_i) \, ;$$

$$\delta_i^{KK} = \int d\phi_i \, {}^{(i)}\mathcal{P}_{K_{i-1}}(\phi_i) \, {}^{(i)}\mathcal{P}_{K'_{i-1}}(\phi_i) \, ;$$

$$P_f^{i\partial} = \int d\phi_i \, {}^{(i)}\mathcal{P}_{K_{i-1}}(\phi_i) f(\phi_i) \frac{\partial}{\partial\phi_i} \, {}^{(i)}\mathcal{P}_{K'_{i-1}}(\phi_i) \, ; \qquad \text{(A.7)}$$

$$P_f^{i\partial^2} = \int d\phi_i \, {}^{(i)}\mathcal{P}_{K_{i-1}}(\phi_i) f(\phi_i) \frac{\partial^2}{\partial\phi_i^2} \, {}^{(i)}\mathcal{P}_{K'_{i-1}}(\phi_i) \, ;$$

where the $^{(i)}\mathcal{P}_{K_{i-1}}(\phi_i)$ are the hyperspherical polynomials of eq. (2.60).
If the nubers l and K are called inside a sum over an index i, they are intended to be l_i and K_{i-1}. Finally, the labels of the angular functions:

$$
\begin{aligned}
c &\rightarrow \cos; \\
s &\rightarrow \sin ; \\
c^2 &\rightarrow \cos^2 ; \\
1/c^2 &\rightarrow 1/\cos^2 .
\end{aligned}
\tag{A.8}
$$

Of course each hyperangular matrix element has to be multiplied by the appropriate hyperradial element, following the association shown in eq. (A.2).

Appendix B

Lists of Parameters for 2-body YN Potentials

In table B.1 we report the parameters of the 2-body Bodmer-Usmani YN potential employed in the benchmark calculations of chapter 4.

TABLE B.1: List of constants defining the 2-body part of the Bodmer-Usmani interaction [46].

Constant	Value	Unit
W_c	2137	MeV
$\bar{r}$	0.5	fm
a	0.2	fm
$\bar{v}$	6.15	MeV
v_σ	0.24	MeV
c	2.0	fm^{-2}
$1/\mu_\pi$	1.429504	fm

In table B.2 the parameters of the NSC97f simulated YN interaction of ref. [14] are shown. The labels C, T and LS are related to the operators associated to the corresponding radial function, in particular central, tensor and spin-orbit.

TABLE B.2: List of constants defining the NSC97f simulated
YN interaction [14].

i	1	2	unit
β_i	0.5	1.2	
$^{0,1}V^{C}_{N\Lambda-N\Lambda}$	732.08	-99.494	MeV
$^{0,1}V^{C}_{N\Lambda-N\Sigma}$	61.223	-15.997	
$^{0,1}V^{C}_{N\Sigma-N\Sigma}$	1708.0	80.763	
$^{0,3}V^{C}_{N\Sigma-N\Sigma}$	695.39	-109.37	
$^{2,1}V^{C}_{N\Lambda-N\Lambda}$	1068.8	-45.490	
$^{2,1}V^{C}_{N\Lambda-N\Sigma}$	-770.21	68.274	
$^{2,1}V^{C}_{N\Lambda-N\Sigma}$	863.76	28.284	
$^{2,3}V^{C}_{N\Sigma-N\Sigma}$	-181.08	23.282	
$^{2,1}V^{T}_{N\Lambda-N\Lambda}$	-243.31	-10.413	
$^{2,1}V^{T}_{N\Lambda-N\Sigma}$	287.54	62.438	
$^{2,3}V^{T}_{N\Sigma-N\Sigma}$	333.05	22.234	
$^{2,1}V^{LS}_{N\Lambda-N\Lambda}$	1023.8	-17.195	
$^{2,1}V^{LS}_{N\Lambda-N\Sigma}$	-19.930	22.299	
$^{2,3}V^{LS}_{N\Sigma-N\Sigma}$	-462.31	0.0023	

Appendix C

Benchmark Results for Systems with A$= 3 \div 5$

In table C.1 some benchmark results for binding and separation energies with unrealistic YN gaussian potentials are shown. The parameters for the potentials and the notation are shown in section 3.5.3. NSHH results are compared with AFDMC [70] and NCSM ones [71].

TABLE C.1: Benchmark calculation for light Λ hypernuclei.
Minnesota NN potential, no Coulomb. Energies in MeV.

$NN + \Lambda N$ potential	System	AFDMC	NCSM	NSHH
Minnesota + MN $T = 0 \times 0.9$	$^3_\Lambda$H B_Λ	-2.38(12) 0.21(13)	-2.29(2) 0.07(2)	-2.27(1) 0.05(1)
	$^4_\Lambda$H B_Λ	-18.12(15) 10.07(17)	-17.9(3) 9.51(30)	-17.694(3) 9.304(3)
	$^5_\Lambda$He B_Λ	-70.41(25) 39.67(25)	— —	-70.70(1) 39.92(1)
Minnesota, centr only+ MN $T = 0 \times 0.9$	$^4_\Lambda$H B_Λ	-28.87(15) 20.82(17)	— —	-29.02(20) 20.64(20)
Minnesota+ MN $T = 1 \times 0.9$	$^4_\Lambda$H B_Λ	-9.01(13) 0.96(15)	-10.06(1) 1.67(1)	-10.06(1) 1.68(1)
AV4′+ MN $T = 0 \times 0.9$	$^3_\Lambda$H B_Λ	-2.35(12) 0.17(13)	— —	-2.30(5) 0.08(5)
	$^4_\Lambda$H B_Λ	-19.11(16) 10.39(18)	— —	-18.831(5) 9.62(10)
	$^5_\Lambda$He B_Λ	-72.34(35) 39.58(36)	— —	-72.8(6) 40.1(6)

Bibliography

[1]   J. Kadyk, G. Alexander, J. Chan, P. Gaposchkin, and G. Trilling, Nucl. Phys. B **27**, 13 (1971).

[2]   V. G. J. Stoks, R. A. M. Klomp, M. C. M. Rentmeester, and J. J. Swart, Phys. Rev. C **48**, 792 (1993).

[3]   A. A. Usmani and F. C. Khanna, J. Phys. G **35**, 025105 (2008).

[4]   E. Hiyama, M. Kamimura, T. Motoba, T. Yamada, and Y. Yamamoto, Phys. Rev. C **65**, 011301 (2001).

[5]   H.-J. Schulze and T. A. Rijken, Phys. Rev. C **88**, 024322 (2013).

[6]   H. Polinder, J.Haidenbauer, and U. Meißner, Nucl. Phys. A **779**, 244 (2006).

[7]   J. Haidenbauer, S. Petschauer, N. Kaiser, U.-G. Meißner, A. Nogga, and W. Weise, Nucl. Phys. A **915**, 24 (2013).

[8]   D. Gazda, J. Mares, P. Navratil, R. Roth, and R. Wirth, Few-Body Syst. **55**, 857 (2014).

[9]   R. Wirth, D. Gazda, P. Navratil, A. Calci, J. Langhammer, and R. Roth, Phys. Rev. Lett. **113**, 192502 (2014).

[10] D. Gazda and A. Gal, Phys. Rev. Lett. **116**, 122501 (2016).

[11] A. Nogga, H. Kamada, and W. Glöckle, Phys. Rev. Lett. **88**, 172501 (2002).

[12] D. Lonardoni, S. Gandolfi, and F. Pederiva, Phys. Rev. C **89**, 014314 (2014).

[13] E. Hiyama, Few-Body Syst. **53**, 189 (2012).

[14] E. Hiyama, S. Ohnishi, B. F. Gibson, and T. A. Rijken, Phys. Rev. C **89**, 061302 (2014).

[15] M. Gattobigio, A. Kievsky, and M. Viviani, Phys. Rev. C **83**, 024001 (2011).

[16] S. Deflorian, N. Barnea, W. Leidemann, and G. Orlandini, Few-Body Syst. **54**, 1879 (2013).

[17] D. Lonardoni, *From Hypernuclei to Hypermatter: a Quantum Monte Carlo Study of Strangeness in Nuclear Structure and Nuclear Astrophysics* (Ph.D. Thesis, Universitá degli Studi di Trento, 2013).

[18] J. Beringer, J. F. Arguin, R. M. Barnett, et al., Phys. Rev. D **86**, 010001 (2012).

[19] M. Danysz and J. Pniewski, Philos. Mag. **44**, 348 (1953).

[20] S. N. Nakamura, Nucl. Phys. A **914**, 3 (2013).

[21] T. Sato, T. Takahashi, and K. Yoshimura, *Particle and Nuclear Physics at J-PARC* (Springer, 2010).

[22] R. Lea, Nucl. Phys. A **914**, 415 (2013).

[23] F. Garibaldi et al., Nucl. Phys. A **914**, 914 (2013).

[24] A. Esser et al., Nucl. Phys. A **914**, 1016 (2013).

[25] A. Feliciello et al., Mod. Phys. Lett. A **28**, 1330029 (2013).

[26] T. Yamamoto, M. Agnello, Y. Akazawa, et al., Phys. Rev. Lett. **115**, 1 (2015).

[27] E. Botta, T. Bressani, and A. Feliciello, Nucl. Phys. A **960**, 165 (2017).

[28] A. Esser et al., Phys. Rev. Lett. **114**, 232501 (2015).

[29] C. Rappold et al., Phys. Rev. C **88**, 041001 (2013).

[30] A. Gal and H. Garcilazo, Phys. Lett. B **736**, 93 (2014).

[31] H. Garcilazo and A. Valcarce, Phys. Rev. C **89**, 057001 (2014).

[32] M. Juric, G. Bohm, J. Klabuhn, et al., Nucl. Phys. B **52**, 1 (1973).

[33] S. N. Nakamura, A. Matsumura, Y. Okayasu, et al., Phys. Rev. Lett. **110**, 012502 (2013).

[34] D. H. Davis, Nucl. Phys. A **754**, 3 (2005).

[35] N. Nakazawa, Nucl. Phys. A **835**, 207 (2010).

[36] M. Danysz et al., Nucl. Phys. **49**, 121 (1963).

[37] O. Hashimoto and H. Tamura, Progr. Part. Nucl. Phys. **57**, 564 (2006).

[38] T. Rijken and Y. Yamamoto, Phys. Rev. C **73**, 044008 (2006).

[39] H. J. Schulze and T. Rijken, Phys. Rev. C **88**, 024322 (2013).

[40] H. Polinder, J. Haidenbauer, and U.-G. Meißner, Phys. Lett. B **653**, 29 (2007).

[41] J. Haidenbauer, U.-G. Meißner, and S. Petschauer, Nucl. Phys. A **954**, 273 (2016).

[42] H. Dapo, B. J. Schaefer, and J. Wambach, Eur. Phys. J. A **36**, 101 (2008).

[43] J. Hao, T. Kuo, A. Reuber, K. Holinde, J. Speth, and D. J. Millener, Phys. Rev. Lett. **71**, 1498 (1993).

[44] T. A. Rijken, V.G.J.Stocks, and Y. Yamamoto, Phys. Rev. C **59**, 21 (1999).

[45] E. Hiyama, M. Kamimura, T. Motoba, T. Yamada, and Y. Yamamoto, Progr. Theor. Phys **97**, 881 (1997).

[46] A. R. Bodmer and Q. N. Usmani, Nucl. Phys. A **477**, 621 (1988).

[47] D. Lonardoni, S. Gandolfi, and F. Pederiva, Phys. Rev. C **87**, 041303 (2013).

[48] M. Gattobigio, A. Kievsky, M. Viviani, and P. Barletta, Phys. Rev. A **79**, 032513 (2009).

[49] V. Aquilanti and S. Cavalli, J. Chem. Phys. **85**, 1355 (1986).

[50] N. Y. Vilenkin, G. I. Kuznetsov, and Y. A. Smorodinskii, Sov. J. Nucl. Phys. **2**, 645 (1966).

[51] N. Barnea, *Exact Solution of the Schrödinger and Faddeev Equations for Few Body Systems* (Ph.D. Thesis, The Hebrew University of Jerusalem, 1997).

[52] J. Avery, *Hyperspherical Harmonics. Applications in Quantum Theory* (Kluwer Academic Publishers, 1989).

[53] V. D. Efros, Sov. J. Nucl. Phys. **15**, 128 (1972).

[54] I. S. Gradshteyn and I. M. Ryzhik, *Table of Integrals, Series and Products* (Alan Jeffrey and Daniel Zwillinger, 2007).

[55] N. Barnea, W. Leidemann, and G. Orlandini, Nucl. Phys. A **650**, 427 (1999).

[56] N. Barnea, W. Leidemann, and G. Orlandini, Phys. Rev. C **61**, 054001 (2000).

[57] M. S. Kil'Dyushov, Sov. J. Nucl. Phys. **15**, 113 (1972).

[58] J. Raynal and J. Revai, Nuovo Cimento A **68**, 612 (1970).

[59] A. R. Edmonds, *Angular Momentum in Quantum Mechanics* (Princeton University Press, 1957).

[60] A. Novoselsky and J. Katriel, Phys. Rev. C **51**, 412 (1995).

[61] K. Suzuki and S. Y. Lee, Progr. Theor. Phys. **12**, 603 (1980).

[62] K. Suzuki and R. Okamoto, Progr. Theor. Phys. **92**, 1045 (1994).

[63] B. R. Barrett, P. Navratil, and J. P. Vary, Progr. Part. Nucl. Phys. **69**, 131 (2013).

[64] N. Barnea, W. Leidemann, and G. Orlandini, Phys. Rev. C **67**, 054003 (2003).

[65] C. C. Paige, J. Inst. Maths. Applics. **10**, 373 (1972).

[66] D. Baye, Phys. Rep. **565**, 1 (2015).

[67] D. R. Thomson, M. LeMere, and Y. C. Yang, Nucl. Phys. A **286**, 53 (1977).

[68] R. B. Wiringa and S. C. Pieper, Phys. Rev. Lett. **89**, 182501 (2002).

[69] H. Kamada et al., Phys. Rev. C **64**, 044001 (2001).

[70] D. Lonardoni (Private Communications).

[71] D. Gazda (Private Communications).

[72] C. Manzata, *Ground State and Photodisintegration of Beryllium-9 in Cluster Effective Field Theory* (Ms.C. Thesis, Universitá degli Studi di Trento, 2016).

[73] N. Barnea, V. D. Efros, W. Leidemann, and G. Orlandini, Few-Body Syst. **35**, 155 (2004).

[74] V. D. Efros, Few-Body Syst. **32**, 169 (2002).

[75] R. B. Wiringa, R. A. Smith, and T. L. Ainsworth, Phys. Rev. C **29**, 1207 (1984).

[76] P. Lancaster and L. Rodman, *Algebraic Riccati Equations* (Oxford University Press, 1995).

[77] N. Barnea (Private Communications).

[78] F. Ferrari-Ruffino, D. Lonardoni, N. Barnea, et al., Few-Body Syst. **58**, 113 (2017).

[79] T. A. Rijken, V. G. J. Stoks, and Y. Yamamoto, Phys. Rev. C **59**, 21 (1999).

[80] A. Nogga (Private Communications).

[81] A. A. Usmani, Phys. Rev. C **73**, 1 (2006).

[82] E. Hiyama, M. Kamimura, T. Motoba, T. Yamada, and Y. Yamamoto, Progr. Theor. Phys. **97**, 881 (1997).

Acknowledgements